FACULTY OF ELECTRICAL
ENGINEERING
AND COMMUNICATION

Department
of Electrical and Electronic
Technology

24th ABAF

BRNO 2023

Advanced Batteries, Accumulators and Fuel Cells

INTERNATIONAL CONFERENCE

August 27th - August 30th 2023

Organised by:

Department of Electrical and Electronic Technology,
Faculty of Electrical Engineering and Communication,
Brno University of Technology

Organizing committee:
Marie Sedlaříková
Tomáš Kazda

Honourary Scientific Committee:

- Petr Vanýsek, *Northern Illinois University, DeKalb, Illinois, USA*
- Arnaldo Visintin, *INIFTA, La Plata, Argentina*
- Günter Fafilek, *TU Wien, Vienna, Austria*
- Elena Shembel, *USCTU, Dnipro, Ukraine*
- Vito Di Noto, *University of Padova, Padova, Italy*
- Harry Hoster, *Universität Duisburg-Essen, Duisburg, Germany*
- Boris Markovsky, *Bar-Ilan University, Tel Aviv, Israel*
- Philipp Adelhelm, *Friedrich Schiller University, Jena, Germany*
- Laurence Hardwick, *University of Liverpool, Liverpool, UK*
- Renata Oriňáková, *UPJŠ, Košice, Slovakia*
- Andrea Fedorková-Straková, *UPJŠ, Košice, Slovakia*
- Grzegorz Lota, *Poznan University of Technology, Poznan, Poland*
- Mariusz Walkowiak, *Institute of Non-Ferrous Metals, Poznan, Poland*

Organisation Committee:

- Marie Sedlaříková, *FEEC BUT, Brno, Czech Republic*
- Tomáš Kazda, *FEEC BUT, Brno, Czech Republic*
- František Klein, Brno, *Czech Republic*
- Vítězslav Novák, *FEEC BUT, Brno, Czech Republic*
- Miroslav Zatloukal, *FEEC BUT, Brno, Czech Republic*
- Jiří Libich, *FEEC BUT, Brno, Czech Republic*
- Ondřej Čech, *FEEC BUT, Brno, Czech Republic*
- Tomáš Binar, *FEEC BUT, Brno, Czech Republic*
- Jiří Švarc, *University of Defence, Brno, Czech Republic*
- Pavlína Sedlaříková, *Brno, Czech Republic*

Program Committee:

- Marie Sedlaříková, *FEEC BUT, Brno, Czech Republic*
- Arnaldo Visintin, *INIFTA, La Plata, Argentina*
- Mariela Ortiz, *INIFTA, La Plata, Argentina*
- Petr Vanýsek, *Northern Illinois University, DeKalb, Illinois, USA*
- Günter Fafilek, *TU Wien, Vienna, Austria*
- Boris Markovsky, *Bar-Ilan University, Tel Aviv, Israel*
- Harry Hoster, *Universität Duisburg-Essen, Duisburg, Germany*
- Grzegorz Lota, Poznan *University of Technology, Poznan, Poland*
- Mariusz Walkowiak, *Institute of Non-Ferrous Metals, Poznan, Poland*
- Ondřej Čech, *FEEC BUT, Brno, Czech Republic*
- Vítězslav Novák, *FEEC BUT, Brno, Czech Republic*
- Petr Bača, *FEEC BUT, Brno, Czech Republic*
- Tomáš Kazda, *FEEC BUT, Brno, Czech Republic*
- Helena Polsterová, *FEEC BUT, Brno, Czech Republic*
- Miroslav Zatloukal, *FEEC BUT, Brno, Czech Republic*
- Kristýna Jandová, *FEEC BUT, Brno, Czech Republic*
- Andrea Fedorková-Straková, *UPJŠ, Košice, Slovakia*
- Jiří Libich, *FEEC BUT, Brno, Czech Republic*
- Tomáš Binar, *FEEC BUT, Brno, Czech Republic*

ISBN 978-80-214-6176-5

Main sponsors:

SKUPINA ČEZ

pragolab

RENISHAW®
apply innovation™

Other sponsors:

BioLogic

ERA
Elektro Recycling Austria

EVC group

EV Battery

TechSoft

co-sponsored by

ISE
INTERNATIONAL SOCIETY OF ELECTROCHEMISTRY

Springer
Monatshefte für Chemie - Chemical Monthly

We would like to express our thanks to the Brno University of Technology, Faculty of Electrical Engineering and Communication for support and help with organising 24th ABAF conference.

FACULTY OF ELECTRICAL
ENGINEERING
AND COMMUNICATION

Contents

Lithium Batteries and Related Systems

Supercapacitors

Fuel Cells

Aqueous Batteries

New Systems of Batteries

Photovoltaics

Corrosion, Applications and Simulations

Model-based optimization of electrolyte filling using laser structured electrodes

Mauritz Biebl[a], Harry Hoster[a]

[a] Chair of Energy Technology, University of Duisburg-Essen, Duisburg, Germany

The wetting of battery electrodes with electrolyte is a time- and cost-intensive process. One of the biggest challenges is the time it takes for the liquid electrolyte to be absorbed into the porous electrode. To reduce this wetting time, laser-structured electrodes can be used. The resulting grooves facilitate deeper penetration of the electrolyte during the wetting process, leading to faster wetting. Multiphysics simulations and measurement data will be used to optimize the wetting process and to investigate the influence of the structuring geometry on the wetting time.

Introduction

The structuring of electrodes for lithium batteries has gained significance in recent years as it affects both battery performance and production. By introducing structural modifications, a 3D electrode is created, enhancing lithium-ion transport and leading to higher battery cell performance. This opens up the possibility of combining high-energy and high-power cells [2]. Furthermore, structured electrodes offer advantages in battery production. They enable faster and more energy-efficient drying processes and thus improving the manufacturing process. In particular, the wetting time during the electrolyte filling process can be significantly reduced [3]. Wetting is a time-consuming and cost-intensive step, as the liquid electrolyte needs to penetrate the porous electrode structure [1]. Due to the small pore size and low porosity of the electrode material, permeability is low, resulting in long wetting times. However, the use of structured electrodes can substantially decrease this wetting time. The grooves in structured electrodes have a larger diameter than the pores in the porous material. As a result, the grooves have a higher permeability, allowing the electrolyte to penetrate quickly into the electrode. Figure 1 shows a microscope image of structured electrodes.

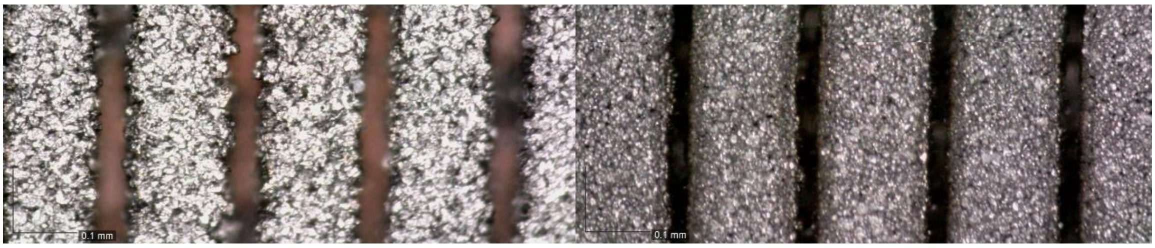

Figure 1. *Microscope image of a structured anode (left) and a structured cathode (right).*

So far, there have been a few studies on the wetting of structured electrodes, mostly based on experimental investigations that give limited insight into the exact distribution within the electrode. This work focuses on detailed multiphysics simulations to investigate the influence of structured electrodes on the wetting process. This study analyses the distribution of the electrolyte within the electrode during the wetting process and investigates the influence of the structural geometry on the wetting time.

Results and Discussion

To investigate the wetting process of unstructured and structured electrodes a simulation model was created in the software *COMSOL MULTIPHYICS*. To reduce the simulation time to a reasonable level, the model was simplified to a 2D model. The physical model of Darcy's Law and Phase Transport in Porous Media were used to create a multiphysics model. Using the created model, the wetting behavior of a structured electrode was simulated and compared with the wetting of an unstructured electrode. Figure 2 illustrates the electrolyte saturation profile for an unstructured electrode (top) and a structured electrode (bottom) for two different time steps.

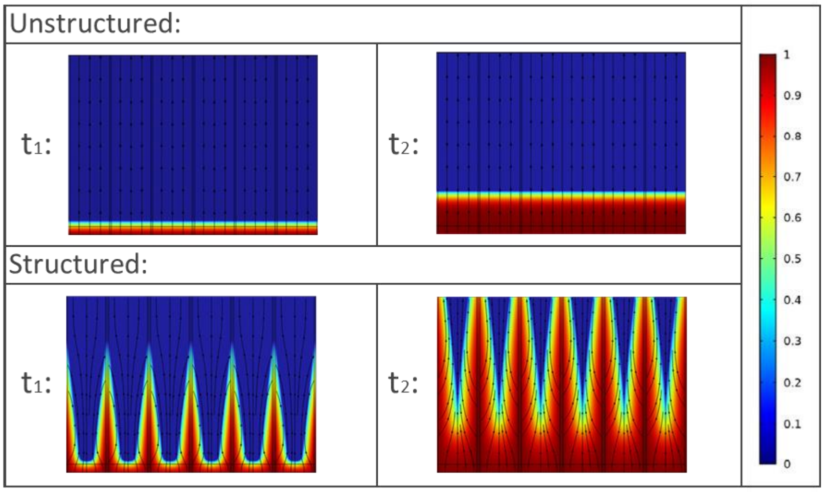

Figure 1. *Saturation profile of unstructured (top) and structured (bottom) electrodes for two different time steps ($t_1 < t_2$) in COMSOL MULTIPHYSICS*

It can be seen that the unstructured electrode shows a very homogeneous wetting behavior, while the structured electrode shows a very heterogeneous wetting pattern. The liquid electrolyte wets the grooves faster than the porous structure of the electrode. When the grooves are wetted, the electrolyte is distributed from there into the porous electrode. This effect results in a faster wetting process.

The simulation result shows that in this simulation the wetting time of a structured electrode could be 15-25 times faster than the wetting time of an unstructured electrode, depending on the structuring geometry, the electrode and the electrolyte. The result agrees well with the measurement data from the literature [1-3]. Furthermore, the sensitivity study showed that the wetting time increase for a higher groove distance.

Conclusion

The electrolyte filling process is a time- and cost-intensive step in battery production. In this study, the filling process was investigated and optimized using multiphysics simulations for both unstructured and structured electrodes. The results demonstrate that structured electrodes significantly reduce the wetting time. Furthermore, it was shown that the wetting time can be further reduced by choosing a suitable structuring geometry.

Acknowledgments

The dissemination of this work is funded by the European Union (HORIZON.2.5 – Climate, Energy, Mobility), Project Title: Carbon Neutral European Battery Cell Production with Sustainable, Innovative Processes and 3D Electrode Design to Manufacture (BatWoMan), ProjektID: 101069705

References

1. Jan B., Habedank et al. (2019) Rapid electrolyte wetting of lithium-ion batteries containing laser structured electrodes: in situ visualization by neutron radiography. The International Journal of Advanced Manufacturing Technology. https://doi.org/10.1007/s00170-019-03347-4
2. Wilhelm, Pfleging et al. (2014) A new approach for rapid electrolyte wetting in tape cast electrodes for lithium-ion batteries. Journal of Materials Chemistry A. doi: 10.1039/c4a02353f
3. Wilhelm, Pfleging et al. (2014) Laser generated microstructures in tape cast electrodes for rapid electrolyte wetting – new technical approach for cost efficient battery manufacturing. Green Photonics Best Paper Award. doi: 10.1117/12.2039635

Battery2030+ initiative and smart functionalities : Sensors and Selfhealing materials for enhanced safety Lithium ion cells

Silvia Bodoardo[1], Piera Di Prima[2], Davide Dessantis[2], Sebastiano Bellani[3], Hossein Beydaghi[3], Francesco Bonaccorso[3], Carlotta Francia[1], Julia Amici[1], Daniele Versaci[1]

[1]Electrochemistry Group Department of Applied Science and Technology – Politecnico di Torino – Corso Duca degli Abruzzi 24, 10129 Torino -Italy

[2]Department of Energy – Politecnico di Torino – Corso Duca degli Abruzzi 24, 10129 Torino -Italy

BeDimensional S.p.A., Genova, 16163, Italy

[3] Politecnico di Torino, (Dept. Of Applied Science and Technology), 10129-Turin, Italy

More and more automotive manufacturers introduce BEVs (battery electric vehicles) to the automotive market. Lithium-ion battery (LIB) cells are known to be sensitive to fast charging and high voltage operations. Pushing the charging limits, overcharging or an internal defect causing a short circuit can result in a thermal runaway causing a fire. Degradation of LIBs is an extremely complex process and is not yet fully understood, consequently many underlying degradation processes are not included in current BMS. The capability to measure in real-time internal battery cell key parameters like temperature, pressure, etc. would greatly help to understand these processes and LIB safe while using the full battery capacity. Accurate sensing of internal parameters leads to improved insight in the batteries condition and its usage history. These aspects together with some ideas on selfhealing materials are developed within H2020 SENSIBAT1 project and Battery20230+2 which ideas are explained in the presentation.

In order to study the anode and cathode behavior in working conditions, an internal reference electrode can provide fundamental information; therefore, a novel sensing technology consisting of printed auxiliary electrodes has been developed inside SENSIBAT project. A sensor working as reference electrode must possess stable voltage in the cell working conditions: for this reason, two different chemistries were chosen (Lithium Iron Phosphate -LFP- and Lithium Titanate Oxide -LTO-) as printed sensors. Different materials, including single-/few-layer graphene (SLG/FLG), reduced graphene oxide (RGO), carbon black (CB), were tested for LFP and LTO electrodes formulation and printability. The morphological and surface properties of the produced electrodes, hence, their suitability for the relevant applications, were characterized with X-Ray Diffraction (XRD), Scanning Electron Microscope (SEM) and Raman analysis to study the local composition and impurities on the interfaces.

Then, the reference electrodes were printed onto the cell separator (Celgard2500) and positioned between the active anode (graphite) and cathode (NMC622) in full pouch cells of 3 cm2 as shown in Figure 1. Finally, 3-electrodes cells were electrochemically characterized performing galvanostatic charge and discharge (GCD) cycles at different C-rates and EIS. The obtained results indicate that the printed LFP and LTO reference electrodes do not alter the pouch cell operation and can be used to accurately monitor distinctively the potentials and the impedances of the battery electrodes.

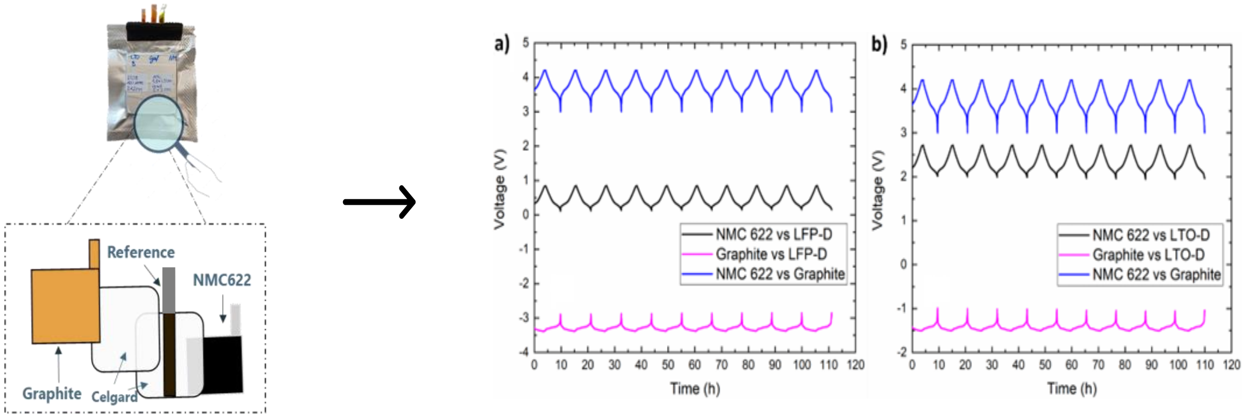

References

1. https://sensibat-project.eu
2. https://battery2030.eu

SENSIBAT - Integrating Sensing Capabilities for State Estimation and Performance Assessment in Li-ion Pouch Cells

Bernd Eschelmüller[1], Gregor Glanz[1], Katja Fröhlich[1], Marcus Jahn[1]

[1] Battery Technologies, AIT Austrian Institute of Technology GmbH, Vienna, Austria

As part of the BATTERY 2030+ research initiative, the project SENSIBAT (Cell-integrated SENSIng functionalities for smart BATtery systems with improved performance and safety) focuses on developing smart sensing functionalities, novel battery management system strategies, and state determining algorithms considering economic and environmental aspects. With the help of these sensors, integrated in Li-ion pouch cells, a better understanding of the battery behavior during its operation is gained.

A profound knowledge about the actual cell conditions (SoC, SoH) during cycling can be used for a better prediction of the cell behavior. Indicators for degradation processes and failure mechanisms can be determined and enable a more accurate control of the cells in a battery pack, leading to improved BMS state estimation functions apart from an estimation based on the electrical dipole behavior. That way, a significant increase in safety, lifetime and quality is achieved. The introduction of sensors into pouch cells is currently not done at industrial scale because several problems can arise within the process. One of them is incompatibilities during integration of the sensors during the pouch cell assembly. Especially at the sensor feedthrough, it needs to be ensured that electrolyte leakage is avoided, and air tightness of the pouch cell is given. Additionally, chemical reactions between the sensor and cell components, which can cause side reactions and unwanted by-products, should be avoided, as this can negatively influence the performance of the cell [1, 2, 3].

The research focus of the SENSIBAT project is on the use of potential, temperature, and pressure sensors to determine the State of Health (SoH) and State of Charge (SoC) of lithium-ion batteries. By integrating these sensing capabilities, the project developed accurate and reliable methods for assessing the health and performance of the cells, enabling proactive battery management strategies, and facilitating the optimization of battery utilization and lifetime. In addition to that, a profound recyclability and cost benefit assessment was also done within the project. With these approximations the holistic approach of implementing sensor units into LIBs and its advantages at industrial scale could be proven.

This project has received funding from the European Union's Horizon 2020 research and innovation programme under Grant Agreement no. 957273.

References

1. Vincent Dreher, Daniel Joch, Harald Kren, Jannik H. Schwarberg, Michael P.M. Jank, „Ultrathin and flexible sensors for pressure and temperature monitoring inside battery cells", 2022 IEEE Sensors | 978-1-6654-8464-0/22/
2. Valentin Sulzer, Peyman Mohtat, Antti Aitio, Suhak Lee, Yen T. Yeh, Frank Steinbacher, Muhammad Umer Khan, Jang Woo Lee, Jason B. Siegel, Anna G. Stefanopoulou, David A. Howey; "The challenge and opportunity of battery lifetime prediction from field data", 2021 Elsevier Inc. Joule 5, 1934–1955
3. Lukas Marthaler, Piotr Grudzien, Maarten Buysse, Marcos Ierides, Amy McCready, „KEY TECHNICAL, POLICY AND MARKET DEVELOPMENTS INFLUENCING THE ELECTRIC VEHICLE BATTERY LANDSCAPE", 2022 Cobra, Grant Agreement 875568, Market Intelligence Report

BatWoMan:
A superhero approach towards carbon neutrality in battery cell production in Europe

Katja Fröhlich

Competitiveness in battery cell production from a European perspective can only be achieved via high quality productions with minimum scraps and lowest carbon footprint for enhanced sustainability of the battery cell production processes.

The BatWoMan project develops new sustainable and cost-efficient Li-ion battery cell production concepts to reach the ambitions goal of carbon neutral cell production within the European Union.

This is pursued via the following concepts and improvements:

- Processing of three-dimensional patterned electrodes based on slurries with high dry mass content and without volatile organic compounds;
- Innovative electrolyte filling process and significantly reduced dry room needs to an absolute minimum;
- Low-cost and energy-efficient cell conditioning – namely wetting, formation and ageing.

An artificial intelligence driven manufacturing platform will digitally support and steer the implementation of these improvements, via smart re-tooling in response to changes in the desired cell properties. A battery passport contains all essential information about the manufacturing process, materials and their sources and the carbon footprint and efficiency of the individual production steps. All newly introduced processes and concepts will be carefully monitored and evaluated via life cycle assessment.

At the bottom line, this would put Europe into the driver’s seat of making battery production not only cost-efficient but also more sustainable.

Non-crystallizing electrolytes for lithium-ion batteries

M. Kasprzyk [a,*], L. Niedzicki [a], M. Broszkiewicz [a], A. Zalewska [a], B. Świątkowska [a],
M. Pyzik [a], E. Iwanek [a]

[a] Faculty of Chemistry, Warsaw University of Technology, Warsaw 00-664, Poland

This work is concentrated on application of non-crystallizing liquid electrolytes. The mixtures of ethylene carbonate (EC) with various poly(ethylene glycol)s (PEGs) are making base for the electrolytes preparation. Liquid electrolyte based on such solvent mixtures do not exhibit any crystallization or melting points. They also show quite high conductivity at temperatures much below 0°C. The electrochemical and physicochemical study of these electrolytes will be presented herein. Initial study on electrode morphology changes after keeping at extremely low temperature will be discussed.

Introduction

Modern world is concentrating on preserving and securing constant energy supplies. That is why the energy storage is now so important. We may collect energy by means of solar cells but then very often we need to save this energy for later (for instance to use it during night). This is why the lithium-ion batteries are still developing.

In standard lithium-ion batteries the liquid electrolytes are still used as standard electrolytes. Unfortunately, most of these electrolytes do crystallize. Crystallization risk at temperatures below 0°C is very high. During that process various parameters of electrolyte may change rapidly, i.e.: conductivity, viscosity and density. Due to volume changes we often observe the damage to electrodes. Because of that very often we cannot use the battery again, even if the temperature increases back to the standard operating values. Damage to electrodes may cause the damage to the battery system and may be responsible for fatal battery failure (fire outbreak). If the battery still works after freezing, the significant change in capacity may be observed. That is why the non-crystallizing electrolytes may be the answer to this important issue.

We should be able to preserve the energy during winter time. The unbroken energy supply chain may be crucial then. The low temperatures at the surface of Earth are very often observed on both poles and in high mountains. Reliable energy source is needed there as well. That is why the electrolyte which works at the temperatures much below 0°C would be a perfect solution to these issues.

Experimental and results

The presented work is about liquid electrolytes and their electrochemical properties. The electrolytes with either $LiPF_6$ (lithium hexafluorophosphate) or LiTDI (lithium 4,5-dicyano-2-(trifluoromethyl)imidazolide) salts will be presented. The selected mixtures of EC:PEG with various chain lengths will be used as the basis for non-crystallizing electrolyte preparation.

The conductivity, cyclic voltammetry, lithium transference number and other electrochemical measurements will be shown. Selected physicochemical properties of solvents and electrolytes will be discussed. The microscopic images of electrodes will be presented and discussed.

These electrolytes exhibit quite high conductivity (above 1 mS cm^{-1} at 20°C). They show relatively high conductivity at temperatures much below 0°C as well. The high electrochemical stability window of these electrolytes is also observed, up to 4.8 V vs. Li.

Acknowledgments

This work was financially supported by Faculty of Chemistry, Warsaw University of Technology.

References

1. M.C. Smart, B.V. Ratnakumar, S. Surampudi, *J. Electrochem. Soc.*, **149(4)**, A361 (2002).
2. M. Kasprzyk, A. Zalewska, L. Niedzicki, A. Bitner, M. Marcinek, W. Wieczorek, *Solid State Ionics*, **308**, 22 (2017).
3. M. Kasprzyk, A. Zalewska, W. Wieczorek, *J. Phys. Chem. C.*, **124(9)**, 5046 (2020).

LiTDI and LiPDI Imidazole Salts for Li-ion Electrolytes – Thermal Stability and Water Scavenging Properties

K. Czyżewski[a], K. Rogala[a], A. Zalewska[a], M. Kasprzyk[a], and L. Niedzicki[a,*]

[a] Faculty of Chemistry, Warsaw University of Technology,
Noakowskiego 3, 00-664 Warszawa, Polska

leszek.niedzicki@pw.edu.pl

Lithium salts LiTDI and LiPDI are investigated for their stability in the water presence. Known for being stable in water solutions and water scavenging, they are also very thermally stable. Here we investigate their behavior in electrolyte upon high water uptake. Thermal stability of the salt and electrolyte, electrode-electrolyte compatibility, electrolyte electrochemical stability and cell properties with water content as high as 20,000 ppm are investigated. It is shown, that LiTDI or LiPDI-based electrolytes and cells are very stable in all aspects up to at least 10,000 ppm, giving very large safety buffer and possibilities towards lowering Li-ion cell manufacturing costs.

Introduction

Li-ion batteries are the backbone of large majority of contemporary fast-responding energy storage and electric automotive field. The European Union and other power players are working on decreasing batteries manufacturing costs, factories costs, etc. One of the important aspects on both raw materials' use as well as manufacturing lines' costs is the need for limiting moisture content in the substrates, components and manufacturing atmosphere. For one, all the materials have to be dried to the single-digit ppm level of trace moisture. It is energy consuming and expensive, increasing price per unit of every component, especially liquid ones, like solvents, but also salts and ready electrodes (tape-casted from the solvent-based paste). Keeping them dry during storage and transport also contributes towards final battery cost. Furthermore, atmosphere during cell assembly needs to be either relatively pure nitrogen/argon or synthetic/dried air with dew point at least below -55°C – level of ca. 20 ppm of water in the air (preferably below -65°C, i.e. 5 ppm). It is not only contributing towards energy consumption and increasing the cost of the battery per unit, but also increases upfront cost of the manufacturing line – at the level of the design of the building containing such a line. Finally, dry atmosphere is making the whole process more complex, as in case of employees it requires short shifts, or it needs fully automated lines and machines adapted to such atmosphere in terms of lubricants, maintenance, but also their emissions.

Lithium imidazolate salts – LiTDI (lithium 4,5-dicyano-2-trifluoromethylimidazolate) and LiPDI (lithium 4,5-dicyano-2-pentafluoroethylimidazolate), has been previously established to be completely stable even in water solutions, as well they have water scavenging function when used as an additive or main electrolyte salt for Li-ion batteries. They have superior parameters to the most common salt in the market, $LiPF_6$, when it comes to thermal stability (1), chemical stability as well as compatibility with new generations of electrodes (2) (3). It was also found that LiTDI/LiPDI have ability to complex water in a stable manner and "dry" other components of the cell from trace moisture. As a result, cells containing LiTDI have been found to have capacity retention up to 2-3 times longer than cells without them – be it as an additive to $LiPF_6$ or main salt (4).

What has not been investigated so far, is how the electrolyte and cell behave after a long time of scavenging water by LiTDI/LiPDI. What parameters are changing and how it may affect the functional parameters, safety and performance of the cell was the focus of the investigation in this work.

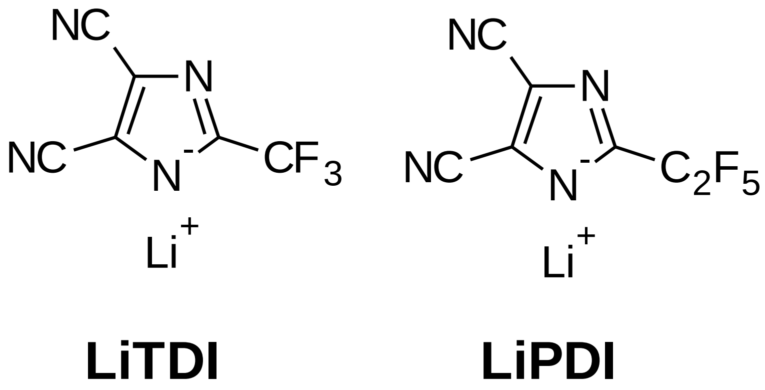

Figure 1. *LiTDI and LiPDI salt semi-structural formulae.*

Results and Discussion

In order to investigate long-term water scavenging, water has been added to the electrolyte in known amounts – measured by Karl Fischer titration. The raw salt containing ca. 300-400 ppm was used as a reference point – purposedly not dried to the battery level grade, which would be below 20 ppm. Such raw salt has been dissolved in typical battery grade solvents (ca. 20 ppm water content), as well as main sample solutions were made to be 5,000, 10,000 and 20,000 ppm water content, roughly equal to 2:1, 1:1 and 1:2 ratios between salt and water, respectively.

In the presented work, the investigation of the water content influence on thermal stability by means of differential scanning calorimetry DSC and on electrochemical stability by means of linear sweep voltammetry LSV and cyclic voltammetry CV of the salt and electrolyte has been performed. Electrolyte-electrode compatibility by means of CV and chemical stability of the electrolyte by means of electrochemical impedance spectroscopy EIS long-term study of the lithium metal contact with electrolyte have been established. Electrolyte conductivity changes have been also tested. All abovementioned results will be shown during presentation.

Conclusions

Results of the investigation have proven that LiTDI/LiPDI-based electrolytes are indeed stable both dry and with high content of the water in the system. Such high amounts of water content (10,000 ppm level) in electrolyte would be impossible to be reached even if standard chemicals (not purposedly dried) be used during manufacturing of components (standard water content of p.a. purity solvents is ca. 500-1000 ppm) and then during the cell assembly under air atmosphere, even if all of it would be scavenged by the electrolyte (LiTDI). Thus, designing new battery factories using LiTDI as a main electrolyte could possibly gain a lot of savings during construction and equipment installation. Also, using this approach requirements towards materials for battery manufacturing could be decreased, resulting in much cheaper manufacturing.

Acknowledgments

This work has been funded by the Warsaw University of Technology.

References

1. L. Niedzicki, S. Grugeon, S. Laruelle, P. Judeinstein, M. Bukowska, J. Prejzner, P. Szczecinski, W. Wieczorek, and M. Armand, *J. Power Sources*, **196**, 8696 (2011).
2. L. Niedzicki, B. Brzozowski, and P. Wieczorek, *Electrochim. Acta*, **174**, 625 (2015).
3. F. Lindgren, C. Xu, L. Niedzicki, M. Marcinek, T. Gustafsson, F. Björefors, K. Edström, and R. Younesi, *ACS Appl. Mater. Interfaces*, **8**, 15758 (2016).
4. M. Armand, P. Johansson, M. Bukowska, P. Szczecinski, L. Niedzicki, M. Marcinek, M. Dranka, J. Zachara, G. Zukowska, M. Marczewski, G. Schmidt, and W. Wieczorek, *J. Electrochem. Soc.*, **167**, 070562 (2020).

Particle Engineering Strategies for Improving the Electrochemical Performance of Lithium-Ion Batteries

Moustafa M.S. Sanad*

*Central Metallurgical Research and Development Institute, (CMRDI) P.O. Box 87, Helwan, Cairo, Egypt

Email: mustafa_sanad2002@yahoo.com, Mobile: 01068320472

Abstract: The worsening of energy supply crisis and the exacerbation of climate change by environmental pollution problems have become the greatest threats on the human life. One of the ways to confront these problems is to rely on renewable energy and its storage systems. Nowadays, huge attentions have been directed to the development of lithium ion batteries (LIBs) as efficient tools for storing the clean energy produced by green sources like solar and wind energies. Accordingly, the demand powerful electrode materials with excellent electrochemical characteristics has been progressively increased to meet fast and continuous growth in the market of energy storage systems. Therefore, developing and engineering highly active electrode materials for rechargeable lithium-ion batteries (LIBs) attracts the attention of scientists and engineers. However, capacity fading, low thermal stability and low capacity retention upon long-term cycling are being the most serious problems facing lithium-ion batteries (LIBs). The intended presentation will demonstrate the new insights and effective ways for enhancing the electrical conductivity and improving the electrochemical performance of Li-ion batteries (LIBs). Besides, the utilization of structural and spectroscopic analyses (e.g. XRD, FESEM, HRTEM, and XPS) for monitoring the changes in the physicochemical properties of electrode materials will be highlighted. Finally, the enhancement in the electrochemical properties of different cathode/anode materials will be discussed through Galvanostatic Cycling (GC), Cyclic Voltammetry (CV) and Electrochemical Impedance Spectroscopy (EIS) technique.

Key words: Structure modification; Particles morphology;, Anode/cathode materials; Lithium-ion Batteries

Regeneration of used batteries from electric vehicles – chemical and electrochemical investigation

Andrea Straková Fedorková[1*], Natália Podrojková[1], Renáta Oriňaková[1], Peter Drgoňa[2]

[1]Institute of Chemistry, Faculty of Science, P.J. Šafárik University, Moyzesova 11,

SK-04154 Košice, Slovak Republic

[2]ZTS – VÝSKUM A VÝVOJ, a.s., Lieskovec 598/75, 018 41 Dubnica nad Váhom,
Slovak Republic

Abstract

The European Commission is totally committed to face the biggest challenge of the today's world: the Climate Change. Thus, a significant number of initiatives and changes have been proposed to achieve a climate-neutral Europe by 2050 The different mobility modes (road, waterborne, airborne, rail) together represent around 25% of total CO_2 emissions in the EU. Significant efforts have led to efficiency improvements (for example, the average emissions from new passenger cars, measured in g [CO_2]/km, decreased by 30% between 2000 and 2018). However, mobility demand continues to grow, and the sector remains the only one that has not been able to reduce its CO_2 emissions (the EU transport emissions have increased by around 20% compared to 1990 levels, while the EU total emissions have decreased by around 20% in the same period). Batteries are playing an increasingly important role in decarbonising light-duty transport (in particular, passenger cars and vans, which represents around 50% of current EU transport sector CO_2 emissions). 2nd life fatteries can also contribute to the decarbonisation of stationary applications.

In this study we are representing electrochemical and chemical analysis of second life batteries from different cars as Toyota and VW.

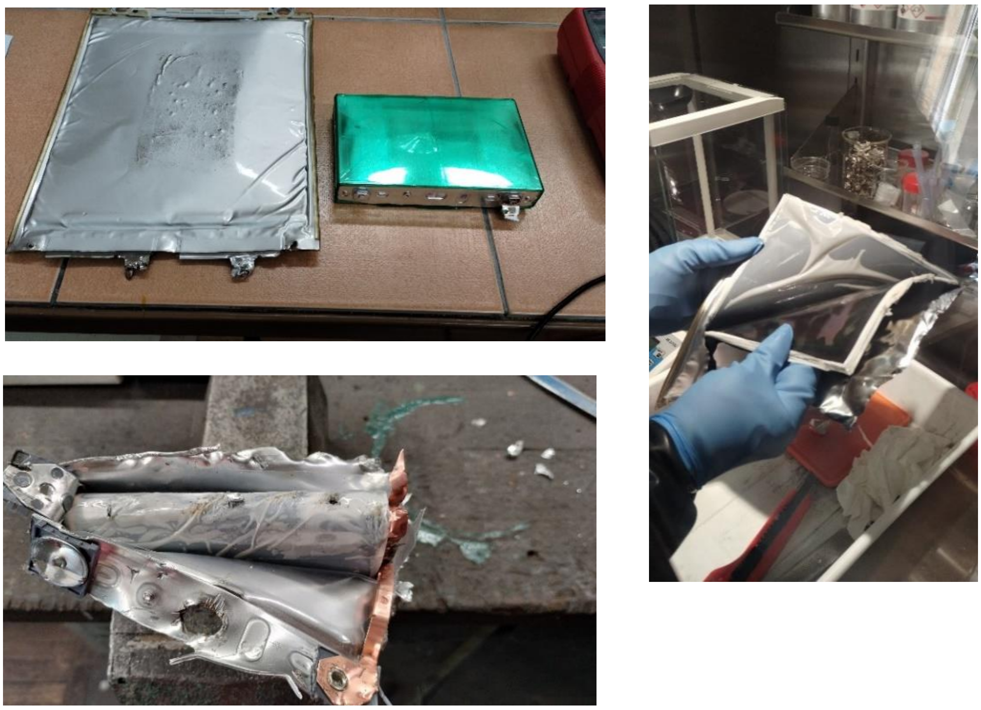

Figure 1. *Batteries from Toyota (silver A4 format) and VW (green prismatic format).*

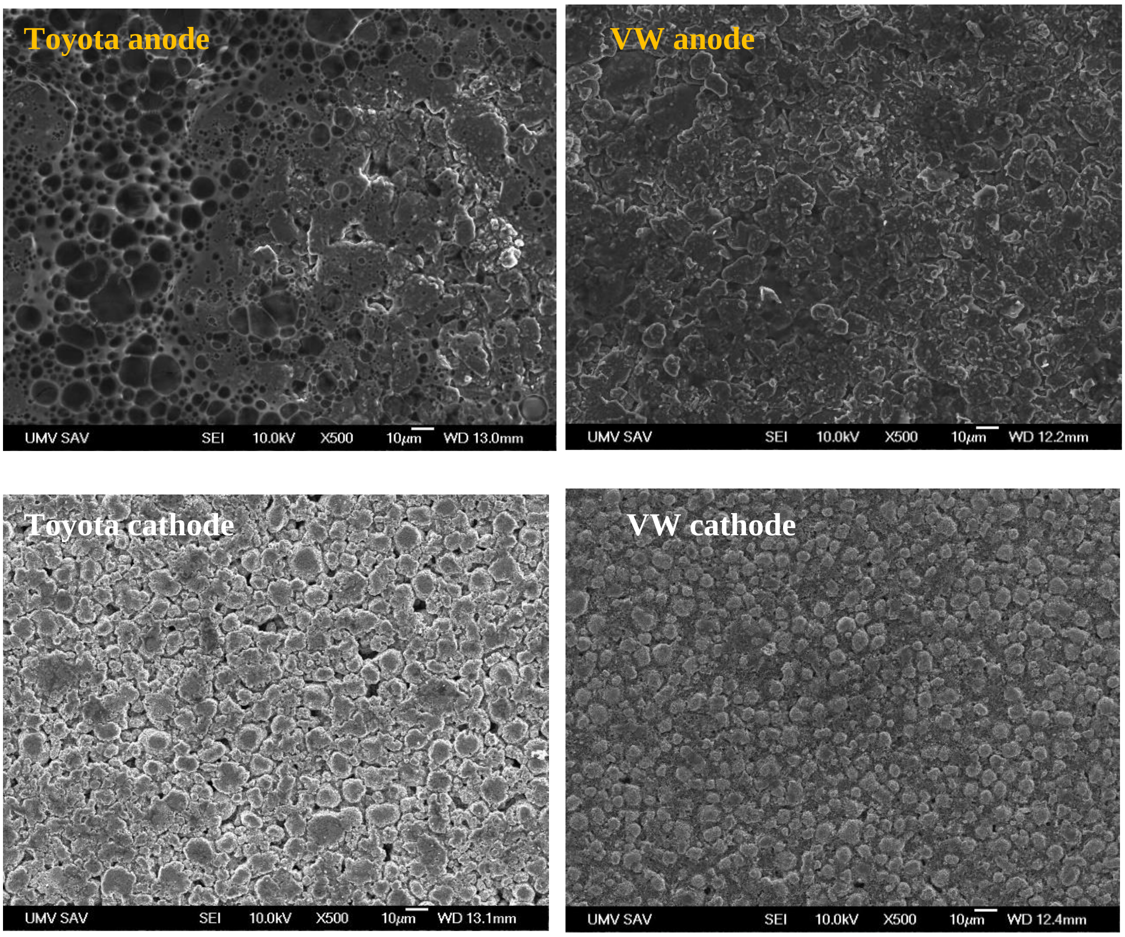

Figure 2. *SEM images of anodes and cathodes from Toyota and VW batteries.*

It is clearly visible that cathode and anode from VW is more homogeneous, and distribution of particles and porosity is better in comparison with materials from Toyota. This observation was also confirmed by EIS measurements. For Toyota batteries we can observe a higher value of resistances. The semicircle at high frequency can be ascribed to the electrolyte resistance and the surface film impedance, and the semicircle at lower frequency can be ascribed to the lithium-intercalation process (Fig. 3). It should be mentioned that the constant phase element (CPE) has been introduced in equivalent circuit instead of pure capacitive element for measurement fitting. We can observe higher charge transfer resistance for batteries from Toyota what is in agreement with SEM analysis and surface inhomogeneities observations.

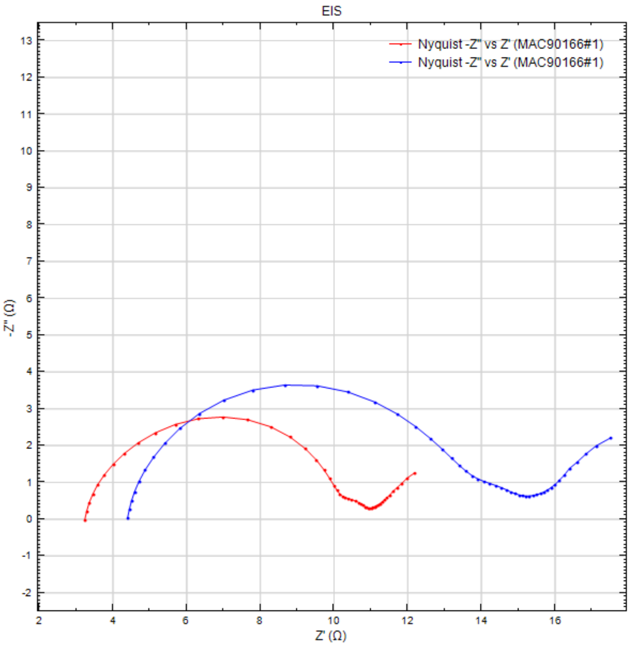

Figure 3. *EIS Nyquist plots for batteries from Toyota (blue line) and VW (red line).*

Acknowledgement

This research was sponsored by the APVV-20-0138, APVV-20-0111, iCoTS project ITMS No. 313011V334 and by the Operational Programme Integrated Infrastructure for the project: Regeneration of used batteries from electric vehicles, ITMS2014+: 313012BUN5, which is part of the Important Project of Common European Interest (IPCEI), called European Battery Innovation in the Operational Program Integrated Infrastructure, call code: OPII-MH/DP/2021/9.5-34, co-financed from the resources of the European Regional Development Fund.

LNMO/LFP blended cathode materials for lithium-ion batteries

Daniele Versaci,[1] Roberto Colombo,[1] Giorgio Montinaro,[1] Julia Amici,[1] Mihaela Buga,[2] Carlotta Francia,[1] Silvia Bodoardo[1]

[1] Electrochemistry Group, Department of Applied Science and Technology (DISAT), Politecnico di Torino, Corso Duca degli Abruzzi, 24, 10129 Torino, Italy

[2] National Research and Development Institute for Cryogenic and Isotopic Technologies – ICSI Rm. Valcea, 240002, Romania

e-mail presenting author: daniele.versaci@polito.it

Electrochemical energy-storage systems, such as lithium-ion batteries (LiBs), have turned out to be the most prevalent technology for a wide range of devices, from small electronics to stationary energy storage applications, and electric mobility. However, to meet the ever-increasing market demand, significant effort is still needed in order to develop batteries with better performance in terms of power and energy density.

In this frame, cathode materials completely cobalt-free and operating at high voltage (e.g. 4.75 V), such as LNMO (lithium nickel manganese oxide – $LiNi_{0.5}Mn_{1.5}O_4$) are particularly interesting and potentially able to increase the electrochemical performance of next-generation high-energy-density LiBs [1].

Unfortunately, LNMO still suffers of some drawbacks such as easy cation leaching during cycling (in particular at high C-rate) and electrolyte decomposition at high voltage. Therefore, one possible approach to mitigate these issues, increasing the safety of the system, the lifetime, and limiting the cost, is using blended electrodes, containing multiple types of active materials.

In the present work, within HYDRA H2020 project, the influence of LFP (lithium iron phosphate – $LiFePO_4$) physically mixed with LMNO was studied both from morphological and electrochemical point of view. LFP was chosen because of its outstanding thermal and electrochemical stability, and its influence on the electrochemical performances of the cathodes, such as cycling performances, lifetime and safety. The role of LFP was studied changing its amount inside the cathode formulation and the electrochemical properties were evaluated both in half-cell and full-cell configuration.

In particular, the simple and up-scalable physical blending, by resonant acoustic mixing (RAM) technique, provided a good distribution of LFP and LNMO particles, resulting in increased electrochemical performances. The blended LNMO/LFP cathode was able to deliver a specific capacity higher than 125 mAh g^{-1} at C/10 and a capacity retention higher than 80% after 1000 cycles at 1C vs. lithium. Analogously, the blended electrode shows a capacity retention close to 74% after 100 cycles in full-cell configuration (vs. graphite), almost 30% higher than the pure LNMO cathode.

Acknowledgments

Authors kindly acknowledge Hydra project (Horizon 2020 innovation program under Grant agreement number: 875527) for funding.

References

1. Chen et al. *ChemElectroChem* **2021**, 8, 608

Smart Functionalities Meet Batteries Under Battery 2030+: Embedding Self-Healing Binder in Advanced Li-Ion Batteries

K. B. Dermenci[a], P. K. Dammala[a], J. V. Mierlo[a], M. Berecibar[a]

[a] Electromobility Research Centre, Vrije Universiteit Brussel, Pleinlaan 2, 1050, Brussels, Belgium

Achieving the best performance from the batteries requires particular attention in the battery assembly processes. Each battery component such as anode, cathode, electrolyte and separator are being manipulated to boost the performance of the batteries. Next-generation batteries target energy density values of more than 350 Wh/kg and more sustainable, abundant, easy-to-recycle battery components with improved safety are aimed to be integrated. In this sense, working with next-generation battery components generates unforeseen challenges to be tackled during battery manufacturing processes. EU-funded BAT4EVER project under Battery 2030+ CSA is aiming to boost the performance of the batteries having Si-containing anodes thanks to the integration of self-healing binder in combination with safer ionic liquid electrolytes. This study concentrates on the battery manufacturing process development from the ionic liquid electrolyte perspective to obtain the best possible performance in terms of short-term and long-term capacity retention.

Introduction

Li-ion batteries (LIBs) span a number of diverse application areas extending from devices of Industry 4.0 and private households including mobile and smart household equipment, for decentralized smart grids, e-vehicles, public city transport, drones for consumer use and security/defense and public protection, as well as in Internet of Things (IoT) applications regarding digitalization driven systems and for electronics such as smartphones, smartwatches, tablets, digital cameras, media players [1-2]. These applications require safe and sustainable systems such as no danger of explosion and leakage, as well as longer cycle life and durability.

Silicon anodes offer a promising alternative to graphite anodes with their abundance, high theoretical capacity and high working potential making the cells suitable for high-energy and power applications. However, silicon is prone to failure mechanisms because of drastic volumetric changes which lead to particle pulverization and uncontrolled SEI formation over cycles [3]. Self-healing binders have been investigated quite recently to maintain the overall electrode integrity against extensive volume changes during the operation of the cells. Thanks to the self-healing mechanism triggered by internal mechanical stresses generated during the operation of the cells, broken polymeric binder chains will be recovered limiting the degradation caused by particle pulverization and total loss of active material [4].

Electrolytes play an important role to maintain the performance of the cells in a longer period. Commercially available Li-ion Batteries (LIBs) for consumer electronic devices and electric vehicles are using organic liquid electrolytes, that are composed of organic solvents such as EC, DEC and Li-salts such as $LiPF_6$ and LiTFSI. However, they are toxic and harmful to the environment limiting their widespread use. Besides, they generally require SEI stabilizing agents such as FEC while working with Si-based anodes that result in practical challenges such as reduced shelf-life [5]. In this regard, ionic liquids are considered an important replacement for conventional electrolytes that can exploit the use of novel battery chemistries including Si-based systems [6].

BAT4EVER project targets the development and optimization of self-healing functionalized high energy density, high voltage and long-term stable next-generation LIBs. It offers novel battery chemistries comprising self-healing binders, ionic liquids, Si/C anodes as well as tailored core-shell structured NMC cathodes to achieve its ambitious targets supported by multiscale modeling. BAT4EVER also establishes a structured understanding of upscalability up to 2Ah battery fabrication thanks to the battery manufacturing process development [7]. Figure 1 summarizes the BAT4EVER approach to implement self-healing functionalities to Si anodes.

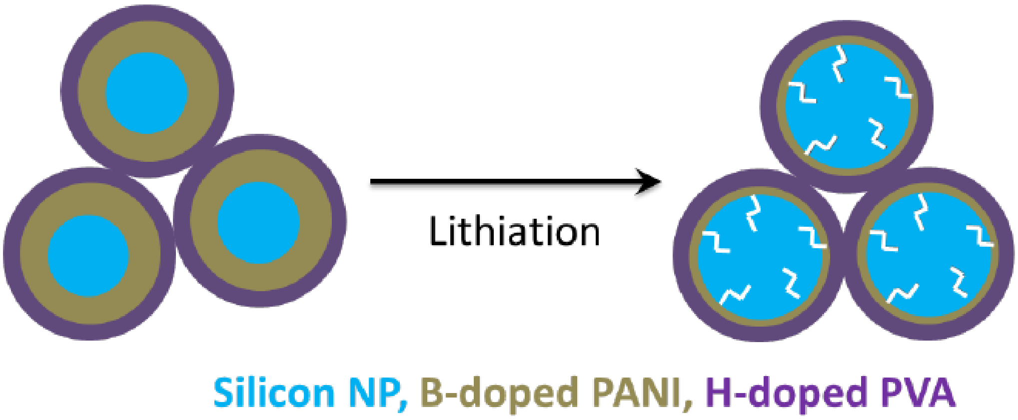

Figure 1. *BAT4EVER approach to implement self-healing functionalities to the Si anodes*

In this study, parameters investigated to understand battery manufacturing processes with the batteries having ionic liquid will be discussed. It concerns the electrochemical stability of the ionic liquid that is going to be used within the BAT4EVER project from single-layer NMC-Graphite pouch cells. Then, the appropriate separator type will be assessed. Finally, battery formation conditions (such as formation cycle number, cut-off voltages and C-rate) will be revisited to obtain the highest possible battery performance. In the end, know-how developed in view to build large capacity cells having ionic liquids as electrolytes will be presented from the battery manufacturing process conditions perspective.

Methodology

The chemical formula of the ionic liquid used is 1.3M LiTFSI in 1-methyl-1-propylpyrrolidinium bis(trifluoromethylsulfonyl)imide (IOLITEC). In order to evaluate the electrochemical stability window, Linear Sweep Voltammetry (LSV) is firstly applied between the voltage range of 0-6V. Then, single-layer pouch cells having a nominal capacity of 40 mAh are assembled in order to investigate the factors affecting the battery performance unless stated otherwise. Here, ionic liquids are tested with three different types of separators namely, polypropylene (PP), Polyamid (PA) and glass fiber (GF). Pre-coated NMC532 and Graphite sheets were purchased from NEI Corp. As-prepared cells are subjected to a formation cycle. The main parameters investigated are ionic liquid loading, cut-off voltages, number of cycles and C-rate.

Acknowledgments

This research has received funding from the European Union's Horizon 2020 research and innovation programme under Grant Agreement No. 957225, project BAT4EVER. Authors would like to thank IOLITEC for providing the ionic liquids used in this research.

References

1. Pech-Rodríguez, W. J., Rocha-Rangel, E., Armendáriz-Mireles, E. N., Suarez-Velázquez, G. G., & Ordóñez, L. C., In *Innovation and Competitiveness in Industry 4.0 Based on Intelligent Systems* (pp. 175-195). Cham: Springer International Publishing (2023).
2. Correia, V., Costa, C. M., & Lanceros-Méndez, S, *Sustainable Energy Storage in the Scope of Circular Economy: Advanced Materials and Device Design*, 291-306. (2023).
3. Liu, Y., Shao, R., Jiang, R., Song, X., Jin, Z., & Sun, L., *Nano Research*, **16** (2023).
4. Chen, H., Wu, Z., Su, Z., Chen, S., Yan, C., Al-Mamun, M., ... & Zhang, S., *Nano Energy*, **81** (2021).
5. Etacheri, V., Haik, O., Goffer, Y., Roberts, G. A., Stefan, I. C., Fasching, R., & Aurbach, D., *Langmuir*, **28** (1), (2012).
6. Lewandowski, A., & Świderska-Mocek, A., *Journal of Power sources*, **194**(2) (2009).
7. www.bat4ever.eu

Development of advanced next generation solid-state batteries for electromobility applications: presentation of the ADVAGEN project

J. Amici[i], D. Dessantis[j], D. Ferrero[j], M. Santarelli[j], C. Francia[i], S. Bodoardo[i]

[i] Electrochemistry Group, DISAT, Politecnico di Torino, c.so D.ca degli Abruzzi 24, 10129 Torino, Italy

[j] STEPS Group, DENERG, Politecnico di Torino, c.so D.ca degli Abruzzi 24, 10129 Torino, Italy

e-mail presenting author: julia.amici@polito.it

To date, the battery market is dominated by lithium-ion (Li-ion) chemistries, as the energy density has more than doubled and their costs have dropped by a factor of at least 10. However, conventional Li-ion batteries are reaching their performance limits in terms of energy density and additional features are needed to ensure safe batteries. Therefore, new battery generations are required, such as Solid-State Batteries (SSBs), as well as the creation of a new industry value chain in Europe towards their commercialization. To do so, the development and deployment of new manufacturing technologies, enabling the large-scale production of SSBs, is crucial.

Thus, it is key to develop next solid-state battery generations with innovative and scalable manufacturing techniques to accelerate cost reduction, energy savings, and enhanced safety and enable its implementation in commercial applications

The ADVAGEN project is doing so by developing a novel lithium metal (LiM) battery cell technology, based on high performing hybrid solid-state electrolyte (oxide-sulfide based), which will be safer and more reliable. Therefore, the aim is to gain a technological advantage over the current world market, especially Asian competition, hence sustainably strengthening the EU as a technological and manufacturing leader in batteries.

The main objective of ADVAGEN is to develop, manufacture and validate the most performant, stable, and safe 10Ah solid-state pouch cells, by developing novel materials for each of the parts that constitute a battery (i.e., the electrolyte, anode and cathode). In particular, the focus is on an innovative hybrid oxide-sulfide ceramic electrolyte to be integrated with a lithium metal anode and a high Ni-rich content-based cathode.

Given that the ADVAGEN consortium covers the full battery value chain, it is in an excellent position to successfully conceive significant battery developments, as well as to adequately produce and test these results in a small scale and ramp up to production to find a use case in the EV industry. Moreover, the recycling process developed for the ADVAGEN solid-state batteries aims at developing a circular economy approach.

The developed technology within the ADVAGEN project aims to have impacts at different levels.First, towards increasing global competitiveness of the European battery ecosystem through generated knowledge and leading-edge technologies in battery materials, cell design, manufacturing and recycling. Then, towards accelerating the growth of innovative, competitive, and sustainable battery manufacturing industry in Europe, and speeding up the spreading of electrified mobility through increased attractiveness for citizens and businesses, offering lower prices, better performance and safety. Last but not least, towards increasing grid flexibility, increasing share of renewables integration, and facilitated self-consumption and participation in energy markets by citizens and businesses, as well as increasing the overall sustainability and improved Life Cycle Assessment of each segment of the battery value chain.

This project has received funding from the European Union’s Horizon Europe research and innovation programme under grant agreement No. 101069743 (ADVAGEN).

The analysis of the conversion of thin-layer SiO_2 in the redox reaction with lithium

R.D. Apostolova, E.M. Shembel

SHEI Ukrainian State University of Chemical Technology, Dnipro, 49005, Ukraine

This presentation focuses on the analysis of the conversion of thin-layer SiO_2 dioxide in the redox reaction with lithium.

Our analysis of discharge-charge curves and cyclic voltammograms of SiO_2 in redox reactions with lithium shows the distribution of materials into two groups (fig. 1a, 1b).

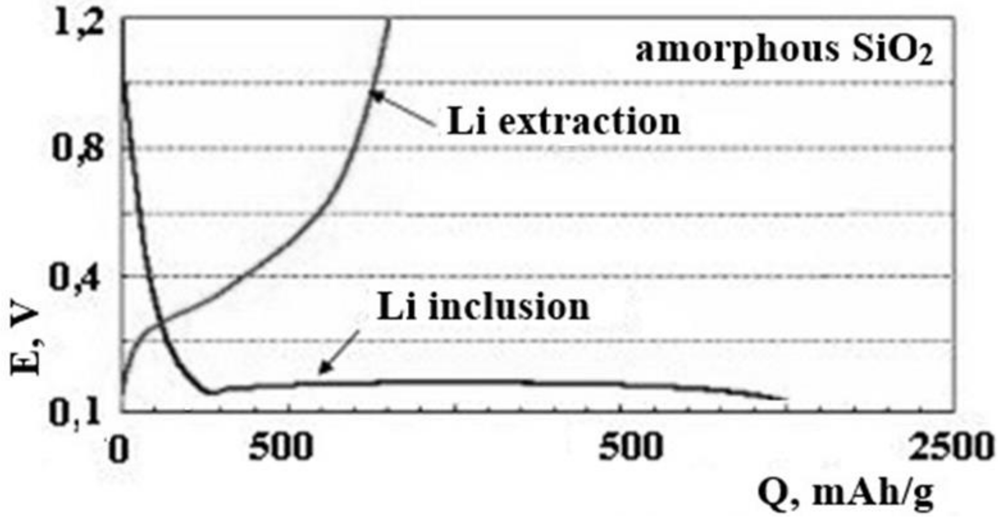

Fig. 1a *– Typical possible profile of the curves for groups 1*

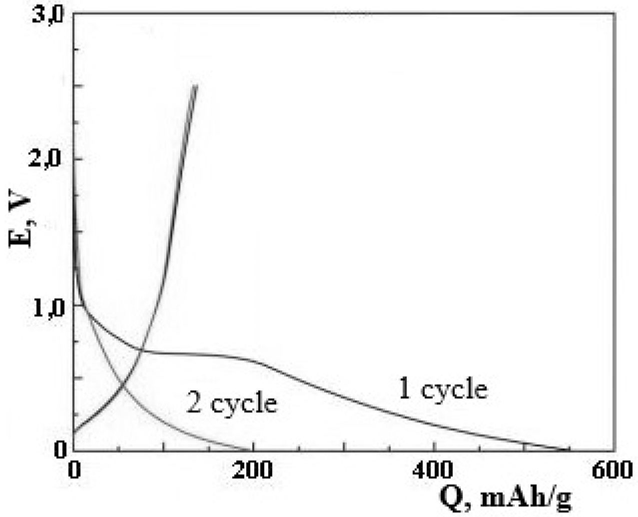

Fig. 1b*– Typical possible profile of the curves for groups 2*

In the first group, the electrode process continues mainly in the region of low potentials - below 0.4 V relative to the Li^+ / Li electrode – Fig.1a (see [1-3, etc).

In the second group, along with the characteristics of low-voltage conversion, the electrode is also transformed within higher values of the potentials of the electrode, clearly expressed in [4-8, etc.], the profile of the recovery curves which can be similar to Fig. 1b.

Silicon and silicon oxide compounds are considered as a promising family of materials for high-energy lithium batteries (LB), due to their high theoretical capacity, widespread in nature, low cost, environmental safety, ease of synthesis. Silicon oxide compounds SiO, SiO_2, SiO_x, and SiOC have replaced silicon in the hope of improving the discharge characteristics of LB. Oxides of SiO and SiO_x are closest to commercialization. Significant volume expansion and irreversible loss of capacity of silicon oxides during cycling in the initial cycles are an obstacle to their large-scale practical use. SiO_2 dioxide is more resistant to bulk expansion than silicon. Various structural formats of nanometer SiO_2 have been developed and tested for lithium batteries such as nanotubes, nanorods, nanowires, nanoparticles, thin films.

A significant number of studies of SiO_2 and Si have been conducted using modern instrumental methods and it has been determined that the reduction processes at potentials of 0.90-0.65 V relate to the decomposition of the electrolyte with the formation of the SEI surface film. Si, Li_2O, Li_xSi silicates are formed after reaching a potential below 0.5–0.4 V. However, the interpretation of the mechanism of the obtained curves by different authors is ambiguous and sometimes does not coincide with the proposed and experimentally confirmed mechanism. Thus, with the interpretation of the results of the study of the thin-film composite SiO_2 / Ni [4] may not agree. The reduction process of SiO_2 / Ni at 1.4 V is described by the interaction of silicon dioxide with lithium with the formation of $Li_2Si_2O_5$, Li_2O, Li_4SiO_4. In [2], in the case of electrolytically encapsulated silicon dioxide with nickel, similar processes were observed around 1.4 and 0.75 V. A separate study of the nickel base in the electrochemical interaction with lithium was conducted. A method for the synthesis of a thin-layer composite SiO_2 / Ni electrode is proposed, in which amorphous nanometer silicon dioxide obtained by the method of sulfuric acid deposition is enclosed in a nickel matrix for efficient use in negative electrodes of lithium-ion film battery [2]. The synthesized SiO_2 was used for galvanic production of a thin-layer SiO_2 / Ni composite on the cathode of nickel foil with a nickel anode. The cathode was placed horizontally and a suspension of SiO_2 in the electrolyte for nickel plating with thorough stirring was poured into the cell. After 5-20 minutes, during which SiO_2 particles sedimented on a nickel base, the current was turned on for a specified time. The composition of the electrolyte for the deposition of the composite, g^{-L}: $NiSO4 \cdot 7\ H_2O$ – 150; $Na_2SO_4 \cdot 5\ H_2O$ - 25; H_3BO_3 – 15; KCl –10; SiO_2 – 2; pH 5 ÷ 6. $S_{cathode}$: S_{anode} = 1: 20; $i_{cathode}$ = 1.5-2.0 $mA \cdot cm^{-2}$. Heat treatment: 105 ° C, 6-7 h. The size of the synthesized particles is mostly 12-16 nm and does not exceed 22 nm. Discharge-charging curves of the synthesized electrode in the model Li-battery in dimensions CR2016 with electrolyte dimethoxyethane (DME, Merck), dioxolane (DOL, Acros), 1 $mol \cdot^{-L}$ $LiBF_4$ depend on the duration of sedimentation of silica on the Ni-base, which determines its mass in the sediment. At a duration of 5 minutes the starting discharge curve changes monotonically within the voltage of 1.20–0.05 V. At a duration of 15-20 minutes the discharge curve consists of two sections - horizontally inclined within 1.4-1.2 V and purely horizontal – within 0.25-0.35 V at a current density of 20-100 $\mu A\ cm^{-2}$ (Fig. 2). The participation of nickel oxides that exist on the surface of nickel in the redox reaction with lithium was shown. The authors [2] identified the process at the peak position of 1.4 V in a thin-layer a-SiO_2 / Ni composite as a process of reducing Ni-oxide film on the surface of the nickel base of the electrode. The reduction of the Ni-oxide film is damaged and becomes irreversible in the second cycle. In addition, the reaction of formation of lithium silicate $Li_2Si_2O_5$ at the beginning of the cycling of silicon dioxide is considered to be the opposite in many studies, and it occurs at potentials below 0.4-0.5 V relative to Li^+ / Li.

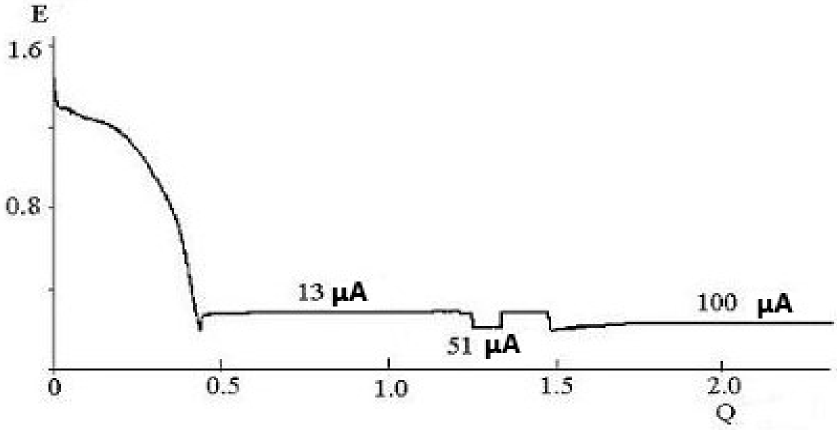

Fig.2 *– Changing the profile of the discharge curve SiO_2 / Ni with a change in current density*

The question arises how to explain the difference in the electrochemical behavior of samples from group 1 and group 2. It should be sought in the experimental conditions. In the case of group 1, the method of obtaining the studied silicon dioxide by grinding in an energy-intensive ball mill without contact with the electrolyte [1, 3] and the method of encapsulating silicon dioxide with nickel [2] were used. These methods allow to limit the negative impact of the electrolyte with contamination of the interface of silicon dioxide with impurities. SiO_2 samples from group 2 were obtained by methods that continue in bulk electrolyte solution. A significant share of irreversible processes of conversion of silicon dioxide with lithium is due to side processes occurring on the electrode surface with oxide film, sensitive to impurities from electrolyte and silicon dioxide contaminated with electrolyte as a result of adsorption, ion exchange and other processes.

The efficiency of electrochemical conversion of the electrode material is known to be determined by the processes associated with the SEI surface film and the retention of lithium ions in the space of the electrode. The difference between the lithium characteristics of the SiO_2 samples of the two groups is due to the different behavior of the SEI film. It is formed in the first cycle with inefficient energy consumption, due to which the discharge capacity of the current source SiO_2 / Li can be lost by almost 50%. Such a significant loss is not observed in the group of amorphous dioxides a-SiO_2, which was obtained by grinding in a ball mill. It is known that the electrode materials synthesized in the ball mill are less contaminated with impurities than synthesized in solutions. Similarly, the encapsulation of nickel by silica synthesized by electrolysis reduces the expected contamination due to the limited contact of SiO_2 with the bulk electrolyte.

In the synthesis of silica in solutions, the possibility of contamination of the final product increases due to adsorption processes, especially when using several reagents in multi-stage synthesis technology. Unfortunately, the lack of control of the synthesized material for purity makes it difficult to identify the causes of degradation of the lithium process and further recommendations. It is necessary to systematize the experimental material in the main areas of study of the qualities of silica obtained by different methods.

In studies of too thin silica films, the authors did not pay attention to the preparation of the electrode substrate and it is not about cleaning the surface. For research in thin films, there are many methods of surface cleaning. The authors sometimes take side processes on the surface of the thin-walled substrate as a significant main electrode process.

When comparing the electrochemical characteristics of silica of different formats, a clear advantage is not observed. The lithium characteristics obtained by different authors by the same method differ. In addition, cycling results are not easy to evaluate when they are obtained at different current densities with different number of cycles.

Some of our comments made in the presentation can be taken as recommendations for improving the performance of silicon dioxide in LB.

References

1. Chang W.-S., Park C.-M., Kim J.-H., Kim Y.-U., Jeong G, Sohn H.-J. Quartz (SiO_2): a new energy storage anode material for Li-ion batteries. *Energy & Environ. Sci*. 2012. 5: 6895.
2. Apostolova RD, Matzievskii NA, Gladun VA, Savchenko MO. Thin-layer electrochemically produced SiO_2/Ni composites in a prototyping lithium-ion battery. *Surf Engin Appl Electrochem*. 2018; 54: 420.
3. Yamamura H, Nobuhara K, Nakanishi S, Iba H, Okada S. Investigation of the irreversible reaction mechanism and the reactive trigger on SiO anode material for lithium-ion battery. *Journal of the Ceramic Society of Japan*. 2011; 119 (110): 855.
4. Sun Q, Zhang B, Fu ZW. Lithium electrochemistry of SiO_2 thin film electrode for lithium-ion batteries. *Appl Surf Sci*. 2008; 254: 3774.
5. Favors Z, Wang W, Bay HH, George A, Ozkan M, Cengiz S, Ozkan C. Stable cycling of SiO_2 nanotubes as high-performance anodes for lithium-ion batteries. *Sci. Rep.* 2014; 4: 4605.
6. Sasidharan M., Liu D, Gunawardhana N, Yoshio M, Nakashima K. Synthesis, characterization and application for lithium-ion rechargeable batteries of hollow silica nanospheres. *Journal of Materials Chemistry*. 2011; 13881.
7. Hao S, Wang Z, Chen L. Amorphous SiO_2 in tunnel-structured mesoporous carbon and its anode performance in Li-ion batteries// *Materials* &. *Designs* 2016; 111: 616.
8. Tang C, Liu Y, Xu C, Zhu J, Wei X, Zhou L, He L, Yang W, Mai L. Ultrafine nickel-nanoparticle-enabled SiO_2 hierarchical hollow spheres for high-performance lithium storage. *Adv. Funct. Mater.* 2017; 28: 1704561.

Effect of pressing pressure on the capacity of recycled graphite anode

Jiří Báňa[1], Tomáš Kazda[1]

[1]Department Of Electrical and Electronic Technology, University of Technology Brno,
Czech Republic

With the ever-increasing consumption of lithium-ion batteries (LIBs), there is a need for an efficient and environmentally friendly method to recycle the batteries. Graphite, as a widely available and cheap material, does not receive as much attention in recycling as other materials, especially precious metals. The direct recycling method of graphite is an environmentally friendly and economically inexpensive operation. However, the resulting capacity of recycled graphite depends on many factors. One of these factors may be the pressing pressure.

Introduction

Graphite significantly dominates to the commercial lithium-ion battery (LIB) market due to its superior electrochemical properties and excellent availability. However, graphite is gradually destroyed during cycling. The repeated intercalation and deintercalation of lithium ions from the graphite anode causes the graphite to change in volume. The cumulative stress eventually leads to cracking and splitting of the graphite particles. Direct recycling strategies for graphite often focus on removing impurities and restoring its crystal structure.

The first step in repairing used graphite is to remove impurities, including residues of SEI (Solid Electrolyte Interphase), polymer binder, conductive substances, contaminants and metal deposits. Several methods are used to remove impurities, such as heat treatment, chemical treatment, acid treatment and water treatment. (1)

Anode material from a discarded battery also contains significant amounts of lithium. Therefore, recycling the anode can provide a valuable source not only of graphite but also of lithium. For this reason, it is believed that lithium recycling is indispensable. (2)

Experiment

Battery used for this work was commercial Motoma LFP 18650 (1500 mAh) with LFP cathode and graphite anode. Long-term cycling was performed to simulate aging of battery. Cycling was performed by 1C-rate in the range declared by the manufacturer as safe for the cell for a total of 500 cycles. Figure 1 shows capacity fade of Motoma LFP battery. Drop of capacity after 500 cycles was 8.4 % to 1375 mAh. The instruments used for electrochemical testing were a Biologic VMP3 with Booster and a ZKETECH EBC-X cycler.

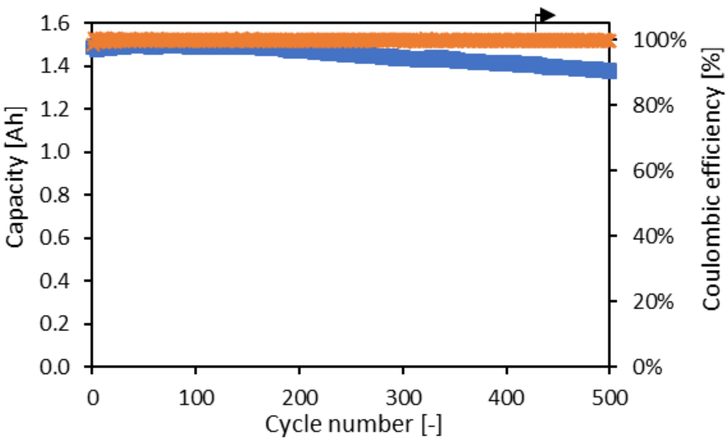

Figure 1. *Capacity fade of Motoma LFP during cycling*

The battery was subsequently dismantled. The anode material (graphite) was separated from the copper collector and weight was measured. Water was used as solvent. The separated graphite was dried and ground. Total graphite content in Motoma LFP was 6.156 g. Therefore, approximate capacity of graphite in Motoma LFP battery was 234 mAh/g after aging. The slurry was made by magnetic stirrer mixing. NMP was used as a solvent. No conductive carbon powder or any other additives were added. The slurry was coated on a copper collector and electrodes were formed, dried for 12h at 60 °C, and then pressed with four different pressures – 1843 N/cm^2, 3840 N/cm^2, 5684 N/cm^2 and 7681 N/cm^2. The fabricated electrodes were used to form electrochemical cells with Li counter electrode. The resulting capacitances for different C-rates are shown in Figure 2.

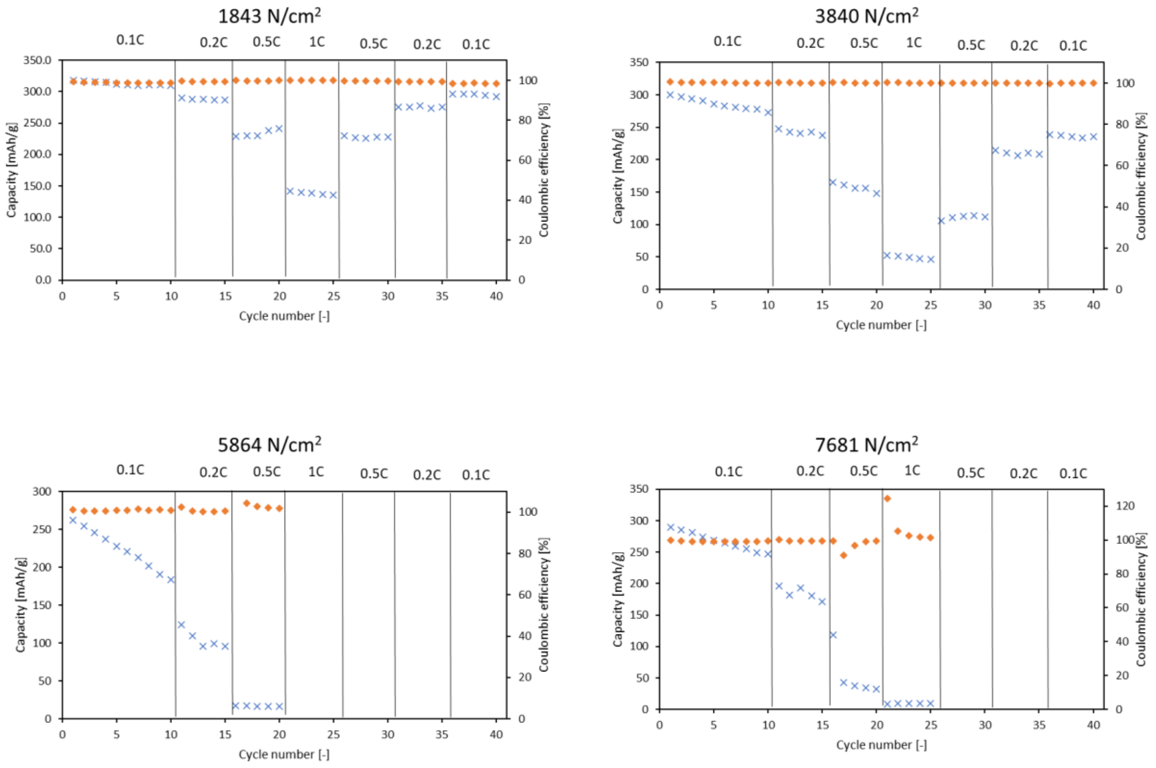

Figure 2. *Capacity of pressing pressures with different C-rates cycling*

As shown in Figure 2, the capacity of the recycled graphite is higher for lower currents than after cycling in the original battery. For a pressing pressure of 1843 N/cm^2, the capacity even exceeds 300 mAh/g. With increasing currents, the capacity gradually decreases for all pressing pressures. For pressing pressure 5684 N/cm^2, the experiment was stopped after 0.5 C and for 7681 N/cm^2, the experiment was stopped after 1 C due to the extreme capacity drop. 1843 N/cm^2 comes out as the best pressing pressure in terms of capacity, pressure 3840 N/cm^2 has higher drops for higher currents, however, for lower currents it competes with 1843 N/cm^2 pressing pressure.

Conclusion

Direct recycling appears to be a suitable method for recycling of spent graphite. Water as anode electrode solvent is a cheap and available resource. Graphite treated in this way, free of impurities, achieves higher capacities than the capacity in the original battery after ageing. Appropriate pressing pressure reduces the differences between C-rates and thus increase the capacity of graphite. Lower pressing pressures proved to be more suitable for achieving higher capacities.

Acknowledgments

This work was supported by the specific graduate research of the Brno University of Technology No. FEKT-S-23-8286.

Bibliography

1. WU, Jiawei, Mengting ZHENG, Tiefeng LIU et al. Direct recovery: A sustainable recycling technology for spent lithium-ion battery. Energy Storage Materials [online]. 2023, 54, 120-134 [cit. 2023-07-18]. ISSN 24058297. Dostupné z: doi:10.1016/j.ensm.2022.09.029
2. LU, Yingqi, Kaiyuan PENG a Lingen ZHANG. Sustainable Recycling of Electrode Materials in Spent Li-Ion Batteries through Direct Regeneration Processes. ACS ES&T Engineering [online]. 2022, 2(4), 586-605 [cit. 2023-07-18]. ISSN 2690-0645. Dostupné z: doi:10.1021/acsestengg.1c00425

Experimental Investigation of Open Circuit Voltage for Lithium-ion Batteries

M. Ceylan[a], A. Balikci[a]

[a] Department of Electronics, Gebze Technical University, Kocaeli, 41400, Turkey

The value of open circuit voltage (OCV) of batteries is a key parameter for state of charge (SoC) estimation. Considering the SoC-OCV curve, the initial SoC can be found by the reciprocal of OCV value as a reference for Coulomb counting during battery operation, and it is crucial for an accurate online SoC estimation algorithm of lithium-ion batteries. The existing methods for the determination of OCV are galvanostatic intermittent titration technique (GITT), which is based on current pulses at different SoC levels, and quasi OCV (qOCV) which is obtained by applying a low discharge current. In this experimental study, the two methods have been investigated at various temperature values and a comparison is provided including entropic effects with respect to operation temperature.

References

1. W. Weppner and R. A. Huggins, Journal of Electrochemical Society. **124** 1569 (1977)
2. K. Takano, Y. Saito, K. Kanari, K. Nozaki, K. Kato, A. Negishi and T. Kato, Journal of Applied Electrochemistry, **32** 251–258 (2002)
3. Q. Zhang and R. E. White, Journal of Power Sources. **173** 2 990-997 (2007)

Lithium-Ion (LCO/NMC, NMC, LFP) Battery Recycling: LCA Study

Michael Fridrich[1], Anna Pražanová[1], Jan Weinzettel[1], Václav Knap[1]

[1] Department of Electrotechnology, Czech Technical University in Prague, Prague, Czech Republic
fridrmi4@fel.cvut.cz

Abstract

As electro automotive industry expands, recycling lithium-ion batteries (LIBs) has become more important today. This work evaluates the environmental impacts (EIs) of recycling different types of automotive LIBs, with black mass (BM) as its output product. EIs were obtained by conducting a gate-to-gate Life Cycle Assessment (LCA) study.

The analysis highlights the benefits of LIBs recycling with a significant recovery yield of secondary aluminum and minor differences in EIs for compared battery types.

Keywords: Material science ● Ecology ● Metals ● Electrotechnology ● Environmental Impacts

Introduction

The increasing number of electric vehicles brings about the necessity of treating waste LIBs. This paper presents an LCA study aimed at evaluating the environmental impacts (EIs) of recycling three different types of lithium-ion batteries (LIBs): Lithium Cobalt Oxide (LCO), Lithium Nickel Manganese Cobalt Oxide (NMC), and Lithium Iron Phosphate (LFP). It focuses on the recycling process, considering black mass as the final output under the conditions of the plant located in the Czech Republic. Black mass represents shredded materials with a significant valuable metal content (such as Co, Mn, or Ni); it is typically used for further specialized metal recovery based on pyro-/hydro-metallurgy recycling methods. [1].

Experimental

The three LIBs types with different material shares (within *anode/cathode active and current collectors materials, electrolyte, separator, and housing*) were compared [2]. In this work, an annual battery mass of 525 tons for recycling was considered. The battery pre-recycling process included the following steps: *discharging*, *dismantling* + *crushing*, *milling*, *sieve separation*, *magnetic separation*, and a *high-temperature furnace* for thermal treatment [3]. The boundaries of the battery recycling system are illustrated in Fig. 1. EIs are evaluated by a detailed gate-to-gate LCA study, which was conducted via SimaPro modeling software using the Ecoinvent database. The results were evaluated by Environmental Footprint (EF) 3.0 life cycle impact assessment method.

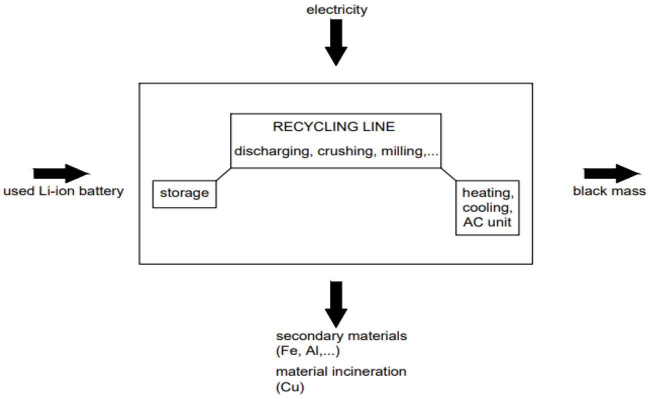

Figure 1. *Recycling system boundaries ● material flows.*

Results and Discussion

The the highest normalized impacts of the system are in EF 3.0 impact categories: Climate Change (-12.9 tons CO_2 eq/ton BM), Acidification (- $0.17 \cdot 10^6$ mol H^+ eq/ton BM), Particulate Matter (-1,4 disease Inc./ton BM), and Resource use − fossil ($-13.6 \cdot 10^6$ MJ/ton BM). The total EIs are negative, which signifies the battery recycling benefits. There is a maximum of 0.3 % nuance between the EIs of each battery type. The main advantages of battery recycling are set for obtaining secondary aluminum.

References

1. Blömeke, S., et al. (2022). Material and energy flow analysis for environmental and economic impact assessment of industrial recycling routes for lithium-ion traction batteries. Journal of Cleaner Production, 377, 134344. https://doi.org/10.1016/j.jclepro.2022.134344
2. Gaines et al. (2011). Paper No. 11-3891 Life-Cycle Analysis for Lithium-Ion Battery Production and Recycling. Transportation Research Board 90th Annual Meeting, Washington, DC.
3. Kwade A., et al. (2018). Recycling of Lithium-Ion Batteries. https://doi.org/10.1007/978-3-319-70572-9

$LiFe_{0.05}Mn_{1.95}O_4$ as a high-rate cathode material for lithium-ion batteries

N. I. Globa[a], Yu. V. Shmatok[a], V. A. Sirosh[a], I. V. Romanova[b], S. A. Kirillov[a]

[a] Joint Department of Electrochemical Energy Systems of the NAS of Ukraine,
38A Vernadsky Ave., Kyiv 03680, Ukraine

[b] Institute for Sorption and Problems of Endoecology of the NAS of Ukraine
13 Gen. Naumov St., Kyiv 03164, Ukraine

Fe-doped lithium-manganese spinel of the composition $LiFe_{0.05}Mn_{1.95}O_4$ was synthesized by means of a citric acid aided route. The influence of annealing temperature on structural and morphological characteristics $LiFe_{0.05}Mn_{1.95}O_4$ is investigated by XRD and SEM methods. Specific and kinetic electrochemical characteristics of $LiFe_{0.05}Mn_{1.95}O_4$ in aprotic and aqueous electrolyte solutions were studied by galvanostatic cycling method, cyclic voltammetry and impedance spectroscopy. $LiFe_{0.05}Mn_{1.95}O_4$ samples annealed at temperatures of 700, 750 and 800 °C demonstrate specific capacity of 114, 102 and 109 mAh/g at the cycling current density of 0.5 C, respectively. The best cycling stability and rate performance with discharge currents up to 50 C were obtained in a case of the sample annealed at 750 °C.

Introduction

Lithium-manganese spinel $LiMn_2O_4$ is one of the most investigated cathode materials for lithium-ion batteries (LIBs) with both non-aqueous and aqueous electrolytes (1). However, its wide application in the industrial production of LIBs is significantly limited due to the relatively low stability of the specific capacity during cycling, especially at elevated temperatures (above 40 °C). Doping spinel with other metal ions is one of the possible ways to improve its characteristics. The main function of the dopant ion is to replace a part of Mn^{3+} ions in the $LiMn_2O_4$ structure, which makes it possible to reduce the influence of the Jahn-Taler effect and related harmful processes that occur during cycling. Changes in the structural, dimensional, and morphological properties of spinel and, as a result, its electrochemical characteristics depend on the nature of the dopant cation, as well as on the method of synthesis. Thus, the choice of a suitable dopant, its content in the material and the synthesis method used make it possible to obtain spinels with improved electrochemical characteristics. Characteristics of Fe-doped spinels $LiFe_xMn_{2-x}O_4$ obtained by various methods of synthesis are reported in the literature (2). However, the problems of specific capacity stability during long-term cycling and high discharge currents both in non-aqueous and aqueous electrolytes remain open.

In this work, the effect of the annealing temperature on the structural and morphological properties of $LiFe_{0.05}Mn_{1.95}O_4$ spinel and their influence on the electrochemical behavior during long-term cycling and discharge at high current densities is considered.

Experimental

$LiFe_{0.05}Mn_{1.95}O_4$ samples were obtained by pyrolysis of citrate precursors obtained from solutions of metal nitrates and citric acid, similarly to the procedure described earlier (3). Citrate precursors were decomposed at a temperature of 400 °C for 8 hours. The intermediate products obtained after that were annealed at temperatures of 700, 750 and 800 °C also for 8 hours. Depending on the annealing temperature, the obtained $LiFe_{0.05}Mn_{1.95}O_4$ samples are further marked as LFMO-700, LFMO-750 and LFMO-800, respectively.

Phase composition and structure parameters of spinel samples were investigated by X-ray diffraction method on a DRON 4-07 diffractometer with Cu-Kα radiation. Morphology was studied on a JEOL JSM-6700F scanning electron microscope.

Electrochemical studies in the non-aqueous system were carried out in 2016 coin cells with a metal lithium anode, and in the aqueous system in 2- or 3-electrode teflon cells with an activated carbon counter electrode and Ag/AgCl as a reference electrode. Cathodes consisted of 80 % of synthesized $LiFe_{0.05}Mn_{1.95}O_4$, 10 % of Super C65 carbon black and 10 % of a poly(vinylidene difluoride) binder. The electrode slurries were cast on an aluminum foil for the non-aqueous system and nickel or stainless-steel current collector for the aqueous system. A 1M solution of $LiPF_6$ in a mixture of ethylene carbonate/dimethyl carbonate/diethyl carbonate with the volume ratio (1:1:1) from Sigma-Aldrich and aqueous solutions of Li_2SO_4 and $LiNO_3$ with salt concentrations of 2 M and 5 M, respectively, were used as electrolytes. Electrochemical investigations were performed on a Neware battery testing system and SPG-200 or P-30 potentiostats in different testing modes.

Results and Discussion

According to XRD patterns, $LiFe_{0.05}Mn_{1.95}O_4$ samples annealed at different temperatures have cubic crystal structure of space group *Fd*3*m* identical to common $LiMn_2O_4$ with characteristic reflections from crystal planes with (111), (311), (222), (400), (331), (511), (440) and (531) indices. An increase in the annealing temperature leads to a relative increase in the crystallinity of spinels, which is evidenced by an increase in the intensities of the corresponding peaks. Apart from small peaks corresponding to Mn_2O_3 (for the samples LFMO-700 and LFMO-750 °C) and Mn_3O_4 (sample LFMO-800) impurities, no additional peaks were found. Structural parameters calculated from XRD patterns presented in Table 1. The lattice parameters (a) and volume (V) are sufficiently close to each other regardless the annealing temperature and are similar to those presented in the literature (4). The change in the crystallite size ($d_{(400)}$) is not so noticeable compared to the change in the particles size, which increased by almost an order of magnitude.

***Table 1.** Structural parameters, crystallite and particle sizes of $LiFe_{0.05}Mn_{1.95}O_4$.*

Sample	a, Å	V, Å^3	$d_{(400)}$, нм	Particle size (SEM), nm
LFMO-700	8.246	561	26	80-100
LFMO-750	8.225	556	26.3	~100
LFMO-800	8.245	560	30.6	400-600

The specific capacity, registered at 10 cycle at cycling current density of 0.5 C (74 mA/g), is 114, 102 and 109 mAh/g for LFMO-700, LFMO-750 and LFMO-800, respectively. The best stability of the specific capacity during cycling, as well as the best rate characteristics (Figure 1), are demonstrated by LFMO-750, despite its lower capacity output compared to the other samples. The results obtained are summarized in Table 2.

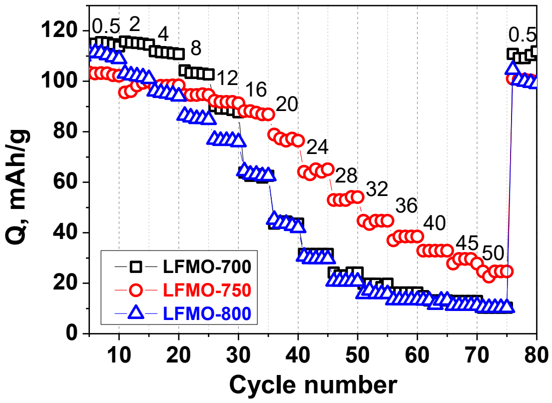

Figure 1. *Cycling performances* $LiFe_{0.05}Mn_{1.95}O_4$ *at different discharge currents (charge current 0.5 C).*

Table 2. *Cycling performances of* $LiFe_{0.05}Mn_{1.95}O_4$

Sample	Discharge capacity, mAh/g			Capacity retention, %	
	0.5 C	20 C	50 C	After rate test	100 cycles at 0.5 C
LFMO-700	114	44	10	97.4	88
LFMO-750	102	76	25	99	96
LFMO-800	109	42	10	91.7	80

In aqueous solutions, the stability of the specific capacity during cycling in the potential range 0.25-1.3 V was lower, despite the close initial capacity of about 100 mAh/g. The decrease in specific capacity for 40 cycles was about 20 %. This may be due to an increase in the side process of oxygen release. Its impact can be reduced by optimizing the electrode composition and the selection of the current collector material.

The dependences obtained may be caused by differences in the structural properties of the particles that determine the rate of lithium diffusion in the solid phase; in the formation of solid electrolyte interface, which affects the charge transfer resistance at the electrode-electrolyte interface; in the macrostructure of the electrode, which provides the required level of electronic and ionic conductivity. The influence of these factors will be discussed further on the basis of an analysis of the potentiodynamic dependences, impedance spectra, and technological parameters of the electrode.

References

1. Y. Huang, Y. Dong, S. Li, J. Lee, C. Wang, Z. Zhu, W. Xue, Y. Li, J. Li, *Adv. Energy Mat.*, **11**(2), 2000997 (2021).
2. A.H. Marincaş and P. Ilea, *Coatings*, **11**(4), 456 (2021).
3. A.V. Potapenko, S.A. Kirillov, *Electrochim. Acta*, **258**, 9 (2017).
4. H. Gu, G. Wang, C. Zhu, Y. Hu, X. Zhang, W. Wen, X. Yang, B. Wang, X. Gao, X. Zhan, J. Li, Z.-F. Ma, Q. He, *Electrochim. Acta*, **298**, 806 (2019).

Electrochemical study comparing liquid and gel electrolytes for lithium-ion batteries based on LiTDI and $LiPF_6$

M. Kasprzyk [a,*], A. Kulka [b], A. Plewa [b], K. Walczak [b]

[a] Faculty of Chemistry, Warsaw University of Technology,
Noakowskiego 3, Warsaw 00-664, Poland

[b] Faculty of Energy and Fuels, AGH University of Science and Technology,
Mickiewicza 30, Cracow 30-050, Poland

Liquid and gel electrolytes based on common commercial and recently commercialized salts for application in lithium-ion batteries are presented herein. Various solvent mixtures and electrolytes based on them are presented. The electrochemical study of these systems will be presented and discussed. Selected organic carbonates' mixtures are chosen as the base for these electrolytes. LiTDI (lithium 4,5-dicyano-2-(trifluoromethyl)imidazolide) and $LiPF_6$ (lithium hexafluorophosphate) are chosen to compare the behavior and the electrochemical properties of the investigated systems. The base for gel electrolytes is PVdF-HFP co-polymer (poly(vinylidene difluoride-*co*-hexafluoropropylene)).

Introduction

Constant development of the lithium-ion battery technology is needed due to constantly increasing demand for more stable energy sources. Lithium batteries are applied in most of small portable devices, smart grids or electric vehicles.

Herein we show new liquid and gel electrolytes based on either LiTDI or $LiPF_6$ salts. $LiPF_6$ was investigated as a benchmark salt, commonly used in batteries. LiTDI is known to be more stable in comparison to $LiPF_6$. The imidazolide salt is stable up to ca. 240 °C and is perfectly stable in presence of water. Decomposition of $LiPF_6$ in presence of even small traces of water or at temperatures higher than 70°C, may lead to gas products evolution. Due to that the inner pressure of cell could increase rapidly and this may cause fire outbreak. That is why the LiTDI salt is considered to be safer and better for long term use.

Liquid electrolytes present quite high conductivity. Unfortunately, especially when volatile solvents are used, the pressure inside the cell may also increase. This may lead again to issues with battery safety. In this work the liquid electrolytes are mostly presented as the benchmark to compare their properties with parameters of gel electrolytes.

Experimental and results

Various systems based on both cyclic and linear carbonates will be presented. Liquid and gel systems containing either $LiPF_6$ or LiTDI will be compared. The conductivity, stability investigated through means of cyclic voltammetry, lithium transference number and results of other electrochemical measurements will be presented. The gel electrolytes have been prepared by so-called Bellcore method. The soakability time will be presented and discussed.

These liquid electrolytes exhibit quite high conductivity (much above 1 mS cm^{-1} at 20°C). The high electrochemical stability window of these electrolytes is also observed, up to 4.7 V vs. Li.

Acknowledgments

This work was financially supported by The National Centre for Research and Development, Project: PROGRAM LIDER XI Nr LIDER/36/0131/L-11/19/NCBR/2020

References

1. J.M. Tarascon, A.S. Gozdz, C. Schmutz, F. Shokoohi, P.C. Warren, *Solid State*
2. *Ionics*, **86-88,** 49 (1996).
3. M. Walkowiak, A. Zalewska, T. Jesionowski, M. Pokora, *J. Power Sources,* **173**, 721 (2007).
4. L. Niedzicki, M. Kasprzyk, K. Kuziak, G.Z. Żukowska, M. Armand, M. Bukowska, M. Marcinek, P. Szczeciński, W. Wieczorek, *J. Power Sources*, **192,** 612 (2009).

Analysis of Degradation Mechanisms in Prismatic Li-ion cell

O. Klvač[a,b], Z. Štubianová[c], J. Báňa[a], and T. Kazda[a]

[a] Department of Electrical and Electronic Technology, Faculty of Electrical Engineering and Communication, BUT, Technická 10, 616 00 Brno, Czech Republic

[b] Thermo Fisher Scientific Brno, Vlastimila Pecha 12, 627 00, Brno, Czech Republic

[c] Central European Institute of Technology, Brno University of Technology, Brno, Czech Republic

This work focuses on the analysis of the degradation mechanisms of prismatic Li-ion cells using a correlation between X-ray computed tomography (CT) and scanning electron microscopy (SEM). CT analysis was performed at the beginning of cycling and after cycling to reveal significant changes in structure. SEM analysis was performed on cells disassembled in a fully charged state, which allows observation of the inactive regions of the anode and preparation of a cross-section through the regions with electroplated lithium. Finally, an event diagram describing the rapid aging of the battery is presented and possible solutions are discussed.

Introduction

Thanks to the fast-growing electromobility market, lithium-ion batteries (LIBs) are currently the most commonly used electrochemical power source, and large funds are invested in development [1][2][3].

Previously, cylindrical cells were widely used for this application. Such batteries are well cooled, but due to the shape of the cylindrical cells they do not use the space well and the whole battery becomes bulkier than the flat type cells - pouch and prismatic. On the other hand, flat-type cells can suffer from gassing, where the uncompressed structure can lead to inactive spots and gassing. For this reason, the cells should be clamped in a rigid mechanical casing [3][4].

Electrochemical methods commonly used in battery analysis can determine essential cell parameters, including capacity, internal resistance, and plateau position. However, understanding the reasons behind changes in these parameters is often limited to theoretical estimations. Gaining more comprehensive knowledge in this area is crucial for research, performance enhancement, and the application of new materials [6].

For evaluating larger-scale changes at the cell design level in a non-destructive manner, CT (Computed Tomography) methods can be applied [7]. Nevertheless, for investigating processes at the microstructure level, the resolution provided by CT methods might be inadequate. SEM, combined with EDS (Energy-Dispersive X-ray Spectroscopy), is capable of observing most of the significant changes in battery structure, along with providing information about the chemical composition [8]. In such cases, the battery is usually disassembled after a defined number of cycles, and the electrode surface or cross-section is scanned [9][10]. For cross-section preparation, the typical method employed is using a focused ion beam (FIB) for small regions, for whole electrodes, broad ion beam (BIB) polishers are preferred [11].

Due to safety considerations related to handling charged cells, the battery is typically discharged before disassembling. However in such cases, certain charging phenomena, for example, lithium plating, cannot be directly observed [12]. The advantage of the cell in a charged state is also the maximum lithium ions are transferred to the anode, resulting in discoloration to golden in the case of graphite anode. This allows the electrochemically active region to be visibly distinguished from the inactive areas [5].

In this work, we focus on a prismatic type cell L402025 from Cellevia cells with a capacity of 150 mAh, which was purchased without a rigid mechanical casing. The cell was subjected to 100 cycles with a maximum datasheet current load of 1C. To compare the condition of the cycled cell at the beginning of cycling and after cycling, X-ray analysis was performed using Thermo Scientific HeliScan micro-CT with space-filling helical trajectory scanning. To verify the results, the cycled cell was disassembled together with a non-cycled cell from the same production used as a reference, both at 100 % State Of Charge. The selected region was further analyzed from the surface and in cross-section using Thermo Scientific Scios 2 SEM. In the case of the cross-sections, Thermo Scientific CleanMill BIB was used for sample preparation. Transfer between the glovebox and other devices was provided by the Thermo Scientific CleanConnect inert gas transfer system to avoid sample degradation and observation in the native state. To describe these processes, an event diagram has been created which shows the inappropriateness of using flexible packaging for Li-ion batteries of the prismatic type.

Acknowledgments

This work was supported by the specific graduate research of the Brno University of Technology No CEITEC VUT/FEKT-J-22-7899 and FEKT-S-23-8286. The work was developed in cooperation with Thermo Fisher Scientific Brno.

References

1. X. Lai et al., Renewable and Sustainable Energy Reviews, 146 (2021).
2. J. A. Sanguesa et al., Smart Cities, 4, 372-404 (2021).
3. P. N. Halimah et al., “Battery Cells for Electric Vehicles,” (2019).
4. P. N. Halimah et al., International Journal of Sustainable Transportation Technology, 2, 54-57 (2019).
5. F. Grimsmann et al., Journal of Energy Storage, 15, 17-22 (2018).
6. L. Li and X. Zhang, (I2MTC), p. 1-5, IEEE (2018).
7. P. Pietsch and V. Wood, Annual Review of Materials Research, 47, 451-479 (2017).
8. H. Liu et al., Journal of Power Sources, 306, 300-308 (2016).
9. Kovachev et al., Batteries, 5 (2019).
10. T. Waldmann et al., Journal of The Electrochemical Society, 163, A2149-A2164 (2016).
11. A. Gholinia et al., Ultramicroscopy, 214 (2020).
12. T. Waldmann et al., Journal of Power Sources, 262, 129-135 (2014).

Analysis of Traditional and Alternative Lithium-Ion Batteries Recycling Methods

Oleksii Korzhenko, Yuliya Polishchuk

Ukrainian State University of Chemical Technology, Dnipro, 49005, Ukraine

The purpose of this research paper is to critically analyze the existing traditional and alternative methods of used lithium-ion batteries recycling and to prepare recommendations for the creation of recycling centers in Ukraine.

In recent years, the market for lithium-ion batteries (LIBs) has developed rapidly. This is due to several factors:

1) Li-ion batteries are recognized as the best source option for electric vehicles (EVs), portable electronic devices, and hybrid electric vehicles (HEVs) because of their high voltage and energy density [1, 2];

2) gradual depletion of natural resources of metals, in particular, lithium [3];

3) expanding the range of cathode and anode materials for Li-ion batteries [4-10].

The market expansion for this type of power source is gradually leading to an increase in the number of used LIBs. Realizing the obvious consequences of accumulating batteries in landfills, countries, and economic unions are implementing bills and measures to reduce them. In particular, back in 2006, the EU introduced Directive 2006/66/EC of the European Parliament on waste electrical and electronic equipment and batteries, which aimed to limit the presence of used batteries in landfills [11].

Structurally, the common components of all types of lithium-ion batteries include the body, the electrode structure, and the electrolyte. It is clear that the greatest interest in the development of LIBs recycling methods is associated with the possibility of extracting valuable metals: copper (Cu), aluminum (Al), lithium (Li), cobalt (Co), manganese (Mn), nickel (Ni), etc. [12]. Moreover, Co is considered to be the most valuable among them [13, 14]. When it comes to lithium metal, in January 2022, its price reached USD 40,000 per ton [15]. Assuming that the valuable metal content of lithium-ion battery cathodes can be effectively recovered in pure metal form, end consumers and companies will have to take their e-waste for recycling to a licensed recycler of electrical and electronic equipment. Thus, the possibility of recovering components of spent LIBs provides an economic incentive for the development of processes and technologies for recycling lithium-ion batteries. Authors [16] note that depending on the design, degree of use, and condition of the batteries, they can be subjected to remanufacturing, repurposing, and recycling.

Currently, the most common technologies for recovering valuable metals (Ni, Co, and Li) from waste batteries, including LFP, are pyrometallurgy and hydrometallurgy [17-24]. Typically, chemical processing is preceded by mechanical separation of components, which separates plastic elements, some metals (e.g., aluminum and copper), and a mixture containing valuable components. This mixture is then processed by pyrometallurgical recycling, which is a high-temperature melting process that burns off plastic residues and electrolytes while recovering valuable metals to copper, cobalt, nickel, and iron alloys [25]. Hydrometallurgical processing is used to separate alloys into individual metals. Pyrometallurgical processes have significant disadvantages, such as the release of hazardous gases, long leaching times, and a significant amount of concentrated acids or reducing agents used in leaching [26], and excessive energy consumption [23]. Hydrometallurgical processes

[24, 27] although requiring less energy, are characterized by the presence of by-products in the form of salts.

There are also alternative methods used to recycle waste, for example, microwave treatment [28- 30].

Recycling of carbon materials also attracts the attention of scientists. For example, the works of [31-33] show the prospects for reusing various types of carbon materials obtained through the recovery and utilization of negative electrodes of lithium-ion batteries.

The literature analysis also revealed the absence of a systematic approach to the recycling of large batteries, as there are almost no regulatory documents that govern these processes. On the other hand, the constant search for the synthesis of new electrode materials should be taken into account, which slows down the standardization of recycling processes.

References

1. W. Chen, J. Liang, Z. Yang, and G. Li. *Energy Procedia.* **158,** 4363 (2019). https://doi.org/10.1016/j.egypro.2019.01.783.
2. B. Dunn, H. Kamath, and J.-M. Tarascon. *Science*. **334**, 928 (2011).https://doi.org/10.1126/science.1212741
3. N. Fatima, N. Solangi, F. Safdar, and J. Kumar. *North American Academic Research,* **5,** 76 (2022). https://doi.org/10.5281/zenodo.6970023
4. A. Mishra, A. Mehta, S. Basu, S.J. Malode, N.P. Shetti, et al. *Materials Science for Energy Technologies,* **1**, 182 (2018). https://doi.org/10.1016/j.mset.2018.08.001
5. F. Schipper, P.K. Nayak, E.M. Erickson, S.F. Amalraj, O. Srur-Lavi, et al. *Inorganics,* **5**, 32 (2017). https://doi.org/10.3390/inorganics5020032.
6. Y. Mekonnen, A. Sundararajan and A. I. Sarwat, *SoutheastCon., 2016,* Norfolk, VA, USA, 2016, pp. 1-6. https://doi.org/10.1109/SECON.2016.7506639.
7. P.U. Nzereogu, A.D. Omah, F.I. Ezema, E.I. Iwuoha, and A.C. Nwanya. *Applied Surface Science Advances,* **9**, 100233 (2022). https://doi.org/10.1016/j.apsadv.2022.100233
8. A. Mishra, A. Mehta, S. Basu, S.J. Malode, N.P. Shetti, et al. *Materials Science for Energy Technologies*, **1**, 182 (2018). https://doi.org/10.3390/inorganics5020032.
9. P. Rozier, and J.M. Tarascon. *J. Electrochem. Soc.,* **162**, A2490 (2015). https://doi.org/10.1149/2.0111514jes
10. A. Dixit. *SMC Bulletin*, 10, 151 (2019).
11. Directive 2006/66/EC of the European Parliament and of the Council of 6 September 2006 on batteries and accumulators and waste batteries and accumulators and repealing Directive 91/157/EEC. https://eur-lex.europa.eu/eli/dir/2006/66/oj.
12. P. Gao, P. Yuan, T. Yue, X. Zhao, and B. Shen. *J. of Energy Storage,* **68**, 107652 (2023). https://doi.org/10.1016/j.est.2023.107652
13. T. Georgi-Maschler, B. Friedrich, R. Weyhe, H. Heegn, and M. Rutz. *J. of Power Sources,* **207**, 173 (2012). https://doi.org/10.1016/j.jpowsour.2012.01.152.
14. X. Zheng, Z. Zhu, X. Lin, Y. Zhang, Y. He, H. Cao, and Z. Sun. *Engineering,* **4**, 361 (2018).
15. Unites States Geological Survey. Mineral Commodity Summaries 2020; ESMAP: Reston, VA, USA, 2020. https://pubs.usgs.gov/periodicals/mcs2020/mcs2020.pdf.
16. M. Chen, X. Ma, B. Chen, R. Arsenault, P. Karlson, N. Simon, and Y. Wang. *Joule,* **3**, 2622–2646 (2019). https://doi.org/10.1016/j.joule.2019.09.014.
17. D. Steward, A. Mayyas, and M. Mann. *Procedia Manufacturing,* **33,** 272 (2019). https://doi.org/10.1016/j.promfg.2019.04.033

18. S. Windisch-Kern, E. Gerold, T. Nigl, A. Jandric, M. Altendorfer, et al. *Waste Management*, **138**, 125 (2022).
19. T. Yan, S. Zhong, M. Zhou, X. Guo, J. Hu, et al. *Nanotechnology Reviews*. **9**, 1586 (2020). https://doi.org/10.1515/ntrev-2020-0119.
20. J. Kumar, R.R. Neiber, J. Park, R.A. Soomro, G.W. Greene, et al. *Chemical Engineering Journal*, **431**, 133993 (2022). https://doi.org/10.1016/j.cej.2021.133993.
21. E. Mossali, N. Picone, L.Gentilini, et al. J. of Environmental Management, **264**, 110500 (2020). https://doi.org/10.1016/j.jenvman.2020.110500.
22. B. Huang, Z. Pan, X. Su, and L. An. J. of Power Sources, **399**, 274 (2018). https://doi.org/10.1016/j.jpowsour.2018.07.116.
23. B. Makuza, Q. Tian, X. Guo, K. Chattopadhyay, and D. Yu. *J. of Power Sources*, **491**, 229622 (2021). https://doi.org/10.1016/j.jpowsour.2021.229622
24. J. Jung, P. Sui, and J. Zhang. *J. of Energy Storage*, **35**, 102217 (2021). https://doi.org/10.1016/j.est.2020.102217.
25. L. Gaines. *Sustainable Materials and Technologies*. **1-2**, 2 (2014). https://doi.org/10.1016/j.susmat.2014.10.001.
26. L. Yun, D. Linh, L. Shu, X. Peng, A. Garg, et al. *Resources, Conservation and Recycling*, **136**, 198 (2018). https://doi.org/10.1016/j.resconrec.2018.04.025.
27. M. Joulié, R. Laucournet, E. Billy. *J. of Power Sources*, **247**, 55 (2014). https://doi.org/10.1016/j.jpowsour.2013.08.128.
28. Y. Fu, Y. He, Y. Yang, L. Qu, J. Li, and R. Zhou. *J. of Alloys and Compounds*, **832**, 154920 (2020). https://doi.org/10.1016/j.jallcom.2020.154920.
29. C. Liu, J. Long, Y. Gao, H. Liu, W. Luo, and X. Wang. *J. of Environ. Chem. Engineering*, **11**, 109759 (2023). https://doi.org/10.1016/j.jece.2023.109759.
30. A. Fahimi, I. Alessandri, A. Cornelio, P. Frontera, A. Malara, et al. *Resources, Conservation and Recycling*, **194**, 106989 (2023). https://doi.org/10.1016/j.resconrec.2023.106989.
31. Z. Ma, Y. Zhuang, Y. Deng, X. Song, X. Zuo, X. Xiao, and J. Nan. J. of Power Sources, 376, 91 (2018). https://doi.org/10.1016/j.jpowsour.2017.11.038.
32. E.M. Garcia, V.F.C. Lins, H.A. Tarôco, T. Matencio, R.Z. Domingues, J.A.F. Santos. *Int. J. of Hydrogen Energy*, **37**, 16795 (2012). https://doi.org/10.1016/j.ijhydene.2012.08.118.
33. X. Zhu, Y. Chen, J.Xiao, F. Xu, F. Su, et al. *J. of Energy Storage*, **68**, 107798 (2023). https://doi.org/10.1016/j.est.2023.107798.

Aging in lithium-ion batteries: A mini-review

Seyed Saeed Madani and Carlos Ziebert

Institute of Applied Materials-Applied Materials Physics, Karlsruhe Institute of Technology, 76344
Eggenstein-Leopoldshafen, Germany;

*Correspondence: seyed.madani@kit.edu

Lithium-ion batteries experience deterioration with each use, and it is unlikely that the effects of aging-induced degradation can be completely eliminated. The aging processes of lithium-ion batteries are complex and diverse, closely associated with various interacting factors such as battery types, electrochemical reactions, and operating conditions. Factors like state of charge, charge-discharge rate, cycles, and temperature directly impact degradation, making operating conditions and stressors crucial considerations. Battery aging poses a significant research challenge, affecting the power and energy capacity of batteries over time. This article offers a comprehensive review of different techniques for modeling battery aging and studies conducted on this topic, with a specific focus on indicators used to assess the health status of batteries. The aim of this review is to summarize the findings of estimation methods for lithium-ion battery aging in various applications. The extensive range of studies on battery aging provides a wealth of information in this field, and thus, this paper provides an overview of these diverse approaches.

Introduction

The emergence of electric vehicles (EVs) has been seen as a viable solution to combat global carbon emissions. However, the widespread adoption of EVs faces challenges like range anxiety and battery degradation. The range of an EV heavily relies on the energy density and specific energy of the battery, while battery degradation is influenced by driving behavior and environmental conditions.

Reutilizing electric vehicle batteries presents an opportunity to make use of their remaining energy capacity and extend their lifespan. Second-life applications for these batteries typically require lower power and energy density compared to EVs. However, the technical and economic feasibility of these systems still faces uncertainties. It is crucial to understand the aging and lifespan of reused batteries to facilitate their development.

As electric vehicles gain popularity, the battery plays a critical role in powering these vehicles. Lithium-ion batteries are widely adopted due to their high energy storage density and long lifespan. However, accurately estimating battery life often requires lengthy and costly testing processes. To address this, efficient methods need to be explored to minimize testing requirements by leveraging existing knowledge of aging patterns from different battery chemistries.

Heat generation and thermal transport are crucial factors affecting the performance, aging, and safety of lithium-ion batteries (LIBs). Elevated battery temperatures significantly accelerate aging. Managing temperature and aging during battery operation presents a complex challenge spanning multiple scales, from micro/nanoscale within individual material layers to large integrated LIB packs.

The fire and explosion risks associated with lithium-ion batteries (LIBs) pose significant concerns for their use and transportation in aircraft. Therefore, it is crucial to study the thermal safety issues specific to flight conditions. Lithium-ion batteries are prone to overcharging, which can lead to thermal runaway and potentially dangerous situations. Inconsistent battery performance, charging devices, or failures in the battery management system can contribute to such incidents.

In recent years, there has been growing confidence among stakeholders that retired batteries can be repurposed for less-demanding applications, such as stationary energy storage, providing new value in the energy and transportation sectors. Assessing the feasibility of second-life battery applications from economic and technological perspectives becomes imperative in this context.

Barré et al. [1] presented a comprehensive overview of recent research and developments concerning the aging mechanisms and estimation of lithium-ion batteries. The article discusses various techniques, models, and algorithms utilized for estimating battery aging, including the estimation of state of health (SOH) and remaining useful life (RUL). The methods covered in the paper encompass a wide range, from detailed electrochemical approaches to statistical methods based on data analysis. Furthermore, the accuracy of the currently employed methods is evaluated. The paper also addresses the remaining challenges in battery aging estimation, providing a thorough analysis. It examines the strengths and limitations of existing approaches and explores the possibility of deriving an ideal method by considering the characteristics of these approaches.

In their study, Wang et al. [2] focused on investigating the degradation of a LiFePO4 battery resulting from cycling and developing cycle-life models. The researchers collected extensive data on cell lifespan through a comprehensive cycle-test matrix. This matrix incorporated three key parameters: temperature (-30 to 60 ◦C), depth of discharge (DOD) (10-90%), and discharge rate (C-rate) ranging from C/2 to 10C (with 1C equivalent to 2A). The experimental findings revealed that, at lower C-rates, the battery's capacity loss was primarily influenced by time and temperature, with the impact of DOD being relatively less significant. However, at higher C-rates, the charge/discharge rate had a more pronounced effect on capacity loss. To establish a life model, the researchers utilized a power law equation that linked capacity loss to either time or charge throughput. Additionally, the temperature effect was accounted for using an Arrhenius correlation. By allowing the model parameters to vary with C-rates, the researchers observed that the model effectively represented a wide range of life cycle data. Finally, the paper discusses ongoing efforts aimed at developing a comprehensive battery life model that takes into consideration Ah throughput (time), C-rate, and temperature. Figure 1 shows the test matrix for a cycle-life model for graphite-LiFePO4 cells.

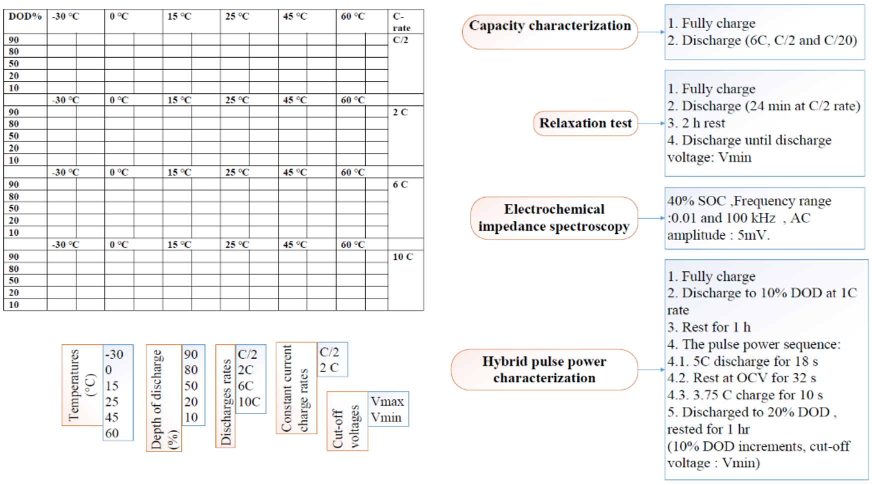

Figure 1. *Cycle-life model test matrix for graphite-LiFePO4 cells [2].*

Discussion and Conclusion

Lithium-ion batteries are highly valued for their compact size and high energy density, making them a popular choice among clean energy sources. The increasing presence of intermittent renewable energy sources has made Stationary Battery Systems (SBS) vital components in power distribution networks worldwide. SBSs serve various purposes, including managing peak loads, shifting loads, regulating voltage, and improving power quality. With their clean and stable characteristics, lithium-ion batteries are widely used in various applications, necessitating the effective management of their health. Accurately predicting the remaining useful life (RUL) of these batteries is a crucial aspect of health management.

The study explores different methods for estimating battery aging, each with its own limitations. It is often observed that existing research tends to focus on capacity fade or resistance increase individually, despite the fact that both factors significantly impact electric vehicle performance. While certain methods excel under specific conditions, such as analyzing detailed data from a single battery or large datasets from vehicle, chemical studies face challenges in terms of reproducibility due to battery design dependencies, and statistical methods require extensive and diverse datasets to capture all interactions effectively.

For users of electric vehicles, having a consistent autonomy range and available power throughout the lifespan of their cars is crucial. Therefore, accurately assessing the health of lithium-ion batteries (LIBs) is vital for evaluating performance and predicting longevity. Numerous solutions have been proposed in the literature to address this challenge. However, the lifetime study of lithium-ion batteries encounters challenges, especially when developing a model-based evaluation system, due to the limited availability of data samples. Conducting extensive battery testing is necessary to establish the relationship between battery degradation and various external factors. Nevertheless, this process is time-consuming and resource-intensive.

Reference

1. Barré, Anthony, Benjamin Deguilhem, Sébastien Grolleau, Mathias Gérard, Frédéric Suard, and Delphine Riu. "A review on lithium-ion battery ageing mechanisms and estimations for automotive applications." Journal of Power Sources 241 (2013): 680-689.
2. Wang, John, Ping Liu, Jocelyn Hicks-Garner, Elena Sherman, Souren Soukiazian, Mark Verbrugge, Harshad Tataria, James Musser, and Peter Finamore. "Cycle-life model for graphite-LiFePO4 cells." Journal of power sources 196, no. 8 (2011): 3942-3948.

Review of Electrochemical Impedance Spectroscopy Methods for Lithium-ion Battery Diagnostics and Their Limitations

Kateřina Nováková[a], Jindřich Sadil[b], Václav Papež[a], Václav Knap[a]

[a] Dept. of Electrotechnology, Faculty of Electrical Engineering, Czech Technical University, Praha, Czech Republic

[b] Department of Transport Telematics, Faculty of Transportation Sciences, Czech Technical University, Praha, Czech Republic

Electrochemical impedance spectroscopy (EIS) is a measurement method widely used for non-destructive analysis and diagnostics in various electrochemical fields. From the measured dependence of the battery impedance on the frequency, it is possible to determine the parameters of various Equivalent Electrical Circuit models of the battery. The conventional method of battery measurement using single-sine EIS is currently one of the most widely used methods for the analysis of Lithium-ion batteries. However, its most significant disadvantage is the relatively long measurement time. For this reason, there is a growing demand for faster methods using Fast-Fourier Transform or Pseudo-Random Sequences. A description of various EIS methods' applications is provided in this paper.

Introduction

Electrochemical impedance spectroscopy (EIS) is a non-destructive method that characterizes electrochemical processes inside the battery. It can be used both in battery steady-state during idling, and dynamically during battery cycling. Subsequently, various dependencies such as state-of-charge, temperature, and C-rates can be covered. During EIS measurements, an AC signal over a wide frequency range is applied to the battery, and the cell response is measured.

With the wider spread of electric cars and the use of traction Lithium-ion batteries, there is increasing pressure to diagnose them as accurately as possible and monitor their SOH while they are in use. For this reason, the speed of measurement using the conventional single-sine method is no longer sufficient.

Newly developed faster methods include the excitation of Lithium-ion batteries using a multi-sine signal, whose response is then processed using Fast Fourier Transform (FFT) or excitation of the battery using a Pseudo Random Sequence (PRS).

This paper provides an overview and a description of various EIS methods and highlights their advantages and disadvantages.

Overview of Electrochemical Impedance Spectroscopy Methods

The paper compares the single-sine method, currently the most widely used method for Lithium-ion battery diagnostics, with innovative methods that use, for example, multi-sine signal processing using Fast Fourier Transforms or battery excitation using Pseudo Random Sequence. Usually, the battery response to the input signal is measured from higher frequencies to lower frequencies; the frequencies are in range from 10 kHz to 0.01 Hz. The single-sine method is currently the most accurate. However, a faster solution for use in the automotive industry is needed. For this reason, the central part of the paper will focus on innovative methods of using EIS that are faster.

Multi-Sinusoidal Excitation and Data Evaluation Based on FFT

The lithium-ion battery is excited by the multi-sine signal, and at the same time, the response of the lithium-ion cell to its excitation is read. The sensed signal is then processed using Fast Fourier transform. This gives the magnitude and phase of the impedance of the measured system for each frequency. These are then plotted in a Nyquist diagram to allow further processing of the EIS curves and determination of the cell's replacement circuit parameters.

Analyzing Step Response Using FFT

As it is generally known, the ideal step change contains all frequencies. This fact is being used by scientists, whose use a step change to excite a Lithium-ion battery and use only the response to this step change to determine the EIS curves, thus reducing the measurement time to the lowest possible limit.

Measuring Techniques of Electrochemical Impedance Spectroscopy Based on PRS

An alternative approach to applying sinusoidal signal injection is to use broadband excitation, such as a pseudo-random sequence. The main advantages of this method are the significant reduction in measurement time, its low complexity, and its online real-time application. A common problem with most measurements based on this principle is the very significant negative impact of noise on the measured values. For this reason, individual research teams try to slightly modify the generated sequence to achieve a higher signal-to-noise ratio.

Conclusions

Diagnostics of Lithium-ion batteries using EIS is a perspective method that can significantly reduce the time required for testing compared to earlier methods, such as capacity tests. Nevertheless, single-sine methods, which are currently the most used methods, are too slow to be used for online battery diagnostics in a Battery Management System. To reduce the time, it is possible to use one of the innovative methods described in this research, such as PRS or the use of multi-sine signal and its post-processing by FFT.

In any case, in all applications using a multi-sine signal or PRS, the quality of the measured data depends on the level of noise in the system, which seems to be a critical parameter determining its useability and it is necessary to properly asses it.

Based on the research presented in the paper, detailed evaluations of the different EIS methods will be introduced and suggestions towards a suitable and quick diagnostic approach will be made.

Acknowledgements

This work was supported by the Grant Agency of the Czech Technical University in Prague, grant No. SGS23/065/OHK3/1T/13 and TACR, project no. TN02000054.

Synthesis and Characterization of $LiMn_2O_4/LiNi_{1/3}Co_{1/3}Mn_{1/3}O_2$ structures as cathode for Li-ion Batteries

M. G. Ortiz[a,b], O. Čech[c], T. Kazda[c], . Čudek[c], A. Visintin[a], M. Sedlaříková[c]

[a] Instituto de Investigaciones Fisicoquímicas Teóricas y Aplicadas (INIFTA), Facultad de Ciencias Exactas (UNLP), CONICET, Diag. 113 y 64, La Plata, Argentina

[b] Centro de Investigación y Desarrollo en Ciencia y Tecnología de Materiales (CITEMA), Universidad Tecnológica Nacional - CICPBA, 60 y 124, 1923, Berisso, Argentina

[c] Department of Electrical and Electronic Technology, Faculty of Electrical Engineering and Communication, Brno University of Technology, Technická 10, 616 00, Brno, Czech Republic

The present work investigates the mixing different cathodes materials (spinel and layered structures) in one electrode. It is considered a promising approach to combine their individual advantages and compensate detrimental properties. The prepared materials were used as cathode material for lithium-ion batteries and the structural characteristics and electrochemical properties are subsequently examined by employing physical and electrochemical techniques such as X-ray diffraction (XRD), scanning electron microscopy (SEM), charge-discharge cycling, the rate capability test, cyclic voltammetry, and electrochemical impedance spectroscopy.

Introduction

Rechargeable lithium ion batteries (LIBs) are considered as one of the most promising power sources for electric vehicle (EV) and hybrid electric vehicle (HEV) applications due to their high energy density, durable cycle life, higher output power and safety issues [1]. Previous research has mainly focused on a single electrode. However, it is difficult for a single cathode material to meet the requirements for EVs and HEVs, and so the combination of different cathode materials in one is proposed [2-4]. This new cathode material (hybrid cathode material) combines several excellent electrochemical properties of each cathode material and has become an alternative to conventional single cathode materials. Current study of hybrid cathode materials focuses primarily on composites of two types of cathode materials. In this work, $LiMn_2O_4/LiNi_{1/3}Co_{1/3}Mn_{1/3}O_2$ structures have been prepared and studied by XRD and electrochemical techniques.

Experimental

$LiNi_{1/3}Co_{1/3}Mn_{1/3}O_2$ was selected as the parent cathode material and was synthesized by the solid-state reaction method. Stoichiometric amounts of NiO, MnO_2, $Co(OH)_2$, and $LiOH{\cdot}H_2O$ were mixed in a ball mill to form homogeneous powder after 1 h. At the following stage, the product was precalcinated at 550°C in the air for five hours to yield the NCM precursor, then this was further annealed under 850°C, for 12 h in the air to obtain the final NCM product. Commercial $LiMn_2O_4$ (Aldrich) was used to prepare the hybrid cathode materials. Then, 0.45 g of $LiMn_2O_4$ was first dissolved with an ultrasonic stirrer in 40ml of ethanol for 2 hrs. Afterwards, 1.05 g of the NCM 850 sample was successively added and ultrasonicated continuously for 1h. Finally, the mixture was subjected to twelve-hour drying at 80°C and then heat-treated at 400°C for 5 hrs to obtain the final $LiMn_2O_4$@NCM-850 material. The as-prepared products were characterized via X-ray diffraction by using a Rigaku Miniflex 600 with Cu kα radiation (1.5406 Å), and the XRD spectra were collected in the range of 10-100° 2θ at the scan rate of 1° $2\theta\text{min}^{-1}$. The working electrodes were prepared by applying 80 wt% of $LiMn_2O_4$@NCM-850 materials; and this was mixed with 10 wt% carbon Super P and 10 wt% polyvinylidene fluoride (PVDF), dissolved in N-methylpyrrolidone (NMP). The slurry of the cathode was deposited onto an aluminium foil as a current collector, and circular electrodes having an area of 2.54 cm^2 each were cut out. The electrochemical experiments were carried out by utilizing the ECC-STD cells (El-Cell, Germany), which had been assembled inside an Ar-filled glove box. A lithium metal foil was employed as the counter and reference electrode. As the electrolyte, we employed a 1.5 M solution of LiPF6 in a mixture of ethylene carbonate and dimethyl carbonate (EC:DMC- 1:2 w/w). The electrochemical measurements were performed with a VMP-2Z multi-channel galvanostat-potentiostat (Bio-Logic).

It was found that the XRD patterns of the final products exhibit the typical hexagonal layered structure of the α-$NaFeO_2$ type with the R-3m space group. No impurity phase peak is detected in these patterns. the addition of LiMn2O4 onto the NCM-850 revealed ameliorating effects. The electrodes deliver the specific discharge capacity value of 143 mAh g^{-1} at the C-rate of 0.2 C; their capacities after 75 cycles remain at 85% of the initial values, and the rate performances as well as cycling stabilities are satisfactory. The mixing of both materials could be promoted the redox reaction kinetics, largely improving the reversibility during cycling and the rate capability of the coated electrodes. The approach also played an important role in stabilizing the surface and, consequently, enhancing the structural stability and the cycle life of the cathode material.

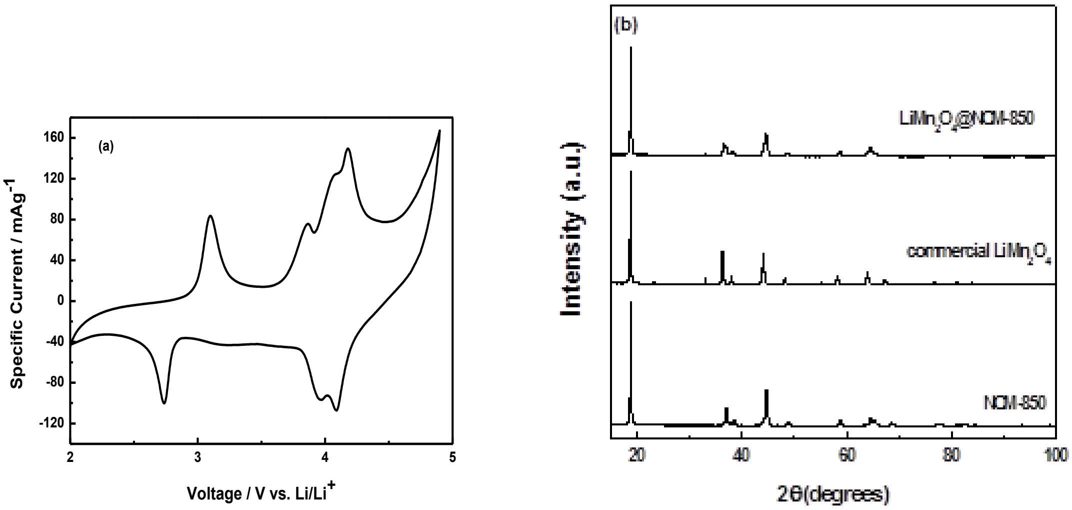

Figure 1. *(a) The CV profiles for the electrode. (b) The XRD patterns of the materials.*

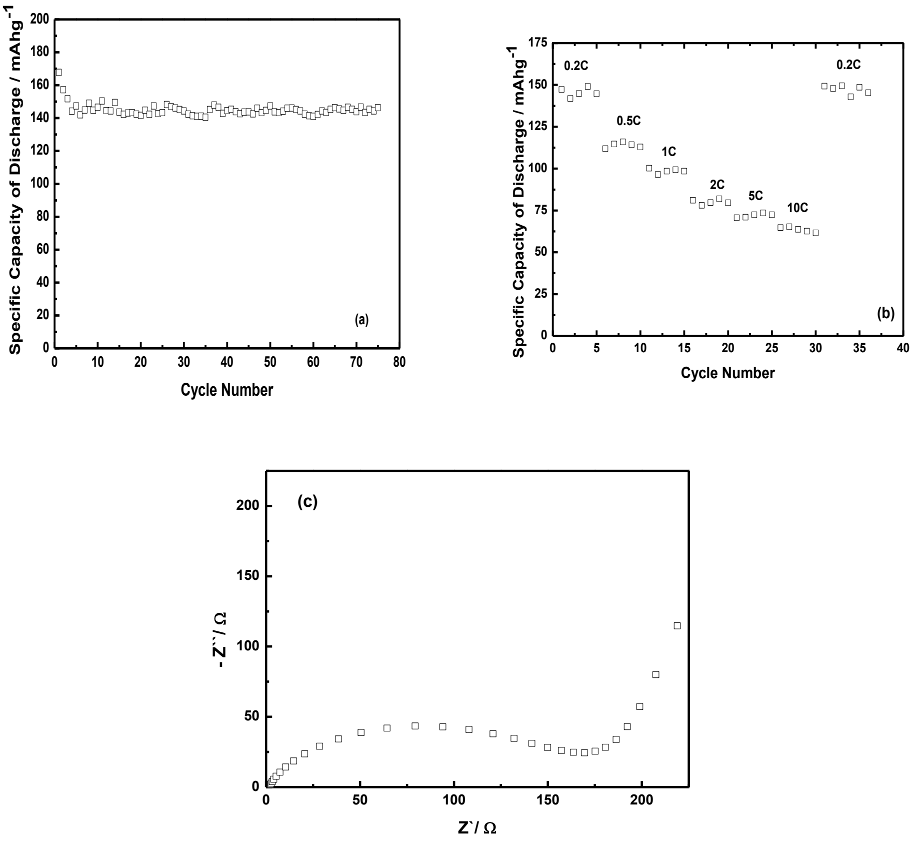

Figure 2. *(a) The discharge cycling performance at 0.2 C, (b) the cycling performances at different current rates, and (c) EIS spectra.*

Acknowledgments

This work was supported by the CONICET (Consejo Nacional de Investigaciones Científicas y Tecnológicas) and ANPCyT (Agencia Nacional de Promoción Científica y Tecnológica).

References

1. Y. Xia, J. Zhengb, C. Wang, M. Gu.,*Nano Energy*. **49**, 434 (2018).
2. B. Zhang, X. Xie, Z. Peng, G. Hua, K. Dua, B. Makuza, Y. Gong, X. Ji, Y. Cao. *J. Power Sources*.**541,**1 231671 (2022).
3. G. Sun, S. Lai, X. Kong, Z. Chen, K. Li, R. Zhou, J. Wang, and J. Zhao. *ACS Appl. Mater. Interfaces*, **10**, 19, 16458 (2018).
4. J-S. Leea, K. Heoa, H-S. Kim, M-Y. Kim, J. Kim, S-W. Kang, J. Lim. *J. Alloys Compd.*, **781**,15, 553 (2019).

TDI-based ionic liquid as a plasticizer in PVdF-HFP membranes

K. Rogala*, L. Niedzicki, M. Kasprzyk, A. Zalewska

Faculty of Chemistry, Warsaw University of Technology, Noakowskiego 3, 00-664 Warsaw, Poland

klaudia.rogala.dokt@pw.edu.pl

In the recent years, interest in electric vehicles powered exclusively by lithium-ion batteries has increased significantly. However, the use of Li-ion batteries, especially in large quantities, can lead to dangerous electrolyte leakage and its ignition or explosion. The use of gel electrolytes may be a solution to this problem. They combine the advantages of solid polymer electrolytes (SPE) and liquid electrolytes. Main advantages of gel electrolytes are: high conductivity, good electrochemical stability and higher safety in case of the battery damage - they will not leak. However, PVdF-HFP membranes used in typical gel electrolytes have very poor mechanical properties. Therefore, we employed MPPyrTDI ionic liquid (1-methyl-1-propylpyrrolidinium 4,5-dicyano-2-(trifluoromethyl)imidazolate) as a plasticizing additive for membranes.

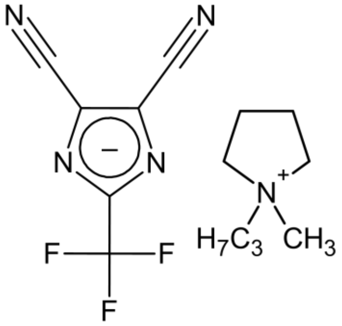

Figure 1. Structure of MPPyrTDI

The research included the synthesis of membranes with a wide range of compositions as for the ionic liquids and PVdF-HFP. The syntheses were done with the use of acetone as a solvent. The obtained membranes were measured using electrochemical, thermal and microscopic techniques. Systems were tested by differential scanning calorimetry (DSC). The electrochemical stability of the membranes relative to the lithium anode was tested using cyclic voltammetry (CV) and linear sweep voltammetry (LSV). Conductivity over a wide range of temperatures was also measured. All electrochemical tests were performed on a multi-channel potentiostatic-galvanostat VMP3 by Biologic Science Instruments with the function of the frequency response analysis.

Gel Polymer Electrolytes in Liquid Ionic - One Way of Increase Conductivity

M. Jahn[a], M. Sedlaříková[a], A. Visintin[b]

[a] Department of Electrical and Electronic Technology, The Faculty of Electrical Engineering and Communication Brno University of Technology, Technická 10,
Brno 612 00, Czech Republic

[b] Instituto de Investigaciones Fisicoquímicas Teóricas y Aplicadas (INIFTA), Facultad

de Ciencias Exactas (UNLP), CONICET, Diag. 113 y 64, La Plata, Argentina

Ionic liquids are classified as conductors of the second category and therefore can be used as electrolytes for accumulators. Research in this sector is focused on classical lithium-ion systems such as LiCoO2-carbon or LiMnNi2O4-carbon, accumulators with gel polymer electrolyte, but is also focused on emerging concepts including Li-S systems, sodium accumulators and lithium-air systems. Due to the mentioned properties of ionic liquids, in terms of high temperature stability, low vapor tension and non-flammability, they are a suitable candidate for use in lithium-ion accumulators with higher fire safety.

Introduction

The goal of this paper is to create a gel polymer electrolyte for use in Li-ion batteries with better properties than existing gel electrolytes. Current developments in the world are aimed at increasing ionic conductivity, widening the potential window and improving long-term chemical and electrochemical stability of the polymer and the solvent.

In the normal operation of Li-ion batteries, one of the most important parameters is their safety. Considering that the electrolyte is the least resistant part of accumulators to increased temperature, the effort is to use an electrolyte with high temperature stability.

Research in the world and in this paper is focused on improving the properties of gel electrolytes for the use in Li-ion batteries.

Some ionic liquids are classified as aprotic electrolytes. These are substances that are composed of an organic cation and an inorganic or organic anion. The melting point of ionic liquids is lower than 100 °C, but nowadays, there are also some that are liquid at room temperature. The main advantages of ionic liquids include, for example: zero vapor tension, high temperature stability, low toxicity, non-flammability and unique solvation properties. Ionic liquids can serve as a suitable substitute for volatile organic solvents.

Materials and Methods

The gel electrolyte with selected ionic liquids consisted of a conductive and a polymer component. The conductive component was a solution of the LiPF6 salt dissolved in the solvent. In the first case, a mixture of aprotic solvents (EC/DEC in a mass ratio of 1:1) was chosen as the solvent, and selected ionic liquids were added to it. Then, ionic liquid was added in volume percentages related to the volume of the aprotic solvent (EC/DEC 1:1 wt.). This volume was considered as 100%. Ionic liquids were added in different percentage amounts of their volume to the solvent volume in the range of 1% - 200%. The chosen molarity of the LiPF6 salt in the resulting solvent mixture was 0.5 M. In another case, the aprotic solvent was completely replaced by only the selected ionic liquid, where, on the contrary, the molarity of the LiPF6 salt in the selected ionic liquid was changed, ranging from 0 to 1.5 M in steps of 0.25 M. The polymeric part consisted of methyl methacrylate (MMA) monomer, ethylene glycol dimethacrylate crosslinker and benzoin ethyl ether (BEE) UV polymerization initiator. The molar ratio of MMA monomer to the conductive component (salt, solvent and ionic liquid or just salt and ionic liquid) was 20 mol%. The molar ratio of the cross-linking agent EDMA to the monomer was 3.5 mol% and at the same time the molar ratio of the polymerization initiator BEE to the monomer was 1.0 mol%. Possible modifications of the composition of the polymeric part are carried out for individual experiments in relevant subsections.

The used ionic liquid were (EMIM TFSI - 1-ethyl-3-methylimidazolium bis(trifluoromethylsulfonyl)imide, EMIM BF_4 - 1-ethyl-3-methylimidazolium tetrafluoroborate, BMIM BF_4 - 1-butyl-3-methylimidazolium tetrafluoroborate, EMIM PF_6 - 1-ethyl-3-methylimidazolium hexafluorophosphate, EMIM DCA - 1-ethyl-3-methylimidazolium dicyanamide, their properties are presented in Table I.

***TABLE I.** Selected ionic liquids*

Ionic liquid	Density [g·cm^{-3}]	Melting point [°C]	Molarity [g/mol]	Conductivity [mS/cm]	Electrochem. window [V]
EMIM TFSI	1.53	-3	391.31	6.63	5.8
EMIM BF_4	1.29	15	197.97	14.10	4.7
BMIM BF_4	1.21	-15	226.02	3.15	4.68
EMIM PF_6	1.35	58-62	256.13	---	---
EMIM DCA	1.11	-21	177.21	17.7	3.0

Sample resp. gel polymer electrolyte is disc with a diameter 16 mm and thickness 0.9 mm, which is cut out from the total area of formed (polymerized) gel. All handling of the gel is performed in a glove box with argon atmosphere. All chemicals are mixed in a vial with a magnetic stirrer in glove box. For all analyses were used potentiostats from Bio-Logic Science instruments® types VSP® and VMP® For the evaluation and comparison of the samples in terms of electrochemical properties, the analyzes chosen were impedance spectroscopy (PEIS) and linear voltammetry (LSV).

Specific conductivity was measured using electrochemical impedance spectroscopy in a metal conductivity cell by EL-CELL, type ECC-STD. The evaluation of the potential window for gel polymer electrolytes was evaluated from the polarization line in a way where the limiting current density, i.e. the current Imax and the voltage Umax when this current density is exceeded, is determined in advance and is taken as a potential window. This method, as well as electrochemical impedance spectroscopy, has a great ability to tell about the measured samples in terms of the electrochemical stability of the entire electrode-electrolyte system, and it can also be determined at what potential electrolyte decomposition occurs. All measurements were performed at room temperature.

Experimental Results

Gel electrolytes with 1-ethyl-3-methylimidazolium hexafluorofosfate and with the addition of an aprotic solvent is given as an example. The negative property of this ionic liquid was its melting point, at room temperature it was in a solid state, so it had to be heated during each manipulation to change its state to liquid. The percentage volume of ionic liquid added ranged from 1 to 15 %.

TABLE II. *Conductivities and potential windows for EMIM PF6 ionic liquid using EC/DEC solvent (1:1 wt.)*

Specific conductance and potential windows			
Added volume *IL* [%]	γ [mS/cm]	E [V] I = 5 µA	I = 10 µA
1	3.35	4.89	>5.10
1.5	4.75	4.58	>5.10
2.5	7.59	>5.10	>5.10
3.5	4.38	>5.10	>5.10
5	3.93	>5.10	>5.10
7.5	1.99	5.07	>5.10
10	2.61	>5.10	>5.10
15	1.87	>5.10	>5.10

The highest specific conductivity was achieved by the gel electrolyte with the addition of 2.5 % of the volume of the ionic liquid, which was 7.59 mS/cm. The sample with the addition of 15 % of the volume of the ionic liquid had the lowest specific conductivity, namely 1.87 mS/cm. Modification with this ionic liquid in the range of 1 to 5 % of the added volume improved the specific conductivity in the order of tens of percent compared to the gel electrolyte without modification. Electrochemical stability of prepared samples was very high. For all samples, at a current of 10 µA, the potential windows exceeded the set measurement range of 5.1 V. This ionic liquid significantly increased the electrochemical stability and the width of the usable potential window. Mechanical properties of all measured samples were excellent and their subsequent handling was also excellent. These gel electrolytes stood out above all for their high mechanical strength.

Based on all observed electrical, electrochemical and mechanical properties, the modification with this ionic liquid proved to be very suitable for use in gel electrolytes. It significantly increased the electrochemical stability and mechanical properties of all prepared samples.

Conclusion

In general, it can be stated that with the use of ionic liquids, as an addition to the selected aprotic solvent, compared with the shows in up to twice the values of specific conductivities, better electrochemical stability were achieved and mechanical properties. The chosen chemical composition and ratios of individual chemical substances of the investigated gel electrolytes were unique and have not yet been published in the world. This part was built mainly on the research of electrolyte liquids in combination with ionic liquids, where generally comparable results were achieved in this paper.

Acknowledgments

This work was supported by the specific graduate research of the Brno University of Technology No. FEKT-S-23-8286

References

1. RAVI, M., Shenhua SONG, Jingwei WANG, Ting WANG a Reddeppa NADIMICHERLA. Ionic liquid incorporated biodegradable gel polymer electrolyte for lithium ion battery applications. Journal of Materials Science: Materials in Electronics. 2016, 27(2), 1370-1377. DOI: 10.1007/s10854-015-3899-x. ISSN 0957-4522.
2. SULTANA, Sharmin, Kumkum AHMED, Prastika Krisma JIWANTI, Brasstira Yuva WARDHANA a MD Nahin Islam SHIBLEE. Ionic Liquid-Based Gels for Applications in Electrochemical Energy Storage and Conversion Devices: A Review of Recent Progress and Future Prospects. *Gels*. 2022, 8(1), 78-91. ISSN 2310-2861. Dostupné z: doi:10.3390/gels8010002
3. EFTEKHARI, Ali, Yang LIU a Pu CHEN. Different roles of ionic liquids in lithium batteries. Journal of Power Sources. 2016, 334, 221-239. DOI: 10.1016/j.jpowsour.2016.10.025. ISSN 03787753.
4. FERNANDES, M., R. LEONES, A.M.S. COSTA, et al. Electrochromic devices incorporating biohybrid electrolytes doped with a lithium salt, an ionic liquid or a mixture of both. Electrochimica Acta. 2015, 2015(161), 226-235.
5. LU, Wen, Kent HENRY, Craig TURCHI a John PELLEGRINO. Incorporating Ionic Liquid Electrolytes into Polymer Gels for Solid-State Ultracapacitors. *Journal of The Electrochemical Society*. 2008, 155(5). ISSN 00134651. Dostupné z: doi:10.1149/1.2869202.

Synthesized Innovative Graphite with Nanostructure and Unique Properties Increases Energy and Power of Lithium Batteries

[1]Y. Pustovalov. [2,3] E. Shembel, [1]D. Kaszuba, [3]Y. Polishchuk, [2] V. Redko, [2]T. Pastushkin, [3]Y. Sknar, [3]A. Markevich, [3]I.Sknar, [3]N. Zaderey, [1]I.Sagirov

[1]INT Sp. Z o.o., Ul Pilsudskiego 17/4, 34-074 Rztszów, Polska

[2]Enerize Corporation, Coral Springs, FL, 33067, USA

[3]Scientific Research Laboratory of Chemical Power Sources of Ukrainian State University
of Chemical Technology, Dnipro, 49005, Ukraine

The synthesis has been developed and the industrial production of unique nano graphites was organized. These nano graphites have special micro and macro structures, high electronic conductivity, low density, catalytic activity for electrochemical reactions, ensure the manufacture of electrodes without binders, have the necessary cohesive and adhesive, and other properties depending on the tasks of the consumer. Nano graphites modify the cathode materials of lithium batteries, and organize the unique anodes.

Introduction

Nano graphite, which produces by INT Sp. Z o.o, are effectively used in Li-ion batteries as: 1) Anode based on nano graphite without a binder. 2) Cathode based on composites: active material, nano graphite, and without a binder. 3) Current collector, which is a thin-layer plate of nano graphite, and without a binder.

Below SEM structural characteristics of various synthesized our nano graphite

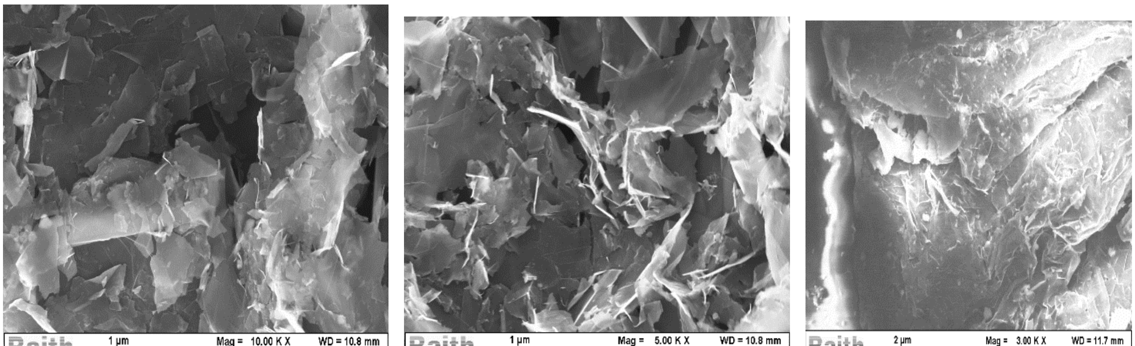

Examples of some of the batteries we are developing with these nano graphites described below. All electrodes without binder

1. Li-ion: the anode is made on the basis of nanographite,
2. Li-ion: the anode is made from a composition of nanographite and Si
3. Li - S: the sulfur cathode is modified with nanographite,
4. Silicon - S is a promising battery: the anode is made from a composition of nano graphite+ Si, and the sulfur cathode is modified with nano graphite

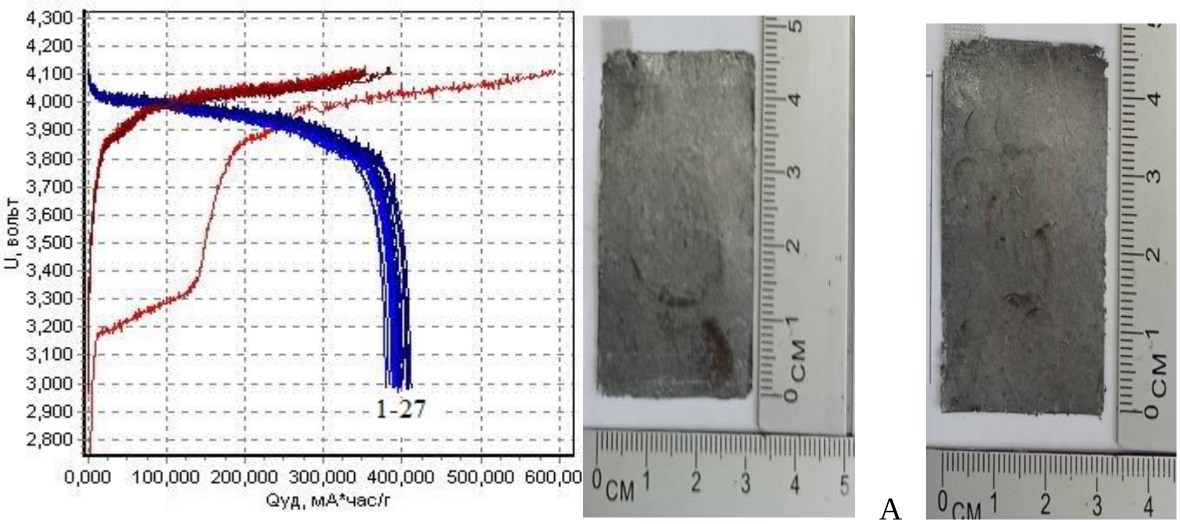

This figure shows the discharge characteristics of the anode of Li-ion battery. Anode is based on nano graphite without the binder. The discharge characteristics of this anode are high and stable. A. Anode based on nano graphite. B. Anode based on nano graphite and Silicon

Below presented the SEM of power the composition of cathode of Li-S batteries: sulfur, nano graphite, composition the sulphur and nano graphite without binder

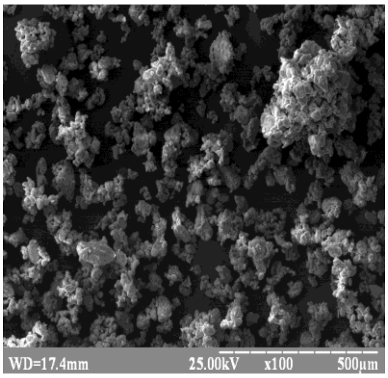

Sulfur powder g

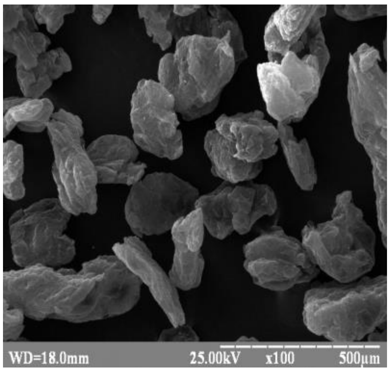

Nano graphite CNS

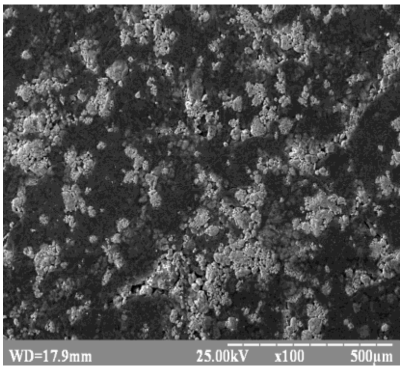

Composition sulphur and nanographite

Discharge characteristics of the Li-S cells with electrolyte: 0.7M LiIm, 0.25M LiNO3, DME:DOL (2:1) are presented below

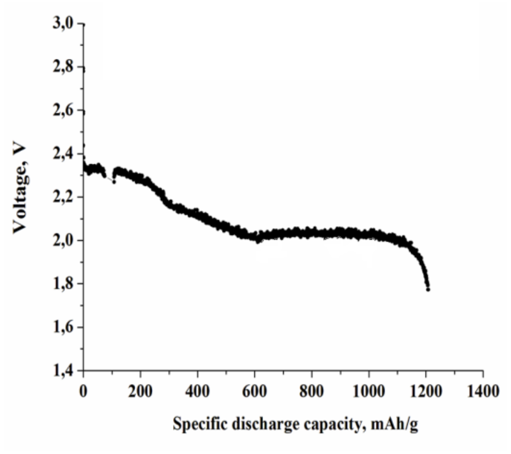

Cathode based on sulfur-79%, nano graphite 21%, without binder

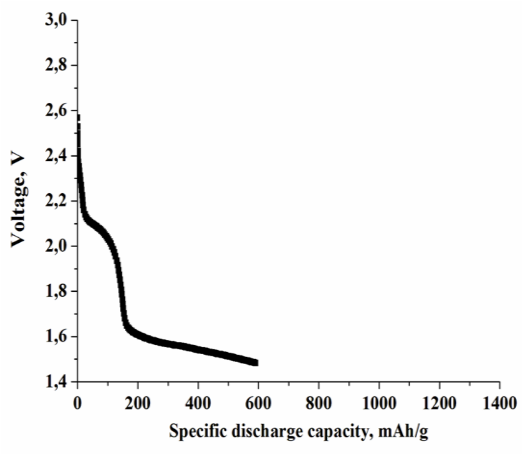

Cathode based on sulfur - 75%, "ordinary" graphite - 10%, carbon black - 10%, binder - 5%.

Conclusions

1. Using of innovative nanostructured carbon compositions for modifying cathodes (for example, based on sulfur, LiMnO4, LiCoO2, LiMnO2, etc.) and without a binder sharply reduces the impedance of Li-S and other batteries, increases energy, power and stability of the battery parameters.
2. High adhesion and cohesion of nanostructured carbon powders with electrode material components allows: to exclude the binder from the electrodes; optimizes the macro- and micro porous structure of the electrode mass.

References

1. J. Gómez, M. V. Sulleiro, D. Mantione. and N. Alegret. A State of the Art. Polymers (Basel). 2021 Mar; 13(5): 745.
2. S.G. Peera, R. Koutavarapu, S. Akula. A Review. Energy Fuels 2021, 35, 15, 11761 11799.Publication Date:July 20, 2021
3. V. Redko, E. Shembel, T. Pastushkin , etc. Method and Device for Rapid Non - Destructive Quality Control of Powdered Materials. US Patent No. 8,102,181
4. Y. Pustovalov, E. Shembel, L. Vishnyakov, etc. Carbon material for electrodes of lithium-ion power sources and method of production thereof. US Patent application No. 10/898631
5. Y, Pustovalov, E. Shembel, V. Redko, T. Pastushkin, etc. PS Global. Word Sience. №2 (42) VoI.1. February 2019

Testing batteries under external force

M.Šedina[a] and T.Kazda[a]

[a] Department of Electrotechnology, Brno university of technology, Brno 61600, Czech Republic

This article briefly shows, how will grow battery production in the world. There is mentioned some studies which are focused on the research of compressed batteries and the last part is describing my research with compressed batteries.

Introduction

With global emission goals and aiming for emission neutrality like EU Fit for 55 and USA Federal Sustainability Plan, scientists need to find ways how to achieve them. One way is using electric vehicles to lower emissions from personal transportation and electric heavy-duty vehicles to lower emissions from goods transportation. With this transition will be many Li-ion batteries (see Figure 1) on the market and in use, after their life in this application will be these batteries reused in the second life or recycled.

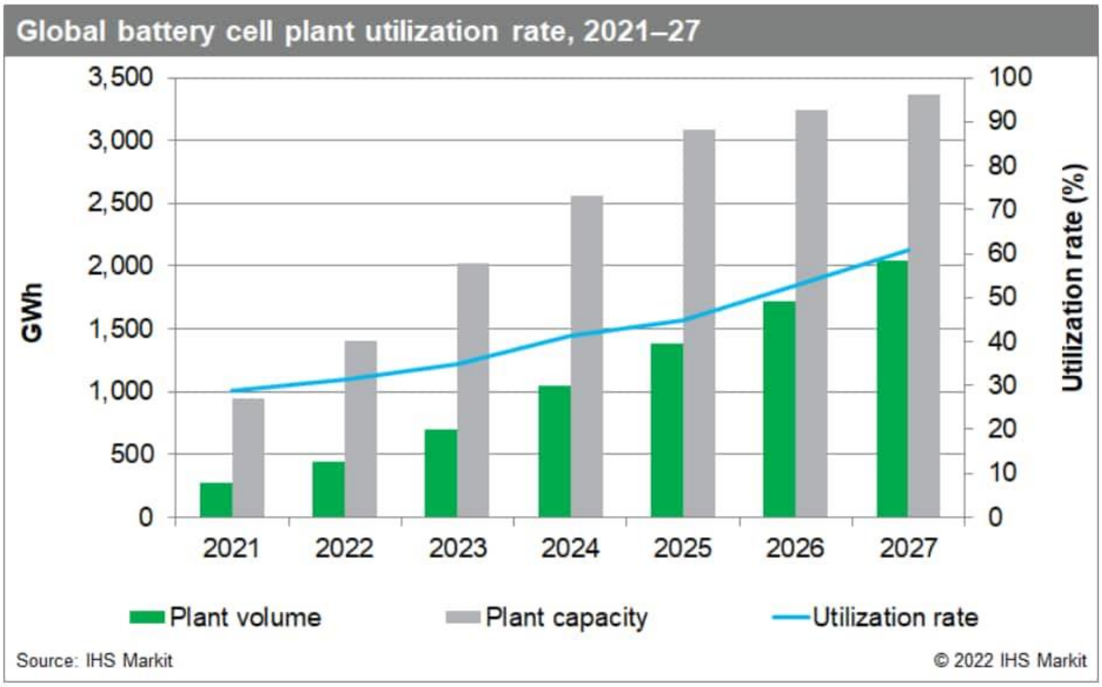

Figure 1. Prediction of global production and production capacity of Li-ion batteries [Chyba! Nenalezen zdroj odkazů.]

Pressure effect on batteries

Applying external pressure to the batteries can significantly extend their lifespan by improving stability, suppressing the growth of internal structures, and enhancing energy efficiency.

Previous studies

There are several articles which focused on studying how external pressure affects the batteries. All these studies are focused on testing small pouch cells made in the laboratory. These studies are mostly focused on the reduction of the negative behavior of next-gen Li-ion batteries with silicon anode, Li-S batteries and Li-ion with solid-state electrolyte.

For example, the study of Müller et al was focused on prolonging the cycle life of batteries with silicon anode and managing of swelling of the battery. The result showed that when you set the right type of pressure, in the study used flexible compression through spring and fixed, and moderate right force, the swelling should be lower, efficiency is stable and the capacity lost is lower [2].

Another study was made by Zhou and his team with a focus to compare compressed and uncompressed NMC pouch cell batteries before and after ageing. The results are that pressure has not had an effect on new batteries but after the ageing, the compression recover partly lost capacity and after decompression didn't lose increased capacity. Better results are achieved by lowering the internal resistance of compressed cells (see Figure 2 A)) and recompressing the layers inside a battery [3], battery layers are decompressed during the ageing because of volume changes, gassing etc. (see Figure 2 B, C).

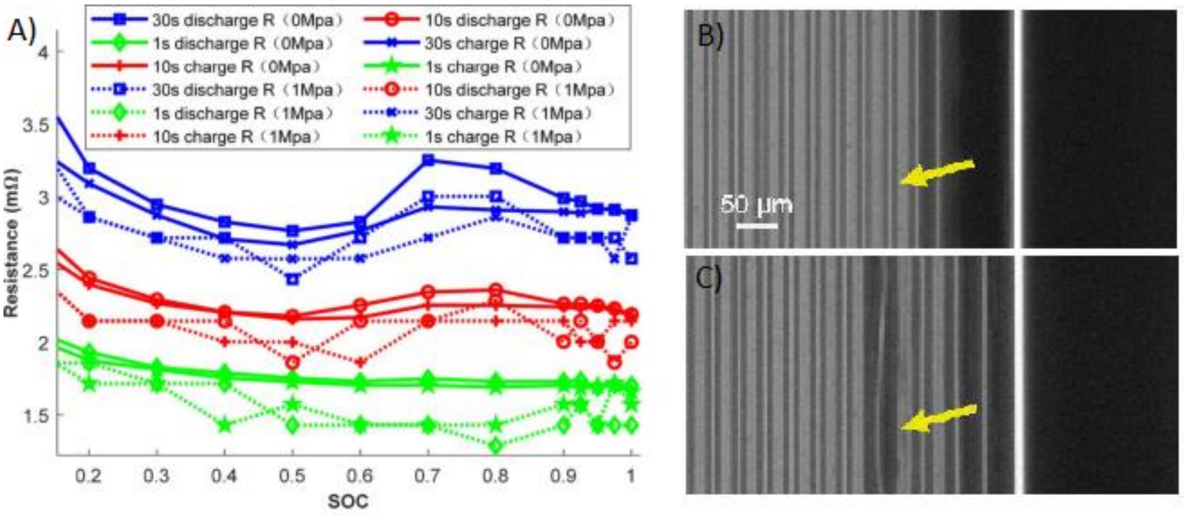

Figure 2. A) Comparison of internal resistance before and after pressure [3] B) Internal structure of cylindrical cell before ageing [4] C) Internal structure of cylindrical cell after ageing [4]

My experiment

In my experiment, I am focusing on applying three levels of external force on automotive pouch cell from the beginning of their life-spam to see how external force affect the capacity during cycling and the current load of the cells. The batteries are 78 Ah cells from Škoda Enyaq. The force is made by a clamp (see Figure 3) with six springs, each spring can make up to 500 N of force. There are used four batteries one is uncompressed, and the other batteries are compressed with a force of 50, 100 and 200 N on each spring. The battery is compressed during the cycling and measuring electrochemical impedance spectroscopy and then is uncompressed and run the parametric test.

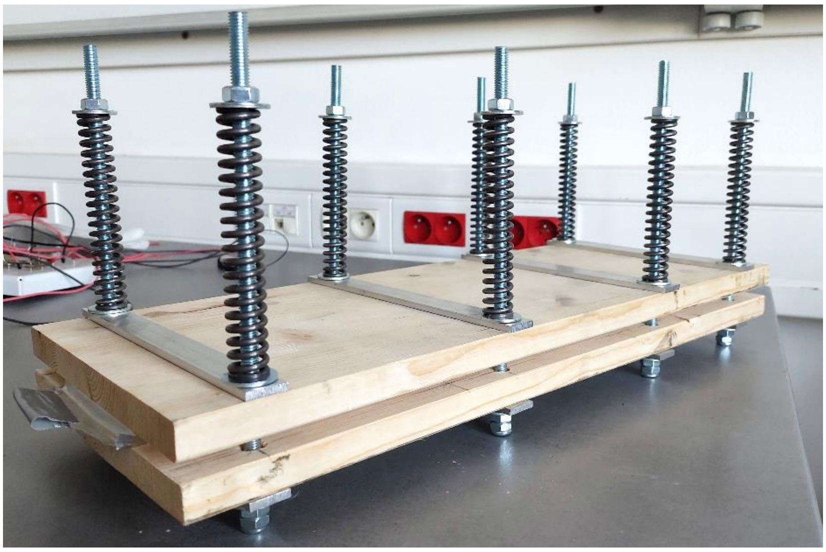

Figure 3. Clamp for an external force

Acknowledgements

This work was supported by the specific graduate research of the Brno University of Technology No. FEKT-S-23-8286. This work was supported by Škoda Auto a.s.

References

1. “Growth of Li-ion battery manufacturing capacity in key EV markets”, *S&P Global*, 02022. https://www.spglobal.com/mobility/en/research-analysis/growth-of-liion-battery-manufacturing-capacity.html (accessed Jul. 12, 2023).
2. V. Müller et al., “Effects of Mechanical Compression on the Aging and the Expansion Behavior of Si/C-Composite|NMC811 in Different Lithium-Ion Battery Cell Formats”, *Journal of The Electrochemical Society*, vol. 166, no. 15, Nov. 2019, doi: 10.1149/2.1121915jes.
3. L. Zhou et al., “A study of external surface pressure effects on the properties for lithium‐ion pouch cells”, *International Journal of Energy Research*, vol. 44, no. 8, Jun. 2020, doi: 10.1002/er.5415.
4. P. Blažek et al., “Multiscale 3D Analysis of Defects and Temporal Development of Electrode Morphology in Lithium-Ion Batteries By X-Ray Computed Tomography”, *ECS Transactions*, vol. 105, no. 1, Nov. 2021, doi: 10.1149/10501.0069ecst.

Electrochemical methods to detect water-contaminated electrolytes for lithium-ion batteries

A. Šimek, T. Kazda and O. Čech

Department of Electrotechnology, Brno University of technology, Brno 616 00, Czech Republic

In this work, the influence of water in electrolytes for lithium-ion batteries is discussed. The focus is on the decomposition of lithium hexafluorophosphate as the most commonly used salt in commercial electrolytes. The presence of water leads to the decomposition of this salt, resulting in a variety of degradation processes in the battery system. The experimental part then deals with electrochemical methods for the detection of changes in reactivity of the electrolyte caused by water content.

Introduction

Lithium-ion (Li-ion) batteries are one of the most commonly used batteries today, and their development is moving forward more and more every year. In general, a Li-ion battery consists of two electrodes (anode and cathode), current collectors (positive and negative), a porous separator and an electrolyte which creates ionic pathway between anode and cathode. The electrolyte is therefore in contact with all structural parts of the battery, so it is essential to pay considerable attention to its development to ensure the time stability and safety of the battery system. [1]

Decomposition of $LiPF_6$ caused by presence of water

Today, the most commonly used type of electrolyte is non-aqueous, which is composed of a lithium salt (most commonly lithium hexafluorophosphate or $LiPF_6$) dissolved in a mixture of organic solvents (such as ethylene carbonate, propylene carbonate, dimethyl carbonate, and others) [2].

$LiPF_6$ undergoes significant degradation when exposed to water, alcohols, or even moisture, although it is stable up to 107 °C in a dry inert atmosphere. It is then described in [3] that the whole degradation process starts with the decomposition of $LiPF_6$ into lithium fluoride (LiF) and phosphorus fluoride (PF_5), which is described by equation (1). The phosphorus fluoride further reacts with water to form hydrofluoric acid (HF) according to equation (2). This reaction is almost negligible at room temperature, but in the presence of organic solvents the equilibrium of the equation shifts to the right, resulting in increased HF acid production according to equation (3). The reaction is not catalyzed by temperature and water alone, but is activated by the release of protons (H^+) during the formation of LiF(s) in the SEI layer. The precipitation of LiF into solid form does not directly affect the formation of HF acid, but the released protons can further react with $LiPF_6$ to form additional HF acid. This process is then described by equations (4) and (5) and figures as a positive feedback in the overall context of HF acid formation. [3]

$$LiPF_6 \rightarrow LiF + PF_5 \tag{1}$$

$$PF_5 + H_2O \rightarrow POF_3 + 2HF \tag{2}$$

$$Li^+ + HF \leftrightarrow LiF(s) + H^+ \tag{3}$$

$$H^+ + PF_6^- \leftrightarrow H - F - PF_5 \tag{4}$$

$$H - F - PF_5 \rightarrow HF + PF_5 \tag{5}$$

The formed HF acid can significantly affect the performance and especially the service life of the battery, as its presence can lead to corrosion of the current collectors, which can be followed by delamination of the active mass and thus a reduction in the overall battery capacity. Another consequence can be etching of the glass separator used in experimental measurements, which can lead to internal short circuits between the electrodes. [3]

Experimental

In the experimental part, the stability of pure electrolyte labeled 1.5M LiPF6 in EC:DMC 1:2 and then electrolyte contaminated with 250 ppm H_2O were measured. For the measurements, different configurations of electrochemical test cells from EL-CELL were used to determine the stability of the electrolyte against the battery components. The configurations included steel-steel, Li-steel, Li-Al and Li-Cu. The assembly of these cells and the overall sample handling was performed in a glove box manufactured by Jacomex in the presence of an argon atmosphere. Electrochemical measurements were then performed on a BioLogic VMP3 multi-channel potentiostat. Figure 1 below shows the cyclic voltammetry results for pure and contaminated electrolyte and change in open circuit voltage (OCV) curves with time influenced by HF acid formation.

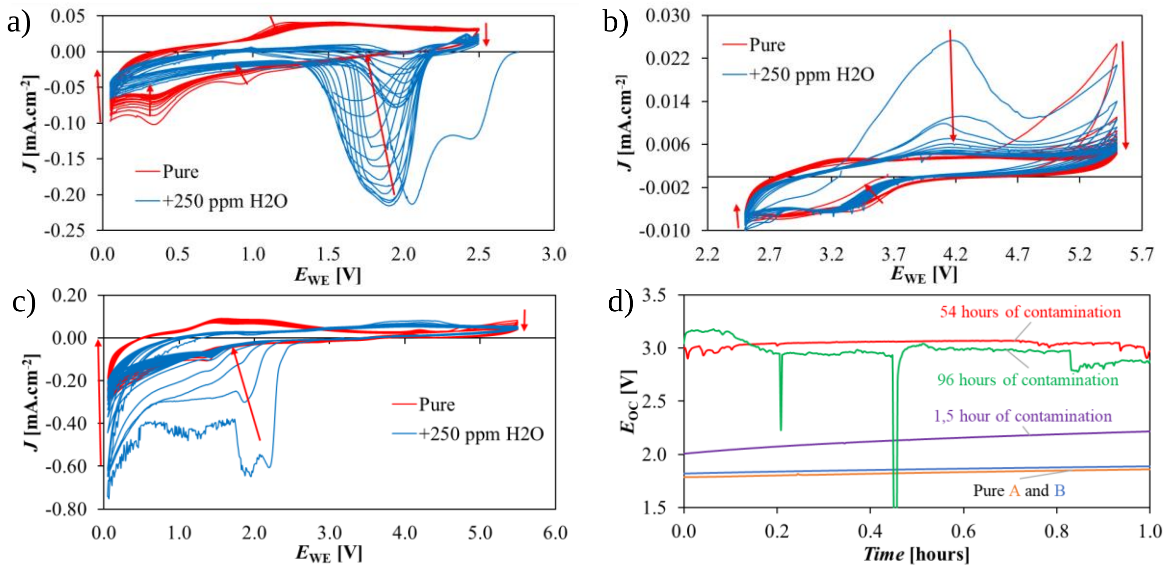

Figure 1. *Cyclic voltammetry results measured on: a) Li-Cu configuration; b) Al-Li configuration and c) Li-steel configuration. d) effect of HF acid evolution on open circuit voltage curves for Li-steel configuration*

Conclusion

The cyclic voltammetry results on Figure 1 shows substantial difference between the curves for clean and water contaminated electrolyte. The significant current response at a potential of 1.5-2.0 V probably corresponds directly to the electrolysis of the water present. The small peaks in the curves are most likely due to etching of the glass separator by the HF acid, which is discussed in the next paragraph.

Figure 1d shows the OCV curves and their change with increasing time from water contamination. It can then be seen from the results that there is an increase in the OCV and a gradual formation of short circuits between the electrodes. These short circuits are caused by the HF acid, the concentration of which increases with increasing time since water contamination. The high concentration of HF then results in etching of the glass separator that was used in the electrochemical test cells.

The presence of water in the electrolyte is highly undesirable as it leads to a rapid degradation of the electrolyte and thus of the entire battery system. This contamination must therefore be carefully controlled during the electrolyte and battery manufacturing process. In this work, rapid electrochemical methods have been presented that can detect contaminated electrolyte. Their use may then find application before further measurements are taken in the laboratory, so that water-degraded electrolyte is not used and the whole measurement is not affected.

Acknowledgments

This work was supported by the specific graduate research of the Brno University of Technology No. FEKT-S-23-8286. We acknowledge CzechNanoLab Research Infrastructure supported by MEYS CR (LM2023051).

References

1. Q. Li, J. Chen, L. Fan, X. Kong, and Y. Lu, “Progress in electrolytes for rechargeable Li-based batteries and beyond”, *Green Energy & Environment*, vol. 1, no. 1, pp. 18-42, 2016.
2. K. Xu, “Electrolytes and Interphases in Li-Ion Batteries and Beyond”, *Chemical Reviews*, vol. 114, no. 23, Dec. 2014, doi: 10.1021/cr500003w.
3. S. F. Lux, I. T. Lucas, E. Pollak, S. Passerini, M. Winter, and R. Kostecki, “The mechanism of HF formation in LiPF6 based organic carbonate electrolytes”, *Electrochemistry Communications*, vol. 14, no. 1, pp. 47-50, 2012.

Spray drying Synthesis of Perspective Materials for Cathodes of Li-ion Batteries with Low Cobalt Content

H. Hálová[a], L. Chladil[a]

[a] Department of Electrotechnology, Faculty of Electrical Engineering and Communication, BUT,
Technická 10, 616 00 Brno, Czech Republic

Our contribution deals with the synthesis possibilities of cathode materials with low cobalt content for Li-ion batteries. There are compared different kinds of synthesis in terms of time, simplicity, and needed temperature in this paper. Among these methods, the spray drying synthesis emerged as the most promising – especially due to the fast process and possibility to operate at low temperatures. The experimental part is focused on the creation of the synthesis apparatus because commercial equipment is not very suitable for laboratory research. During experiments, the attention was paid also to the synthesis temperature, flow rate, length, and temperature of calcination to choose suitable parameters.

Introduction

The selection of cathode material for modern Li-ion batteries is influenced by customer needs. Battery capacity, charging speed, lifespan, and stability play a key role in the customer's evaluation of the device, as well as battery. That is why it is necessary to take into account battery parameters such as voltage against lithium, specific capacity of the material (theoretical as well as practical) and energy density which influence the volume and weight. Another important parameter is also the possibility of recycling and availability of contained elements – such as cobalt which is considered a rare element and its content is being slowly reduced in modern batteries [1] [2].

For the preparation of the cathode material also the process of synthesis is important. According to the published articles the cathode materials are mostly synthesized by solid state reaction, sol gel method, hydrothermal, and solvothermal synthesis. All of these methods have their pros and cons, and it is important to take them into account for the specific cathode material. Another possibility is spray drying synthesis which is often considered the most appropriate for mass production. The advantage of this method is simplicity, operation in low temperatures, particle uniformity, a reduction of calcination time is also expected [3].

The spray drying synthesis can be applied to suspension, solution, or their combination [3] and the main principle of this method is the production of small-sized nanoparticles via atomization and subsequent solvent removal [4]. The first step to maintaining the small-sized particles is to atomize the initial liquid (precursor) by an atomizer. This atomizer can be based on the principle of e.g.: air-shear nozzle, rotary cage atomizer, or ultrasonic nebulizer. The atomizer type plays a key role in droplet production and determines the particle size – the finest particles can be achieved using ultrasonic technique [4]. The droplet diameter is also determined by the viscosity of the solvent, surface tension, and flow rate (direct proportionality). The produced droplets are entrained by the airflow into the chamber where the conversion to the particle is made by solvent removal. That can be achieved by several techniques such as heating by the hot carrier gas, hot furnace, or diffusion drier. After the production of solvent-free particles, it is important to collect them by appropriate technique according to particle diameter. The used methods to collect the particles are e.g.: filtration, gravity settling, cyclone, or electrostatic precipitation.

Instrumentation

The apparatus designed for spray drying synthesis in laboratory conditions consists of 3 important parts of the apparatus – an atomizer, a drying chamber, and a collecting chamber. Regarding the collecting chamber, several variants have been created and modified after initial experiments. The first version of the collecting chamber consisted of a chamber with filter paper Pragolab with different porosity, but after a few experiments, irregular quantity of synthesized particles was observed. As particles were deposited directly on the filter paper, the filter became clogged after some time and the airflow was reduced. Because of that a different option of collecting particles was chosen – the electrostatic precipitator. The apparatus designed for spray drying synthesis in laboratory conditions can be seen in Figure 1 (electrostatic collection of particles).

For the preparation of cathode materials for Li-ion batteries can be used nitrates and acetates (well soluble in water), citrates as precursors together with a liquid e.g.: ethanol, water, or ethylene glycol-cyclohexane. The initial experiments with the laboratory apparatus were undertaken with solution of $Li(OAc) \cdot 2H_2O$, $Ni(OAc)_2 \cdot 4H_2O$, $Mn(OAc)_2 \cdot 4H_2O$ a $Co(OAc)_2 \cdot 4H_2O$ were dissolved in water with the citric acid with mass ratio of 2:1 [5].

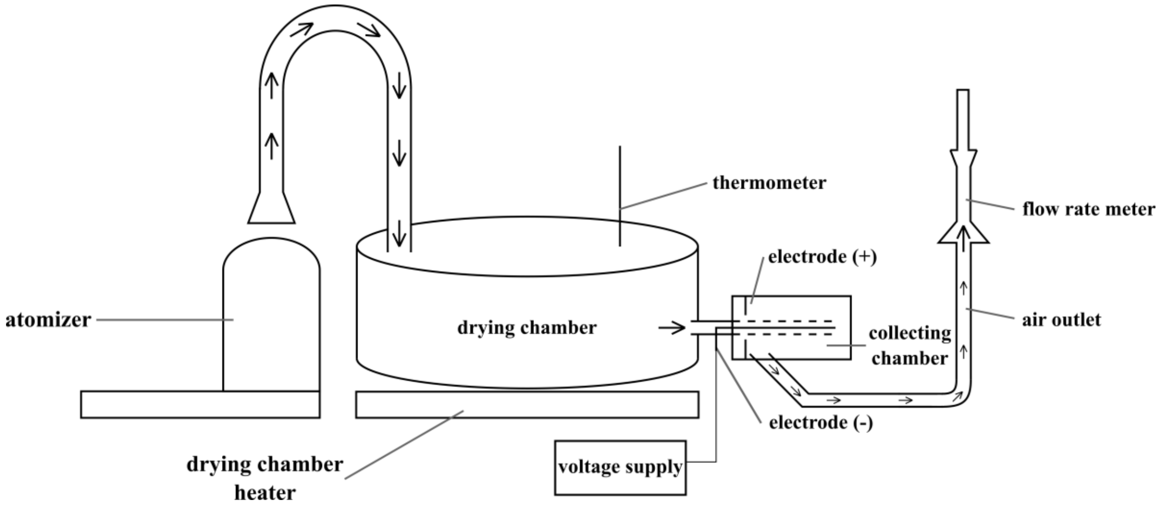

***Figure 1**. Schematic drawing of the apparatus for spray drying synthesis*

Results and discussion

During the synthesis process, the maximum obtained weight of particles was 60 mg (length of synthesis 30 mins). The parameters which influence the effectivity of synthesis and particle diameter were: flow rate 3 l/s, temperature of the drying chamber 170 °C. The synthesized particles can be seen in Figure 2. In Figure 2. it is also visible, that particle size distribution was from 300 nm to 1.1 µm, whereby 70 % of the particles were smaller than 600 nm.

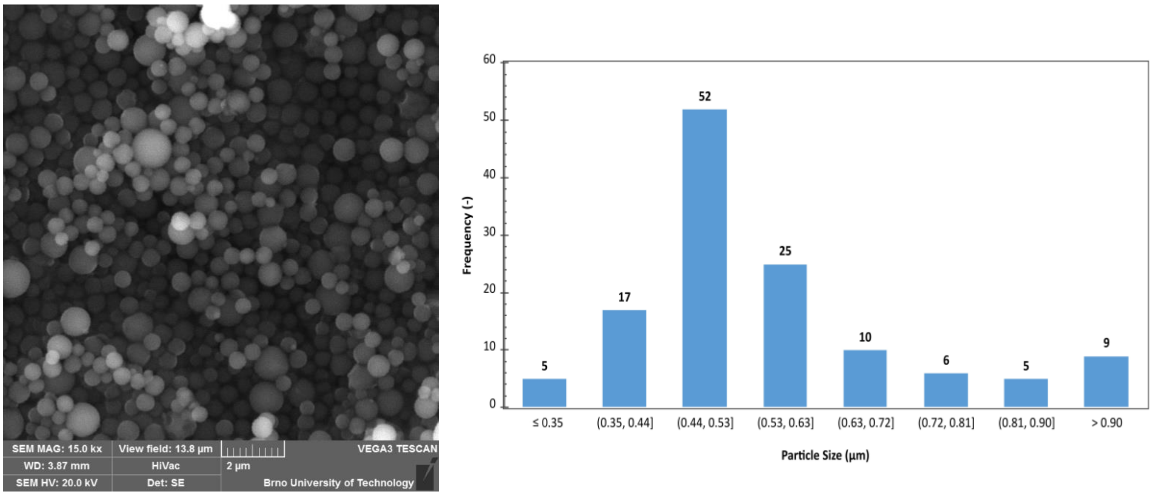

***Figure 2**: SEM picture of synthetized particles, view field 13,8 μm (left), particle size distribution (right)*

Additionally, elemental analysis was performed – the distribution of elements was uniform in the whole sample, and the quantity of each element corresponded to the assumptions.

The synthesis of particles was followed by calcination. During the calcination, weight loss was more than 75 % which is more than expected. The temperature during calcination was maintained at 750 °C – the experiments have shown that at higher temperatures large crystallite form.

Conclusion

This paper focuses on the spray drying synthesis and the possibility of synthesis in laboratory conditions. There were described the parameters of synthesis which influence the particle size and its distribution together with the final apparatus. From the SEM images as well as element analysis we can conclude, that it was possible to modify conventional, but expensive, apparatus to a smaller laboratory one without affecting the synthesized particles.

Currently, the main disadvantage lies still in the low amount of synthesized particles, which is in the amount of milligrams. Another potential problem that will be examined relates to the usage of acetates during synthesis and their reaction with the air humidity after synthesis which can cause wetting of the particles as well as particle magnification.

References

1. M.S. Whittingham, *Chem. Rev.*, **104**, p. 4271-4301 (2004).
2. N. Nitta and F. Wu, *Materialstoday*, **18**(5), p. 252-264 (2015).
3. B. Vertruyen and N. Eshraghi, *Materials* (Basel), **11**(7), p. 1076 (2018)
4. B. D. Nandiyanto and K. Okuyama, *Advanced Powder Technology*, **22**, p. 1-19 (2011)
5. S. Yucheng and Y. Xia, *Electrochem. Acta*, **51**, p. 5581-5586 (2006).

Application of "green" manganese dioxide in solid-state supercapacitors

B. Mladenova[1], K. Pashova[2], I. Hinkov[2], M. Dimitrova[1], A. Stoyanova[1]

[1] Institute of Electrochemistry and Energy Systems, Bulgarian Academy of Sciences,
Acad. G. Bonchev Str., 10, 1113 Sofia, Bulgaria

[2] University of Chemical Technology and Metallurgy, bul. "Kliment Ohridski" 8, 1756 Sofia, Bulgaria

A green synthesis of MnO_2 is presented in this study. MnO_2 was obtained from $KMnO_4$ using plant extracts from Calendula officinalis or Tilia cordata as reducing agents. The obtained materials were structurally and morphologically characterized using by UV-Vis spectrophotometry, transmission electron microscope (TEM), X-ray diffraction (XRD) and Brunauer-Emmett-Teller (BET) methods.

"Green" MnO_2 samples were investigated as positive electrode materials in solid-state supercapacitor cells. The commercial product Aquivion®E87-05S membrane activated in 1M Na_2SO_4 solution was used as separator and electrolyte. Galvanostatic charge/discharge tests between 0.05 and 1.6 V and cyclic voltammetry in the same voltage window were carried out. Cells were subjected to continuous cycling at a current load of 240 mAg^{-1} for up to 1000 cycles.

The synthesized MnO_2 from Calendula officinalis extract was found to exhibit very good capacitive behaviour, high energy density and stability, and is a suitable electrode material for the development of an eco-friendly solid-state supercapacitor.

Acknowledgement:

This research was supported by contract No. DO1-286/ 07.10.2020, funded by the Ministry of Education and Science of Bulgaria, to whom the authors express their gratitude

Comparative Study of Electrochemical Performance of Symmetric Supercapacitors with Aqueous Electrolyte and with Polymer Exchange Membrane

L. Soserov[1], B. Mladenova[1], A. Stoyanova[1], B. Karamanova[1], A. Arenillas[2]

[1]Institute of Electrochemistry and Energy Systems – BAS
10 Acad. G. Bonchev Str., 1113 Sofia, Bulgaria

[2]Instituto de Ciencia y Tecnología del Carbono, INCAR-CSIC, Francisco Pintado Fe 26,
33011 Oviedo, Spain

The symmetric supercapacitors are electrochemical capacitors with higher energy density than conventional. Both their positive and negative electrodes contain the same type of electrode active material.

Carbon xerogels are a type carbon material which properties may be designed, structurally and chemically, in order to fit the requirements for their final application They possess tunable porosity, high purity and electrical conductivity and are very promising as active electrode materials for supercapacitors.

In this study, the electrochemical properties of symmetric supercapacitors based on an activated carbon xerogel (AX-1500) were compared in a polymer Aquivion^{TM} electrolyte membrane (used as electrolyte and separator) and in an aqueous solution of 1 M KOH. The membrane was previously exchanged to the K^+ form by immersion in 1 M KOH. AX-1500 was prepared by polymerization of resorcinol and formaldehyde in a sol-gel process aided by microwave heating. Its physicochemical properties have been characterized by various methods.

Electrochemical tests were carried out by cyclic voltammetry, galvanostatic charge/discharge measurements, impedance analysis and long-term durability tests. The relationship between the structure and morphology of the carbon xerogel and the nature of the electrolyte was established, which may be relevant to the design of supercapacitors that provide high power and energy density.

Acknowledgement

This research was supported by contract No. DO1-286/ 07.10.2020, funded by the Ministry of Education and Science of Bulgaria, to whom the authors express their gratitude

The Potential of *In Operando* Scanning Electron Microscopy for Solid State Chemistry at Elevated Temperature – The Densification of LSM:YSZ Composite

Michal Carda[a], Libor Novák[b], Daniel Budáč[a], Martin Paidar[a], Karel Bouzek[a]

[a] Department of Inorganic Technology, University of Chemistry and Technology, Prague, Czech Republic

[b] Thermo Fisher Scientific, Brno, Czech Republic

The understanding of the course of high temperature processes, such as sintering, still eludes the scientific community despite its importance. Scanning electron microscopy (SEM) is an ideal technique to study such morphological changes. So far, this technique was limited to experiments at ambient temperature. The novel combination of SEM with MEMS heating chip can overcome this limitation. In this work, the application of *in operando* SEM is demonstrated by LSM:YSZ composite densification case study. A well-understood development of microstructure during the sintering process of this composite is crucial to address a necessary compromise between particle interconnection and mass transport. It was shown that the densification of LSM:YSZ occurred in two steps. In addition, the formation of inter particle ligaments was caused exclusively by LSM phase. This case study demonstrated that SEM with heating stage is very promising for *in operando* studies related to numerous technologies operating at high temperature.

Introduction

In operando techniques offer a considerable insight into any investigated system. In addition, they allow to observe intermediate states, which can be a crucial information for numerous technologies. Scanning electron microscopy (SEM) is an optimal technique to study morphological features of materials (and elemental with EDX detector) with high resolution. However, the SEM was, until recently, limited to operate in an ambient temperature. To overcome the operating temperature limitation, we propose the utilization of a novel combination of SEM with MEMS heating chip. Such combination allows to observe processes, which are particularly crucial for solid state chemistry, up to 1200 °C.

In this work, one of many possible applications of *in operando* SEM is demonstrated – the $La_{1-x}Sr_xMnO_{3-\delta}$ (LSM) : ZrO_2:Y_2O_3 (YSZ) composite densification. This LSM:YSZ composite, considered a state-of-the art material for oxygen electrode in solid oxide cells (SOCs), has been studied for several decades by various *ex situ* methods (1-2). The fabrication process of functional ceramics, such as LSM:YSZ electrodes, involves a crucial densification step, which in principle involves heating of a powder precursor to a high temperature for a defined time period to form ligaments between the individual particles. Any morphological changes had been, therefore, impossible to observe by means of conventional SEM. During the densification process a complex inner microstructure is being formed and its properties govern the electrochemical properties of resulting electrodes. In this case, a compromise between particle interconnection and ample mass transport is essential (3). A well-understood development of microstructure and surface composition during the densification process is crucial to address these contradictory requirements (i.e. mass transport and particle interconnection).

So far, only a few experimental studies were published regarding the characterization of *in operando* solid-state chemistry at elevated temperatures, such as X-ray tomography, photoelectron microscopy/spectroscopy, dilatometry, SEM, TEM (4-6). However, none of these groups investigated the densification process of any electrode material, such as LSM:YSZ. Considering the limited applicability of experimental techniques for high temperature processes, a modeling approach can be valuable. The most advanced models are based on the master sintering curve approach or the kinetic Monte Carlo methods in combination with the discrete elements method (7-8). However, the accuracy of these numerical models frequently suffers from the presence of: (i) the estimation of unknown parameters (i.e., kinetic parameters), (ii) non-uniform particle distribution or particle orientation, (iii) multi-phase porous composites with diverse melting points of constituents.

The goal of this study is, therefore, to investigate *in operando* the development of structural, in the manner of elemental surface enrichment of constituents, and morphological changes during the densification process of LSM:YSZ composite. This will help to set the resulting inner microstructure with the applied thermal treatment into relation.

Results & Discussion

The experiments designed to observe morphological changes showed that the LSM:YSZ densification process occur in two steps. The first step has an onset at 900 °C and was associated with the densification of LSM agglomerates. At this point a significant degree of porosity emerged within the composite. The optimal porosity ensures ample mass transport within the resulting electrode, yet a high amount of porosity can be undesirable as the uniformity and mechanical stability of the microstructure may be compromised. The second densification step of LSM:YSZ composite began at 1000 °C with maximum at 1150 °C. This was essentially a self-healing process resulting in a well-interlinked and mechanically stable composite. At this temperature, all LSM particles started to form interparticle ligaments. On the other hand, YSZ particles were not affected by such thermal treatment at all in terms of either morphological or structural changes. This implies that YSZ phase, in this case, acts as inert phase and effectively retarding the sintering process.

The present work includes also a study of surface elemental changes. Particularly, the LSM phase is well-known for its complex defect chemistry, which is directly influenced by temperature, oxygen partial pressure and polarization. The main observed process were: (i) Mn interdiffusion from LSM into YSZ lattice, (ii) the formation of insulating $La_2Zr_2O_7$ phase, (iii) SrO phase segregation from LSM lattice. It was confirmed that no detectable $La_2Zr_2O_7$ phase or Mn interdiffusion was observed at the LSM-YSZ interface after 40 hours at high vacuum. However, we were not able to directly observe the enrichment of the LSM surface by SrO due to the utilized EDX limitations.

Conclusion

To conclude, a slight variation in sintering temperature and/or time leads to a significant difference in a different sintering degree due to the different void fraction in the body of the electrode. This outcome is reflected by a major inconsistency in reported electric conductivity of the commonly utilized 50:50 wt.% ratio of LSM:YSZ.

Although this experimental technique was used only for this case study, it is promising to provide a detailed insight into *in situ/in operando* studies to a number of phenomena (such as sintering, synthesis processes of various materials, formation of new phases, delamination, etc.) relevant to numerous technologies.

Acknowledgments

This work was supported by the Technology Agency of the Czech Republic under project no. TK04030143 and by the Junior research grant of the rector of the UCTP.

References

1. M. Carda, D. Budac, M. Paidar, and K. Bouzek, *ECS Trans.*, **111**, 1279 (2023), http://dx.doi.org/10.1149/11106.1279ecst.
2. O. O. Agbede, K. Hellgardt, and G. H. Kelsall, *Mater. Today Chem.*, **16**, (2020), http://dx.doi.org/10.1016/j.mtchem.2020.100252.
3. D. Budáč, V. Miloš, M. Carda, M. Paidar, J. Fuhrmann, and K. Bouzek, *Electrochim. Acta*, **457**, 142512 (2023), http://dx.doi.org/10.1016/j.electacta.2023.142512.
4. J. Janek, B. Luerßen, E. Mutoro, H. Fischer, and S. Günther, *Top. Catal.*, **44**, (2007), http://dx.doi.org/10.1007/s11244-006-0132-4.
5. B. P. McCarthy, L. R. Pederson, H. U. Anderson, X.-D. Zhou, P. Singh, G. W. Coffey, and E. C. Thomsen, *J. Am. Ceram. Soc.*, **90**, 3255 (2007), http://dx.doi.org/10.1111/j.1551-2916.2007.01890.x.
6. D. W. Ni, K. B. Andersen, and V. Esposito, *J. Eur. Ceram. Soc.*, **34**, (2014), http://dx.doi.org/10.1016/j.jeurceramsoc.2014.04.044.
7. Y. Zhang, C. Xia, and M. Ni, *Int. J. Hydrogen Energy*, **37**, (2012), http://dx.doi.org/10.1016/j.ijhydene.2011.11.020.
8. Z. Yan, S. Hara, and N. Shikazono, *Scr. Mater.*, **146**, (2018), http://dx.doi.org/10.1016/j.scriptamat.2017.10.035.

R&D in Fuel Cells and Hydrogen Based Technologies @ ICPE-CA Bucharest

Gimi A. Rimbu, Nicoleta-Oana Nicula and Eduard-Marius Lungulescu

National R&D Institute for Electrical Engineering (ICPE-CA) 313 Splaiul Unirii, Sector 3, 030138,
Bucharest, Romania

PEM fuel cells (PEMFCs) are among the most promising alternative energy conversion technologies considered for applications in transportation and portable devices. However, the fabrication cost of the system and its components: catalysts, electrode and bipolar plates, is an obstacle for the PEMFC product commercialization. Work at ICPE-CA Bucharest addresses the needs of the PEM fuel cell industry for more efficient and sustainable materials to reduce costs, addresses environmental concerns and supports the growing demand for PEM fuel cells in a wide industrial area. The potential benefits expected will be low cost, high performance and long lifetime PEM fuel cells, that will contribute to the circular economy and clean energy transition, by replacing current materials with sustainable, renewable, and environmentally friendly materials.

Acknowledgements

The financial support was provided by the Ministry of Research, Innovation and Digitization, through contracts: 42N/PN23140102/2023 and 25PFE/2021

Development of Structured Electrodes for Solid Oxide Electrolysis Cells

D. Budáč[a], N. Adamová[a], M. Sádecká[b], M. Carda[a], M. Paidar[a], K. Bouzek[a]

[a] Department of Inorganic Technology, University of Chemistry and Technology, Prague, Czech Republic

[b] Department of Inorganic Technology, Slovak University of Technology in Bratislava, Bratislava, Slovakia

Functional composites of electronic and ionic conductors, are the backbone of oxygen and fuel electrodes in the solid oxide cells. Oxygen electrode is often fabricated from lanthanum strontium manganite and yttria-stabilized zirconia (LSM:YSZ) composite, while fuel electrode is fabricated from Ni:YSZ cermet. There are multiple benefits of using composite electrodes: Mechanical stability is significantly enhanced; Performance is proportional to the amount of simultaneous contact of ionic conductor, electronic conductor and gaseous phase. However, presence of YSZ in the electrode increases ohmic losses. In this study, structure and composition of electrodes is optimized to maximize the performance while maintaining sufficient lifespan. In the case of fuel electrode, the results suggest that presence of YSZ is essential for both, performance and lifespan as it increases the TPB and serves as a scaffold for Ni network. Contrarily, in the oxygen electrode, presence of YSZ has rather a detrimental effect on the electrode performance.

Introduction

Among other electrochemical devices, electrolysers offer an efficient way of electrical to chemical energy conversion suitable for energy storage. On top of that, solid oxide electrolysis cells (SOECs) take advantage of enhanced physico-chemical conditions at elevated operation temperatures at 700 to 900 °C. At such temperature, kinetics of electrochemical reactions are significantly enhanced, thus there is no need for Pt-based electrocatalysts. In addition, the equilibrium voltage of water splitting is lower by 20 % in comparison to conventional low-temperature processes resulting in a significantly more efficient operation (1). Distinctive feature of the SOECs is the use of ceramic materials throughout the cell due to the elevated temperatures. However, the high operation temperature enhances also the kinetics of degradation phenomena. Thus, the challenge lays in development of high-performance cell design with long lifespan.

The SOECs consist of three crucial components, each having its distinctive traits – fuel electrode, oxygen electrode and electrolyte. The electrolyte must be dense and non-conductive for electrons in order to prevent gas diffusion and parasitic currents. In addition, chemical stability in both, reduction and oxidation environment, is required for the electrolyte material. The electrodes need to be highly conductive for electrons, electrochemically active towards the half-cell reactions while being porous in order to ensure sufficient transport of reactants/products. Furthermore, oxygen electrode must be stable in oxidation environment, while the fuel electrode must be stable in reducing environment. Since the whole system is compact, the electrode materials must be inert to the electrolyte to prevent formation of any undesired phases and exhibit similar thermal expansion coefficient to prevent delamination (2). At the same, suitable electrode materials need to be used to ensure high performance.

Performance of the electrodes is governed mainly by three parameters: kinetics of electrochemical reactions, electrical conductivity and transport of reactants/products.

In general, electronic conductors show high electronic conductivity, however they exhibit negligible ionic conductivity. This limits the active area of the electrodes exclusively to so called three phase boundary (TPB) – interface of an electrode, electrolyte and gaseous phase. In the case of electrode composed of exclusive electronic conductor, the TPB is limited only to the contact with the electrolyte component leading to lack of TPB hindering the cell performance. Introduction of electrode material into the electrolyte leads to the increase of the TPB. Such electrodes are called composite electrodes and can be either composites of two ceramic materials or of metal and ceramic, so called cermets. However, electrolyte materials show negligible specific electrical conductivity in comparison to the electrode materials. This leads to decrease in total conductivity in the case of composite electrodes. Thus, the optimization of composite electrode lies in the trade-off between kinetics and conductivity (3).

The optimal trade-off results between kinetics and conductivity can be achieved by grading the composite electrode composition separating the electrode in two distinct layers (4). First, an electrocatalytically active layer with the maximum amount of TPB in direct contact with the electrolyte. Second, highly conductive layer with minimal Ohmic potential drop. The crucial parameter of this design is the thickness of the active layer as it exhibits a significant ohmic potential drop. The aim of this work is to determine the optimal composition and structure of the electrodes for the use in SOECs.

Experimental

Commercially available state-of-the-art powders were used in this study. Yttria-stabilized zirconia (YSZ) was used as electrolyte material, lanthanum strontium manganite (LSM) as an oxygen electrode material (“OE”) and nickel as a fuel electrode material (“FE”). Composites of LSM:YSZ and Ni:YSZ (both 50:50) were used as an active electrode material. Electrolyte was fabricated by uniaxial pressing of the YSZ powder and sintering at 1400 °C. Symmetrical “OE”|YSZ|LSM:YSZ and “FE”|YSZ|Ni:YSZ cells were prepared by screen printing of electrode powder suspensions on the electrolyte and sintering at 1150 °C and 1400 °C, respectively. Both “OE” and “FE” were deposited in three layers (layer thickness ca. 10 μm) with varying number of layers of active electrode material complemented by highly conductive pure electrode material. The fabricated cells were tested in three electrode assembly.

Study results

The results showed that in the case of the fuel electrode, YSZ content is necessary throughout all the electrode material body based on two main findings. Firstly, kinetics of hydrogen evolution reaction is strongly dependent on the TPB length, hence the optimal thickness of the active Ni:YSZ layer was found to be at least 30 μm. Secondly, the results suggest that even the highly conductive layer is required to contain a certain amount of YSZ to prevent undesirable structural changes during the activation of electrode, resulting in electrode degradation.

In the case of the oxygen electrode, the best results were achieved with electrodes composed either by pure LSM or with one active LSM:YSZ layer at the electrode-electrolyte interface. The results suggest that optimal active layer thickness is less than 10 μm in the case of the oxygen electrode. This is probably caused by non-negligible ionic conductivity of LSM decreasing the reliance purely on the TPB (5).

In this study, composition of electrodes suitable for SOECs was optimized. Content of YSZ in the oxygen electrode has no significant effect on its properties, whereas a certain amount of YSZ is required in the fuel electrode to enhance both, mechanical stability and performance. Achieved information is crucial for further development of SOEC stacks.

Acknowledgments

This work was supported by the Technology Agency of the Czech Republic under project no. TK04030143 and Specific University research (A2_FCHT_2023_043).

References

1. L. Mingyi, et al., *J. Power Sources*, **177**(2), p. 493, (2008)
2. A. V. Virkar, *Int. J. Hydrog. Energy*, **35**(18), p. 9527, (2010)
3. D. Budáč et al., *Electrochim. Acta*, **457**, 2023
4. L. C. R. Schneider et al., *Electrochim. Acta*, **52**(9), p. 3190, (2007)
5. M. Carda et al., Curr Opin Electrochem, (2021)

High-performance materials processed by gamma irradiation for special applications – membranes, catalysts and electrodes

Eduard-Marius Lungulescu[1], Nicoleta-Oana Nicula[1], Gimi Rimbu[1], Radu Fierascu[2], Elena Radoi[1]

[1]National R&D Institute for Electrical Engineering (ICPE-CA) 313 Splaiul Unirii, Sector 3, 030138, Bucharest, Romania

[2]National Institute for Research and Development in Chemistry and Petrochemistry – ICECHIM Bucharest, 202 Spl. Independentei, 060021 Bucharest, Romania

Gamma radiation processing of materials is a highly potent technique that has demonstrated its versatility in various industries, including fuel cells, photovoltaic cells, and energy storage materials. This powerful method involves the use of gamma radiation to modify the structure and properties of materials, leading to significant advancements in these specific areas of application.

One notable application is the radiation-grafting of membranes for polymer electrolyte fuel cells, which enables the production of proton exchange membranes (CEMs) for low-temperature PEMFCs, acid-base composite membranes for high-temperature PEMFCs, and anion exchange membranes (AEMs) for PEAFCs.

Additionally, gamma radiation pretreatment of carbon materials shows promise in improving their properties for the development of high-performance supercapacitors, making them suitable for large-scale energy storage applications.

Moreover, gamma radiation synthesis of metal nanoparticles, such as Ag, Au, Pt, Pd, Ru, Rh, Ir, Ni etc. and their alloys, has greater potential to be used in renewable energy applications. These nanoparticles could serve as plasmonic materials in *solar cells*, enhancing light absorption or as catalysts in *hydrogen production*, *fuel cells*, and *batteries*, improving energy conversion efficiency and storage capacity. Furthermore, metal nanoparticles find applications in *photocatalysis*, harnessing solar energy for various renewable energy processes (including hydrogen production).

Compared to conventional methods, the radiation-induced grafting technique offers advantages such as simplicity, cost savings, energy efficiency, and environmentally friendly characteristics. Similarly, radiochemical synthesis of metal nanoparticles provides rapid and controllable synthesis, precise size and shape control, versatility in nanoparticle composition, and reduced chemical and biological waste generation. These attributes make both techniques promising for industrial scalability and the advancement of renewable energy technologies.

Acknowledgements:

The financial support was provided by Ministry of Research, Innovation and Digitization, through contracts: 42N/PN23140201/2023, 612PED/2022 and 25PFE/2021

Hydrogen Production with Reduced Energy Consumption for Use in Fuel Cells and Energy Sector

Volodymyr Nefedov, Yuliya Polishchuk, Vadim Matveev, Mykhailo Sukhyi

Ukrainian State University of Chemical Technology, Dnipro, 49005, Ukraine

Attention to renewable, environmentally friendly energy sources is associated with a critical impact on the environment and the quality of human life of fossil fuel combustion products. Hydrogen is one such attractive material. On the one hand, it can be used as the active substance of a fuel cell. Moreover, the use of hydrogen-oxygen fuel cells does not cause local pollution, since the product of the interaction of these components is pure water. On the other hand, hydrogen can be used as a way of accumulating and transporting energy with its subsequent consumption in transport, various production processes, etc. In addition, hydrogen is characterized by a high specific energy density of 122 kJ/g, which, for example, is approximately three times higher compared to gasoline and other hydrocarbon fuels [1, 2]. However, using hydrogen as an energy source can be unsafe due to its explosive nature. At the same time, data published in 2006 confirmed that hydrogen-powered vehicles are less dangerous than gasoline-powered vehicles [3].

Today, the following methods of hydrogen production are most widely used: thermochemical; electrochemical; photobiological, and photoelectrochemical [4].

Each of these methods has both advantages and disadvantages. The cost of obtaining hydrogen, the purity of the final product, the simplicity of the technological scheme, and environmental friendliness are mainly taken into account.

An important place among methods of obtaining hydrogen is occupied by the method of electrochemical decomposition of water in saline, acidic or alkaline solutions [5]. Electrolytic hydrogen is the purest of industrially produced gases. However, the production of 1 kg of hydrogen requires approximately 260 MJ/kg of energy, and the cost exceeds \$3-5/kg. The cost of hydrogen obtained from natural gas is estimated at \$1.5-3/kg. At the same time, it should be taken into account that the amount of energy consumption will largely depend on the operating current density.

It is possible to somewhat reduce electricity consumption by reducing electrode polarization by changing the structure of electrode materials and applying catalysts to them, primarily platinum group metals [6]. Autors [7, 8] proposed a method of obtaining hydrogen using aluminum alloys. It consists in dissolving aluminum in alkaline solutions with the simultaneous release of hydrogen on aluminum. Such a system can be considered a short-circuited electrochemical cell.

The results of our work are based on the use of a system open for mass transfer [9], At the same time, hydrogen is released on a platinum or nickel electrode with a lower overvoltage than on aluminum, as proposed in [7, 8]. When using soluble Al, the potential difference is -1.66 V. The minus sign in this case means that the process occurs spontaneously, that is, without the application of an electric current. In addition, aluminum goes into a solution, and after additional stages of transformation, it can be used as a coagulant. Aluminum-based coagulants are highly effective in water purification, reducing turbidity and improving other properties [10]. Electrochemical methods of obtaining coagulants based on aluminum are also known [11].

The study of the process of hydrogen release and aluminum dissolution was carried out in an electrolyzer model in potentiodynamic mode with a potential reversal speed of 10 mV/s, and in the potential range from –1.5 to +0.0 V. The working electrode (anode) was an Al plate; the auxiliary electrode (cathode) was a nickel plate. The reference electrode was a saturated silver chloride

(Ag/AgCl) electrode. All potentials were relative to a saturated Ag/AgCl electrode. The electrolyte was a NaOH solution with 1 to 8 mol/L concentration.

Figure 1a shows typical polarization curves of Al dissolution and H_2 release at an alkali concentration of 2mol/L.

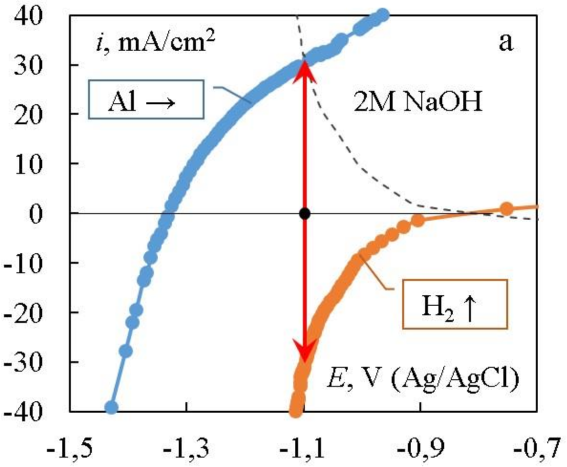

Figure 1. *Polarization curves of Al dissolution and H_2 release at an alkali concentration of 2mol/L (a) and the dependence of the maximum Al dissolution current density (b) on the alkali concentration.*

In general, when the alkali concentration increased from 1 to 4 mol/L, the values of the working current densities of the aluminum dissolution process, i.e., the speed of the process, increased significantly (Fig. 1b). The maximum current density value of ~300 mA/cm^2 was observed at a NaOH concentration of 4mol/L, after which the rate of increase in current density decreased. As the alkali concentration increased at the same rate, the potential difference between the anodic and cathodic processes also increased.

Figure 2. shows the change in current density and specific power generated in a system open for mass transfer.

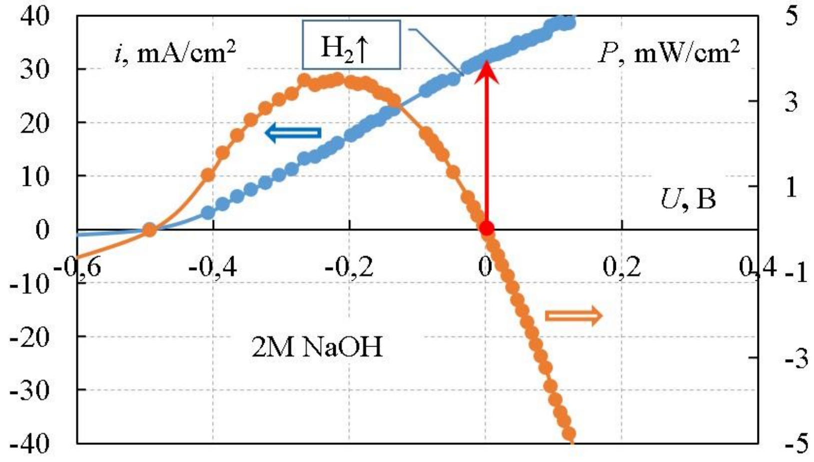

Figure 2. *Change in current density and generated specific power depending on system voltage in 2mol/L NaOH solution.*

The value of the specific power P, which was generated simultaneously with the hydrogen release process, was determined as the product $P = i \cdot U$, where $i$is the current density, A/cm^2; U is the corresponding voltage value, V.

Conclusion

The studies carried out in a system open for mass transfer have confirmed the possibility of extracting pure hydrogen with parallel generation of electricity. The maximum value of the current density of 300 mA/cm^2 is observed in a solution of 4mol/L NaOH. For an alkali with a concentration of 2 mol/L NaOH, the maximum specific power P, which can be generated simultaneously with the process of hydrogen evolution, is ~ 4 mW/cm^2.

It should be noted that the serial connection of several electrochemical cells will make it possible to form a system of any voltage, and by changing the surface of the electrodes, it is possible to adjust the power and amount of hydrogen for its further use in fuel cells.

Acknowledgments

The work was carried out within the framework of the long-term plan for the development of the scientific direction "Technical sciences" Ukrainian State University of Chemical Technology No. BF/17-2021.

References

1. G. Nicoletti, N. Arcuri, G. Nicoletti, and R. Bruno. *Energy Convers Manage*., **89**, 205 (2015). http://dx.doi.org/10.1016/j.enconman.2014.09.057.
2. A. Demirbas. *Energy Sources*., **27**, 7 (2005). https://doi.org/10.1080/00908310490450836
3. W.C. Lattin, and V.P. Utgikar. *Int. J. Hydrogen Energy.,* **32**, 3230 (2006). https://doi.org/10.1016/j.ijhydene.2007.02.004
4. U.K. Zorea, S.G. Yedire, N. Pandi, S. Manickam, and S.H. Sonawane. *Ultrasonics Sonochemistry.,* **73**, 105536 (2021). https://doi.org/10.1016/j.ultsonch.2021.105536
5. S.Y. Tee, Y.W. Khin, S. T. Wee, K. Leng-Duei, L. Shuhua, P.T. Choon, and H. Ming-Yong. *Adv. Sci.* **4**, 1600337 (2017). https://doi.org/10.1002/advs.201600337
6. T. Karchiyappan. *Energy Sources*. **41**, 902 (2019). https://doi.org/10.1080/15567036.2018.1520368
7. C.Y. Ho. *Int. J. of Hydrogen Energy*., **42**, 19622 (2017). https://doi.org/10.1016/j.ijhydene.2017.06.104
8. F. Xiao, R. Yang, and Z. Liu. *Int. J. of Hydrogen Energy*., **47**, 365 (2022). https://doi.org/10.1016/j.ijhydene.2021.09.241.
9. V. Nefedov, V. Matveev, K. Sukhyy, Yu. Polishchuk, A. Bulat, B. Bluss, and A. Mukhachev. *IOP Conf. Ser.: Earth Environ. Sci.,* **1156,** 012034 (2023). https://doi.org/10.1088/1755-1315/1156/1/012034
10. D. Spînu (Gologan), and G. Racoviteanu. *Modelling in Civil Environ. Engin.,* **10**, 9 (2014). https://doi.org/10.2478/mmce-2014-0002
11. Y. Makarov, V. Andronov, and Y. Danchenko. *KEM.,* **925**, 179 (2022). https://doi.org/10.4028/p-i2s5ht.

Microbial Fuel Cells Technology for Bio-remediation and Electrical Energy Harvesting from Organic Solid Waste in Wastewaters

Nicoleta-Oana Nicula, Gimi A. Rimbu and Eduard-Marius Lungulescu

National R&D Institute for Electrical Engineering (ICPE-CA) 313 Splaiul Unirii, Sector 3, 030138, Bucharest, Romania

Microbial fuel cells (MFCs) and water bioremediation have emerged as promising approaches for treating wastewater and polluted water sources, presenting sustainable and economical treatment alternatives. MFCs are systems that generate electricity by breaking down organic matter with the help of microbial substrates. The ability of microorganisms to convert and metabolize various pollutants into harmless substances plays a crucial role in bioremediation, bringing benefits such as minimal energy requirements, low operational expenses, and reduced waste production. However, the efficiency of bioremediation can be influenced by factors like microbial diversity, environmental conditions, and the presence of inhibitors. Moreover, bacteria in microbial fuel cells have the ability to generate electricity while simultaneously breaking down organic materials or waste. This means that using MFCs that harness microbial activity could serve as an alternative to conventional electricity generators both now and in the future. Despite the promising results obtained from MFCs for wastewater treatment, several challenges need to be addressed, including low power density, and scaling up from lab-scale to practical applications. The present research focuses on addressing these challenges and improving the energy efficiency of MFCs.

Acknowledgements

The financial support was provided by the Ministry of Research, Innovation and Digitization, through contracts: 42N/PN23140201/2023 and 25PFE/2021

Portable Power Source Based on PEM Fuel Cell

M. Paidar, D. Budáč, K. Bouzek

Department of Inorganic Technology, University of Chemistry and Technology, Prague,
Czech Republic

Fuel cells are devices for conversion of chemical energy of fuel to electric energy and heat. They find application in various sectors of society. Portable power source with open cathode (breathing) stack was designed. The main attention was paid to the weight of device to enable handheld transport. As dedicated application is emergency situations special focus was paid to air conditioning before entering the stack. The influence of potential pollutants on function of PEM fuel cell was studied.

Introduction

PEM type fuel cells are currently well-known devices for efficient conversion of chemical energy carried by hydrogen into electrical energy. They possess several important advantages as high efficiency, high durability or continuous process operation. The main part the PEM fuel cell stack doesn’t have moving parts. Absence of moving parts is main reason, why fuel cells are silent in comparison to combustion engines. On the other hand, ventilators ensuring air supply or hydrogen recirculation represent typically main source of noise in this device. Beside electricity main products of PEM fuel cells are product water and heat. Due to production of nontoxic emissions the fuel cell systems can be operated as portable power sources inside closed spaces. Houses, caves, mines are examples where combustion engine is problematic to operate. Depending on the required power output the PEM fuel cell unit can also be designed as stationary or portable. High performance power sources have usually more complex system focusing to maximum fuel utilization and efficiency. Smaller portable handheld power sources are designed with attention to minimum weight. The typical PEM fuel cell unit for mobile application has to contain stack of performance 100 -500W. Air is used as oxidant and coolant simultaneously to reduce weight and size of the system, as air compressor and cooling loop are in such case avoidable. Use air for cooling and as oxidant together requires treatment of higher amount of air than required by stoichiometry. Thus, air treatment must be properly designed for secure operation of power source.

Experimental

Particles removal form air are usually solved by HEPA filters. It is common solution for various applications. Chemical contamination is removed by carbon black layer. Its capacity is crucial for proper function of air treatment. The air was contaminated by dosing of selected pollutants. Toluene was chosen as representative of VOC contaminant. The influence of contaminated air on PEM fuel cell performance was monitored. Also, the regeneration of contaminated cell by clean air dosing was monitored. The absorption capacity of carbon black was measured to determine optimal loading to the air filter together with prediction of filter replacement period. Simple laboratory fuel cell and mass spectrometer were used as detectors to identify pollutant penetration through filter.

Results & Discussion

Presence of toluene in air causes serious deterioration of fuel cell performance as shown on Fig. 1. Despite it, partial recovery was observed after clean air dosing. It indicates need of air pretreatment. Absorption capacity of carbon black was studied with respect to toluene and other pollutants. Beside organic compounds ammonia, sulfur dioxide and hydrogen sulfide are often reported as model pollutants.

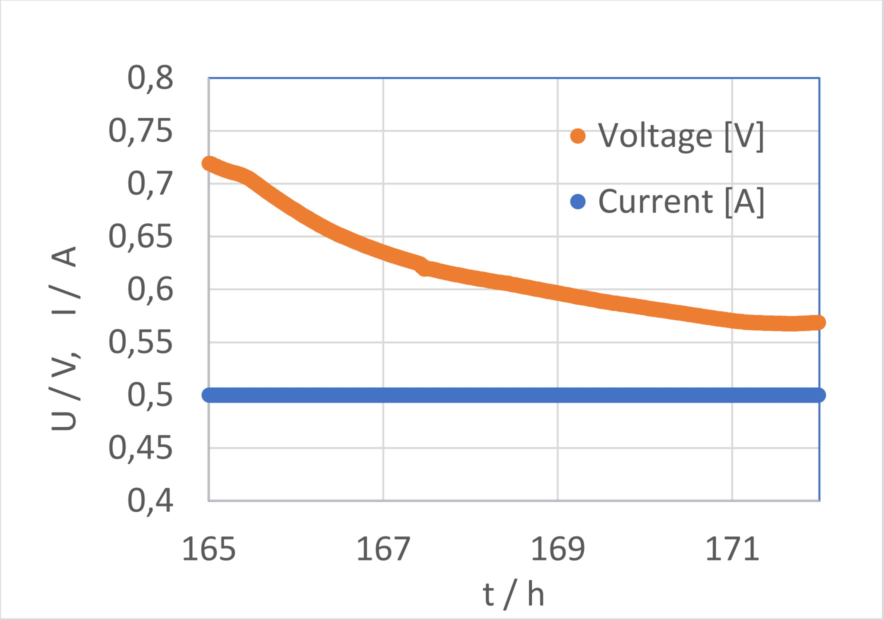

Figure 1. *Performance drop in time of laboratory single fuel cell operated at 0.5 A at 25°C with air contaminated by toluene 0.014 $\%_{WT}$*

Based on measured data it is possible to predict replacement period of active filter in commercial air filters. Also, the development of new air filter is possible. The sorption capacity can be increase with respect to the polluted air expected. Beside absorption of pollutants the pressure drop is crucial to ensure sufficient air flow for cooling and electrochemical reaction. Experiments with wet air was realized. The absorption capacity was impacted by absorbed water but in the case of granular active carbon black the pressure drop remains similar to dry air use.

Conclusion

The importance of air filtration even for small performance stack was proven. Partial recovery of fuel cell performance after poisoning by toluene was observed. The slow deliberation of toluene and ethanol from active carbon filter was observed. It prevents fuel cell poisoning by peak pollution but still allows dosing of residual concentration of VOX. The possibility of use granulated active carbon was identified together with its absorption capacity. Obtained data allows construction of own air filter for portable power sources.

Acknowledgments

This work was supported by the Technology Agency of the Czech Republic under project no TK05020013.

High-Voltage Aqueous Dual-Ion Batteries Based on Water-In-Salt Electrolytes

Jiří Červenka[a], Zahid Ali Zafar[a], Ghulam Abbas[a,b], Farjana J. Sonia[b], Karel Knížek[a], Martin Šilhavík[a], Prabhat Kumar[a], Zuzana Vlčková[b], Otakar Frank[b]

[a] FZU – Institute of Physics of the Czech Academy of Sciences, Prague, Czechia

[b] J. Heyrovsky Institute of Physical Chemistry of the Czech Academy of Sciences, Prague, Czechia

Rechargeable aqueous dual-ion batteries have recently attracted significant attention for grid energy storage applications. Here we demonstrate high-voltage and low-cost aqueous dual-ion batteries based on highly concentrated "water-in-salt" electrolytes of metal perchlorate. We show that the high salt concentration and the chaotropic nature of perchlorate anion can efficiently expand the electrochemical stability window of the aqueous electrolyte up to 2.8-4.0 V depending on the metal cation used. The high concentration of salts in the electrolyte suppresses the dissociation of water at high potentials, facilitating a stable and reversible ClO_4^- anion intercalation into the graphite with a Coulombic efficiency of over 95% for more than 2000 cycles. Our zinc-graphite dual-ion battery delivers a high discharge voltage of 1.95 V with a maximum discharged capacity of 45 $mAhg^{-1}$ at 100 $mAhg^{-1}$ for over 500 cycles. Our work provides a new feasible strategy for designing high-voltage, non-flammable, and low-cost dual-ion aqueous batteries.

References

1. Z. A. Zafar, G. Abbas, K. Knížek, M. Šilhavík, P. Kumar, P. Jiříček, J. Houdková, O. Frank, J. Červenka, *J. Mater. Chem. A* 10, 2064-2074 (2022).
2. Z. A. Zafar, G. Abbas, M. Šilhavík, K. Knížek, O. Kaman, F. J. Sonia, P. Kumar, P. Jiříček, J. Houdková, O. Frank, J. Červenka, *Electrochim. Acta*, 404, 139754 (2022).
3. G. Abbas, Z. A. Zafar, F. J. Sonia, K. Knížek, J. Houdková, P. Jiříček, M. Kalbáč, J. Červenka, O. Frank, *Nanomaterials*, 12 (22), 3932 (2022).
4. G. Abbas, F. J. Sonia, Z. A. Zafar, K. Knížek, J. Houdková, P. Jiříček, M. Bouša, J. Plšek, M. Kalbáč, J. Červenka, O. Frank, *Carbon*, 186, 612-623 (2022).

Development of Novel Design and Chemistries for Redox-Flow Batteries

Andrea Straková Fedorková[1*], Natália Podrojková[1], Igor Derr[2], Tomáš Košický[2]

[1]Institute of Chemistry, Faculty of Science, P.J. Šafárik University, Moyzesova 11,

SK-04154 Košice, Slovak Republic

[2]INO-HUB Energy j.s.a., Tomášikova 30, 821 01 Bratislava, Slovakia

*andrea.fedorkova@upjs.sk

Abstract

The transition to renewable and clean energy sources is one of the greatest challenges and responsibilities of humanity in mitigating the consequences of global warming and assuring a sustainable future for the next generations. Rechargeable batteries are one of the key technologies for storing energy from renewable sources and among these, redox-flow batteries (RFBs) have many advantages such as safety, non-flammability, non-explosive nature, high power density, and cost-effective energy storage solution [1].

INO-HUB Energy was granted by EU IPCEI project for the development of redox flow battery systems. In the first phase of the project a novel organic electrolyte will be developed and tested on a lab-scale. Organic electrolytes were chosen, because of the availability of required resources. After successful testing this electrolyte will be put to work in a kW-scale demonstrator especially developed for this type of electrolyte. The demonstrator development includes the development of a new stack. This new stack design is supposed to be versatile, allowing the stack to be used with organic as well as inorganic electrolytes. Deploying novel organic electrolytes will challenge existing membrane chemistries, which is why we plan to develop a tailor-made and cost-effective membrane for our specific electrolyte in the second phase of the project. After successful testing of the membrane a large-scale demonstrator will be placed in the field to prove the maturity of the overall system design.

The Vanadium redox flow Battery (VRFB) is the best known redox flow systems in academia and the most widespread commercially available system. During charging, V^{3+} is reduced to V^{2+} at the negative side whereas oxidation of $V^{4+}(VO^{2+})$ to $V^{5+}(VO^{+2})$ occurs at the positive side via the exchange of protons and subsequent removal of a water molecule. The electrochemical reaction of positive and negative electrodes constitutes the basic principle of all vanadium redox flow battery. In a VRFB, the fundamental redox reactions are as follows [2]:

- Negative half-cell:

$$V^{2+} \underset{\text{charging}}{\overset{\text{discharging}}{\rightleftarrows}} V^{3+}+e^-, E_-^0 = -0.255\ \mathrm{V} \tag{1-1}$$

- Positive half-cell:

$$VO_2^{+}+2H^{+}+e^{-} \underset{\text{charging}}{\overset{\text{discharging}}{\rightleftarrows}} VO^{2+}+H_2O, E_+^0 = 1.004\ \mathrm{V} \tag{1-2}$$

- Total-cell reaction:

$$V^{2+}+VO_2^{+}+2H^{+} \underset{\text{charging}}{\overset{\text{discharging}}{\rightleftarrows}} VO^{2+}+V^{3+}+H_2O, E^0 = 1.259\ \mathrm{V} \tag{1-3}$$

At INO-HUB Energy we plan to improve the existing VRFB technology and make it more competitive compared with Li-ion and Hydrogen based systems. These improvements include a new stack design with novel component materials as well as an improvement of the most critical electrolyte properties, e.g. concentration of Vanadium or operating temperature window. These newly developed components and materials will have to prove themselves in a large-scale demonstrator.

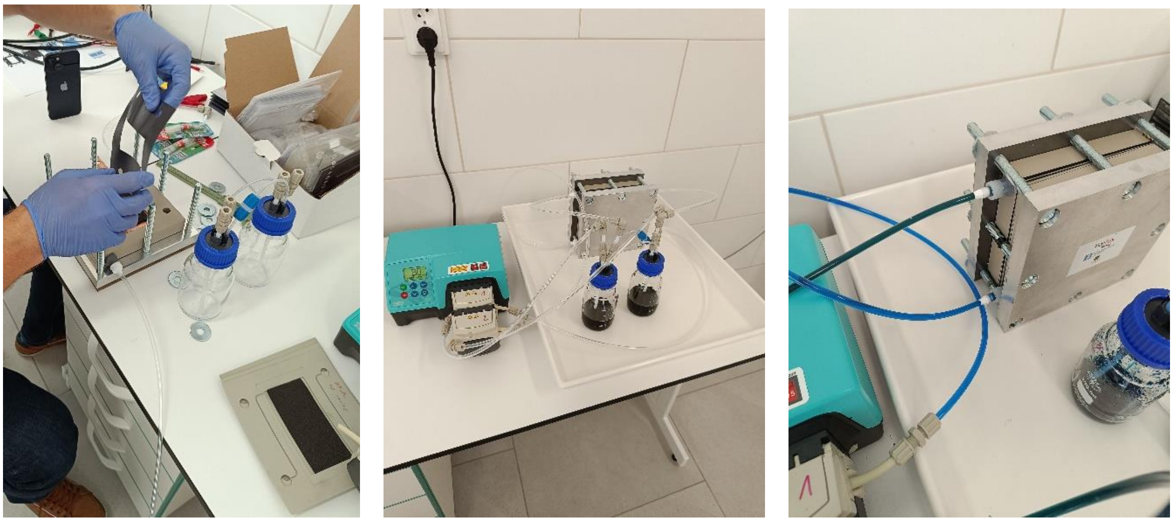

Figure 1. *Assembling and testing of first INO-HUB Energy testing cell.*

The RFB battery structure, degradation, electrochemical reaction, mass transfer process and reaction area distribution have a great influence on the performance of RFB. Several simulations were performed in Comsol to facing the research challenges and performance improvement of RFB while experimental research will consume a lot of time and financial resources. The modeling has an important significance for amplification, performance improvement and control strategy optimization of RFB.

Several simulation models were prepared using Comsol software. Preparation of simulation models consisted of preparation of 2D geometry of the cell and subsequent preparation of 3D geometry, input of material parameters, creation of laminar flow physics and creation of geometry network for laminar flow physics. The models were created on the basis of available literature, to acquire skills in the case of a real model, where the necessary pressure drop values will be simulated to adjust the design of the resulting experimental redox-flow cell.

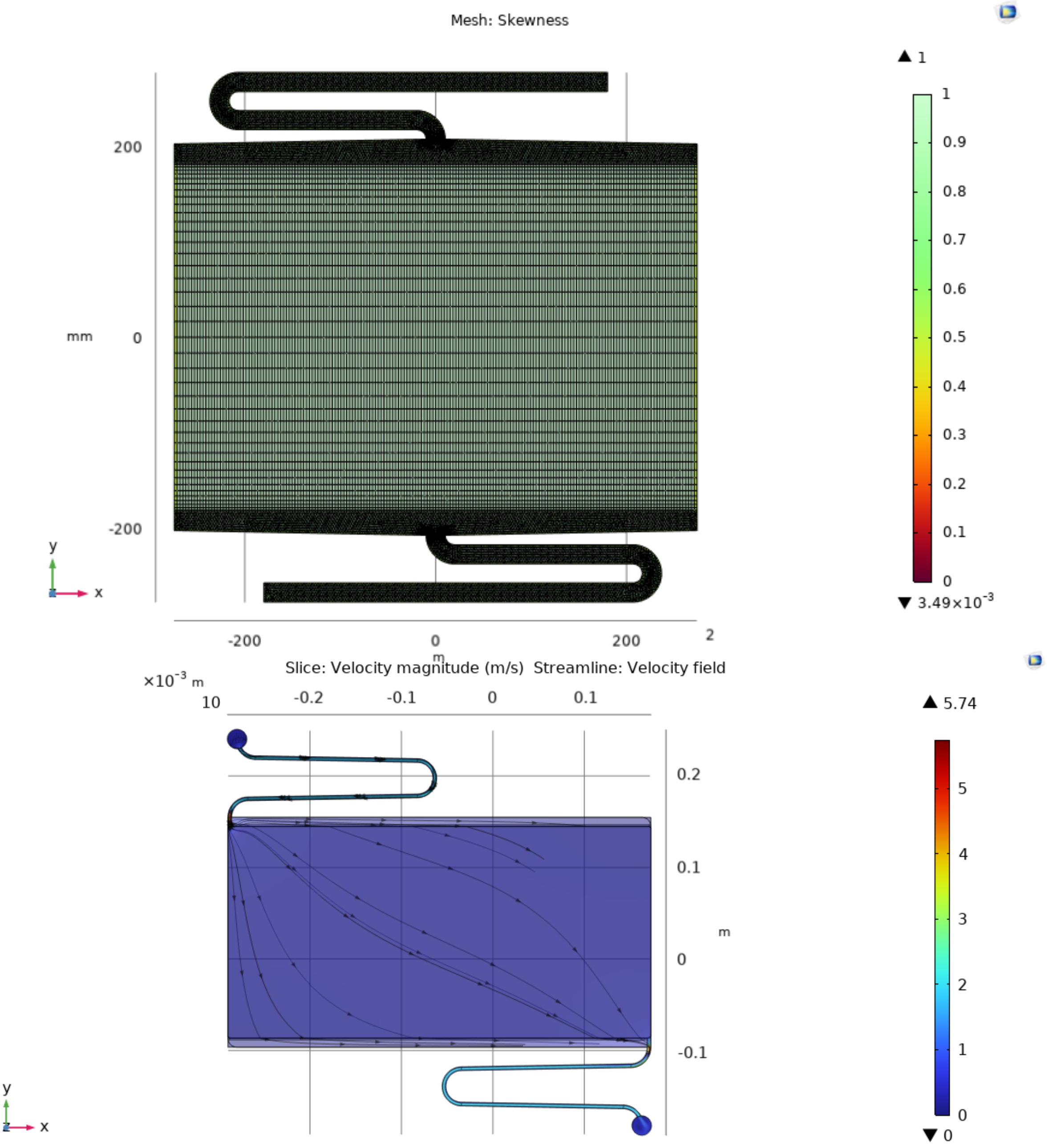

Figure 2. *Preparation of simulation models using Comsol software for INO-HUB cell geometry.*

Acknowledgement

This research was sponsored by the IPCEI project under grant No. ITMS 2014+: IPCEI_IE_FLOW_BESS_012021, 313010BLP2.

References

1. K. Lourenssen, J. Williams, F. Ahmadpour, R. Clemmer, S. Tasnim, *Journal of Energy Storage*, 25 (2019) 100844.
2. F.T. Wandschneider, D. Finke, S. Grosjean, P. Fischer, K. Pinkwart, J. Tübke, H. Nirschl, *Journal of Power Sources*, 272 (2014) 436–447.

Development of zinc-air flow battery

[1]P. Mazúr, P. Richtr[a], D. Graf[a], J. Hnat[a], M. Paidar[a], J. Charvat[b], J. Pocedic[b], P. Hauschwitz[c]

[a]University of Chemistry and Technology Prague, Technicka 5, 166 28 Prague, Czechia;
mazurp@vscht.cz, +420220443360

[b]University of West Bohemia Pilsen, Univerzitni 8, 306 14 Pilsen, Czechia

[c]Hilase Centre, Institute of Physics, Academy of Sciences of the Czech Republic, Za Radnici 828,
Dolni Brezany 25241, Czechia

Ongoing decarbonisation of energetics and mobility sectors emphasizes the needs for reliable, safe and environmentally energy storages for both mobile and stationary applications. The concept of flow battery offers several original features particularly interesting for grid stabilization applications. The zinc-air flow battery particularly provides cheap, non-toxic and non-explosive alternative to more matured vanadium-based system. However, the efficiency and durability needs to be improved to fully exploit the potential of the chemistry. In our contribution, the activities related to R&D of zinc-air flow battery on UCT Prague, UWB Pilsen and Hilase Centre are summarized, covering broad range of topics including electrocatalysis of oxygen reactions, control of zinc deposition morphologies based on local hydrodynamic conditions and optimization of cell/stack design and electrode arrangement.

Development of efficient and stable 3D electrodes for oxygen evolution and reduction reactions is approached by several methods including electrochemically assisted precipitation of Ni-Co spinel catalysts, laser nano-structuration of Ni mesh electrode and hydrophobicity adjustment of gas diffusion electrode catalytic layer.

The detailed study of zinc deposition/dissolution under defined hydrodynamic conditions together with spatially resolved mathematical modelling of electrolyte flow (COMSOL Multiphysics) and detailed deposits inspection (SEM, micro-tomography) is employed to optimize battery operation and construction with respect to the increased homogeneity of Zn distribution. Various strategies for enhanced cyclability of the battery are tested including use of static mixers, electrolyte additives for dendrite-free depositions and choice of substrate (including 3D materials).

The final step is aimed to the battery up-scale from lab-cell to kW-scale stack. This involves optimization of the battery stack design, particularly of the flow fields, with respect to multiple trade-offs to provide homogeneous fluid distribution and to suppress detrimental shunt currents at acceptable pressure drops.

Acknowledgments:

This works was supported by TAČR, program THÉTA2, project no. TK02030001.

Temperature Changes in a Lead-Acid Battery During Cooling

Petr Křivík[a], Jana Zimáková[a], Tomáš Binar[a]

[a] Department of Electrotechnology, Brno University of Technology, Faculty of Electrical Engineering and Communication, 616 00 Brno, Czech Republic

The paper deals with the measurement of temperature changes inside of the battery during cooling by the ambient temperature. It was found that during cooling there is an uneven distribution of the temperatures of the active materials inside of the battery. The highest unevenness there is achieved after 1-2 hours of cooling.

Introduction

The issue of thermal changes in a lead-acid battery in both current on and current off state was presented by several authors [1-5]. To determine the thermal changes of a lead-acid battery, it is necessary to calculate with all the contributions of individual types of heat. It is heat from electrochemical reactions (both exothermic and endothermic), heat from ohmic and polarization losses (Joule heat) and heat exchanged through the contact with the environment.

Heat concentrated in a lead-acid battery is lost mainly by conduction through the individual components of the cells. The battery is cooled dominantly through the side walls of the vessel, which are in contact with the electrolyte and the plates. Air layer on the top surface of the battery has low thermal conductivity and it is isolated from ambient temperature by plastic cover and that is why top surface does not contribute to the cooling of the battery significantly.

Experiment

For investigation the dynamics of temperature changes inside the lead-acid battery during cooling, a maintenance-free 12 V ZAP Plus Calcium 74 Ah battery with dimensions of 275 x 175 x 190 mm was used. The battery is made up of 6 cells connected in series, placed in a vessel made of ABS plastic. Individual cells were separated by plastic partitions.

Three temperature sensors were placed in the vertical plane passing through the center of the battery, see Fig. 1.

With this battery, experiment was started in the charged state with the measurement of temperature changes during cooling from 20 °C to -40 °C. In the experiment, the battery was placed from a room temperature of 20 °C into a freezer box tempered to -40 °C for 12 hours. Temperature of all temperature sensors was recorded at 2-minute intervals.

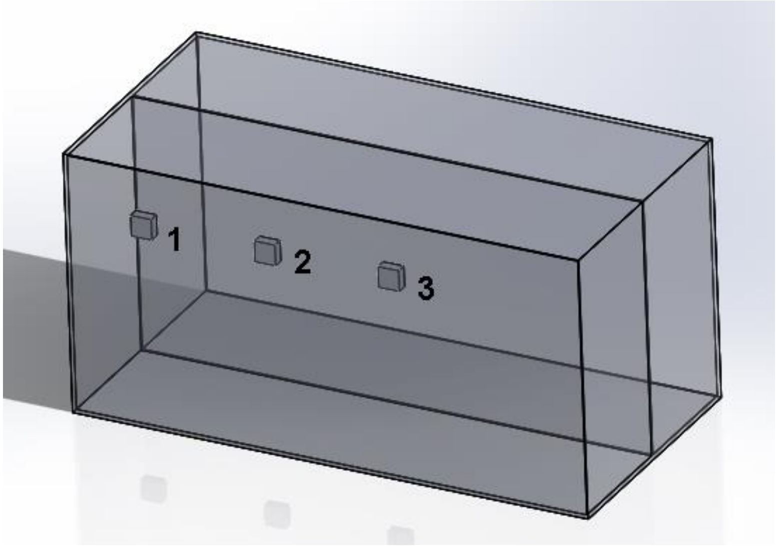

Figure 1. *Location of the 3 temperature sensors.*

Fig. 2 shows temperature dependences of all 3 sensors after placing the battery in the freezer for 12 hours. The temperatures of all the sensors show an exponential decrease. Different temperature course can be seen for the sensor in contact with the side wall of the battery vessel (sensor 1) compared to the other sensors. With that sensor, the highest temperature drop can be observed immediately from the 1st minute. For other sensors, there is almost no change in temperature at the beginning of battery cooling, only after about 20 minutes there is observed a gradual decrease in temperature as the battery cools down and this cooling expands further to the internal parts of the battery. At the areas close to the contact of the active materials with the side wall of the vessel, the highest temperature gradient is observed at the beginning of cooling. Temperature gradient increases the rate of temperature changes. The lowest temperature changes at the beginning of cooling can be observed in the center of gravity of the battery (sensor 3), because there is the lowest temperature gradient.

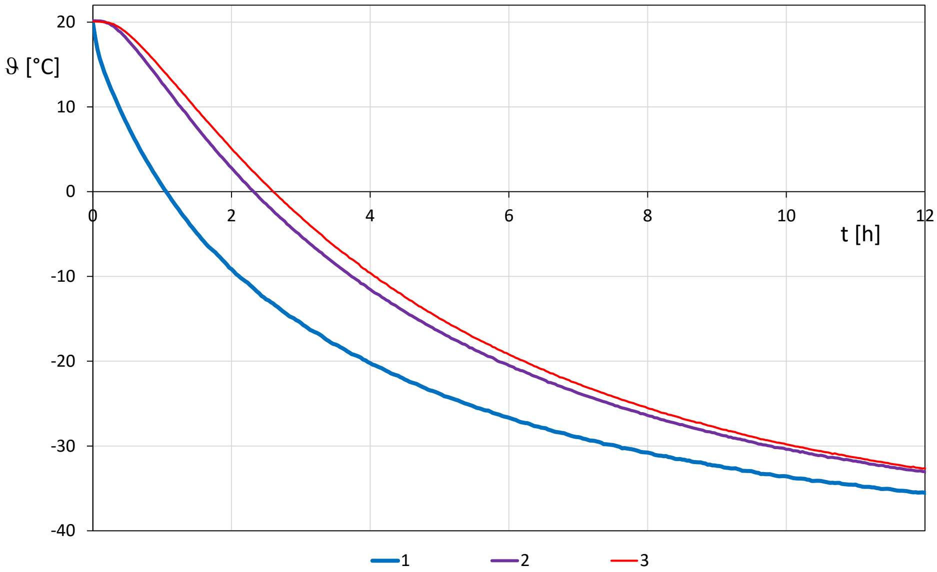

Figure 2. *Temperature dependence of 3 measured locations in a lead-acid battery during cooling from 20 °C to -40 °C for 12 h.*

Conclusion

It can be seen that during cooling from 20 °C to -40 °C, there is an uneven distribution of the temperatures of the active materials inside of the lead acid battery. Temperature differences inside the battery can cause uneven exploitation of active materials due to the different diffusion speed of ions in the electrolyte and also due to the different conductivity of the electrolyte and the active materials of electrodes. Uneven temperature distribution inside the battery has an adverse effect on the capacity and cycle life.

Acknowledgments

This work was supported by the specific research of the BUT FEKT-S-23-8286.

References

1. H. Frank Gibbard, *Journal of the Electrochemical Society* **125** (3), 353 (1978).
2. D. Pavlov, *Journal of Power Sources* **64**, 131 (1997).
3. D. A. J. Rand, R. Woods, R. M. Dell, *Batteries for electric vehicles* (1998).
4. H. A. Kiehne, *Battery Technology Handbook*, second edition (2003).
5. D. Valkovska, M. Dimitrov, T. Todorov, D. Pavlov, *Journal of Power Sources* **191,** 119 (2009).

Bio-renewable gel polymer membranes for sustainable Li-O_2 batteries

J. Amici[a],G. Banaudi[a], M. Longo[a], M. Gandolfo[a], D. Versaci[a], C. Francia[a], S. Bodoardo[a]

[a] Electrochemistry Group, DISAT, Politecnico di Torino, c.so D.ca degli Abruzzi 24, 10129 Torino, Italy

e-mail presenting author: julia.amici@polito.it

The growing need for clean energy production, due to global warming, has addressed the research towards the study of cleaner and more performing energy storage solutions and electric vehicles technologies. One of the most promising technologies currently being studied is the lithium - air battery, thanks to its high theoretical energy density of the order of 11000 Wh kg^{-1}. This extraordinary value is explained by the use of a metallic lithium anodes but, above all, by the use of porous carbon cathodes (GDL) where the active material, oxygen, flows from the outside. The use of metallic lithium anodes, however, results in many drawbacks that limit the stability and cycling of these batteries. For this reason, in this work, two biorenewable polymer gel membranes have been studied for lithium metal protection.

The first membrane studied is based on chitosan, a polysaccharide obtained from the deacetylation reaction of chitin. Such molecules were methacrylated through a simple, one-step reaction, in water, and then cross-linked by UV induced radical polymerization. The obtained membranes were successively activated in liquid electrolyte (LiTFSI 0.5 M in DMSO) and used as lithium protection layer. The cells prepared with protected lithium were able to perform more than 40 cycles at 0.1 mA cm^{-2}, at a fixed capacity of 0.5 mAh cm^{-2}, under a constant O_2 flow of 4 ml min^{-1}, at room temperature conserving 100 % coulombic efficiency. This is actually more than twice the lifespan of a similar cell containing bare metallic lithium, which failed in the same testing conditions, after 19 cycles.

The second studied membrane is based on gelatin which is a waste of the fishing industry as it is extracted from cold water fish skin. In this case as well the gelatin is methacrylated and then reticulated through fast and cheap UV mediated radical polymerization. Interestingly, in this case it is possible to perform the crosslinking reaction directly in presence of the liquid electrolyte (LiTFSI 0.5 M in DMSO) thus obtaining a Li ion conducting organogel in a simple one-pot procedure. The cured membranes displayed a good interfacial stability against Li metal and reversible cycling in a wide range of current densities. Furthermore, the cathodes of the discharged cells were investigated by XRD, and it was observed that the crosslinked gelatin matrix was able to slow down the decomposition of the DMSO, thus increasing the reversibility of the electrochemical reactions.

Investigation of hydroxide formation and resulting degradation at the polymer-metal interface in advanced DS cells

Lars Varain[1], Silvia Larisegger[2], Michael Nelhiebel[2], Günter Fafilek[1]

[1]TU Wien, Vienna/Austria

[2]KAI GmbH, Villach/Austria

Cathodic delamination of insulating and protective coatings on metals is an often-described corrosion phenomenon. It is commonly assumed, that the delamination process is initiated by defects in the coating. This work investigates the possibility of cathodic delamination induced by traces of water present in the polymer coating that are reduced at the interface by electrolysis.

An advanced Devanthan Starchurski setup is used to measure hydrogen formed at a palladium membrane. The current in the input cell and the amount of possibly detected hydrogen provides information about formation of hydroxide or peroxide, two species that contribute to degradation and delamination.

High-Entropy Additives Improving the Performance of Li-Sulfur Batteries

M. Zukalová[1], M. Vinarčíková[1], B. Pitňa Lásková[1], O. Porodko[2] M. Fabián[2] and L. Kavan[1]

[1]J. Heyrovský Institute of Physical Chemistry, v.v.i., CAS, Dolejškova 3, Prague 8, Czech Republic

[2] Institute of Geotechnics, Slovak Academy of Sciences, Watsonova 45, 040 01, Košice,
Slovak Republic

The rechargeable lithium-sulfur battery is regarded as a promising next-generation electrochemical energy storage device, due to the high theoretical capacity (1675 mAh/g) of sulfur, as well as the abundance, low cost, and eco-friendliness of elemental sulfur(1). Nevertheless, the electrochemical stability and commercial application of Li-S batteries are inhibited by the insulative sulfur and Li_2S/Li_2S_2, the shuttling effect in the electrolyte, and significant volume change(2). The main problems are related to the dissolution of lithium polysulfides (PS) in the electrolyte and their parasitic reactions with electrolyte solvents and Li anode. PS diffusion to the anode compartment of the Li-S battery causes severe redox shuttle between the cathode and Li anode. Hence, effective PS immobilization in the cathode compartment of the battery is essential for the optimum performance and cycling stability of the system.

High-entropy oxides and their lithiated oxychlorides or oxyfluorides showed promising results in the fields of batteries, supercapacitors, and electrocatalysis(3). Although these materials have not yet been optimized from the point of view of their electrochemical properties, they can hardly contribute by their inherent electrochemical activity to the redox processes taking place in Li-sulfur batteries analogously to TiO_2(4), because their redox activity occurs at potentials smaller than ca. 1.5 V vs. Li^+/Li, which is outside the usual electrochemical window of Li-S batteries(5-7). Instead, they can, presumably, serve as efficient PS adsorbents due to the presence of oxygen vacancies in their structure. In addition to the adsorption of PS, certain HEOs can also act as electrocatalysts accelerating the redox reactions of PS in Li-S batteries(8, 9).

In our work, we evaluated a novel lithiated high-entropy oxychloride $Li_{0.5}(Zn_{0.25}Mg_{0.25}Co_{0.25}Cu_{0.25})_{0.5}Fe_2O_{3.5}Cl_{0.5}$ (LiHEOFeCl) synthesized by the mechanochemical–thermal route(10). The addition of the LiHEOFeCl material to the P_carbon_sulfur composite cathode in the Li-sulfur battery resulted in improved long-term electrochemical cycling stability and increased charge capacity of the system. The P_carbon_LiHEOFeCl sulfur cathode provided a charge capacity of 530 mAh g^{-1} after 100 galvanostatic cycles, which represents ca. 33 % increase as compared to the charge capacity of the blank P_carbon sulfur composite cathode after 100 cycles (398 mAh g^{-1}). This considerable effect of the LiHEOFeCl material is assigned to its excellent structural and electrochemical stability within the potential window of 1.7 V/2.9 V vs. Li^+/Li. In this potential region, our LiHEOFeCl exhibits no inherent electrochemical activity and acts solely as an electrocatalyst accelerating the redox reactions of PS. This can be beneficial for the Li-S battery performance, as evidenced by reference experiments with TiO_2 (P90).

Acknowledgment

This research was funded by the Grant Agency of the Czech Republic (contract No. 20-03564S).

References

1. R. Yan, M. Oschatz and F. Wu, *Carbon*, **161**, 162 (2020).
2. L. Zhang, W. Zhao, S. Yuan, F. Jiang, X. Chen, Y. Yang, P. Ge, W. Sun and X. Ji, *J Energy Chem*, **60**, 531 (2021).
3. J. W. Sturman, E. A. Baranova and Y. Abu-Lebdeh, *Front Energy Res*, **10**, 862551 (2022).
4. M. Zlámalová, B. Pitňa Lásková, M. Vinarčíková, M. Zukalová and L. Kavan, *J Solid State Electrochem*, **26**, 639 (2022).
5. A. Sarkar, L. Velasco, D. Wang, Q. Wang, G. Talasila, L. de Biasi, C. Kubel, T. Brezesinski, S. S. Bhattacharya, H. Hahn and B. Breitung, *Nat Commun*, **9**, 3400 (2018).
6. T. X. Nguyen, J. Patra, J.-K. Chang and J.-M. Ting, *J Mater Chem A*, **8**, 18963 (2020).
7. O. Porodko, M. Fabián, H. Kolev, M. Lisnichuk, M. Zukalová, M. Vinarčíková, V. Girman, K. L. Da Silva and V. Šepelák, *Z Phys Chem*, **236**, 713 (2022).
8. Y. Zheng, Y. Yi, M. Fan, H. Liu, X. Li, R. Zhang, M. Li and Z.-A. Qiao, *Energy Storage Mater*, **23**, 678 (2019).
9. L. Tian, Z. Zhang, S. Liu, G. Li and X. Gao, *Energy Environ Mater*, **5**, 645 (2021).
10. M. Zukalova, M. Fabian, O. Porodko, M. Vinarcikova, B. Pitna Laskova and L. Kavan, *RSC Adv*, **13**, 17008 (2023).

Inversely Vulcanized Sulfur as Electroactive Material for Li-S Cathodes

Ondřej Čech, David Trochta, Pavel Čudek and Tomáš Kazda

Department of Electrical and Electronic Technology, Faculty of Electrical Engineering and Communication, BUT, Technická 10, 616 00 Brno, Czech Republic

The work deals with the study of lithium-sulfur batteries, which are promising in terms of their high theoretical capacity and low environmental impact. Instead of elemental sulfur, which is the most common electroactive material of the positive electrode, an inversely vulcanized sulfur with an amorphous structure was used, the preparation process of which was improved and optimized.

Introduction

Lithium-ion (Li-Ion) batteries currently dominate energy storage. However, their further development is limited by a theoretical energy density of 400 Wh / kg, which is insufficient to meet the growing demands. A potential solution is to use batteries based on a combination of lithium sulfur (Li-S), which can bring a theoretical energy density of up to 2600 Wh / kg [1]. However, the use of sulfur is problematic due to its low specific electrical conductivity of 10-30 S / cm. During the cycle, polysulfides are also formed, which cause morphological and structural changes, further reducing the effective contact and conductivity of the entire electrode [2]. Higher polysulfides are soluble, migrate through the separator electrolyte, and react irreversibly with the lithium anode. This work is focused on the preparation of materials from inversely vulcanized polymer sulfur (IVS). Current research shows that sulfur in amorphous form achieves higher cyclic stability as well as charge efficiency compared to its crystalline form [2]. The inverse vulcanization method, in which polymer sulfur is crosslinked by reaction with a crosslinking agent such as 1,3-diisopropenylbenzene (DIB), stabilizes the polymer sulfur. This prevents recrystallization, which causes problems in the further use of polymeric sulfur materials.

Experimental

Copolymer material with different ratios of starting materials was prepared by the method of inverse vulcanization (IVS), developed by Griebel, Pyun and colleagues [3]. The temperature of addition of DIB to the sulfur melt proved to be a critical factor in the preparation. If the procedure of the authors of the method was followed, the samples recrystallized sulfur and formed crystalline phases in the sample, which was proved by XRD. Stable results have been achieved by modifying the preparation process, and our preparation method thus produces an amorphous polymeric material which does not recrystallize and precipitate elemental sulfur even after several years.

IVS samples with sulfur, 70, 60, 50 and 40 wt.% Were synthesized. %. In the case of sulfur 70 wt. % was not the resulting solid phase copolymer at room temperature, but was highly viscous. In the case of samples with a sulfur content of 60 wt. % and less the substance was in a glassy state after cooling and in the long run the substance was stable in its properties. As the ratio of the input substances changed, the color shade of the resulting copolymer changed, see Figure. 1

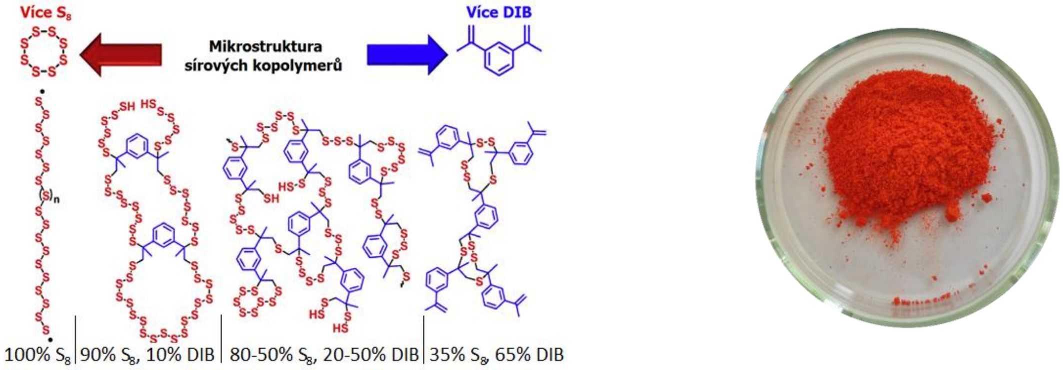

Figure 1. *Left - IVS structure with different degrees of crosslinking using DIB. Right – grinded IVS with 70 wt% of sulfur.*

Electrochemical characterization of electrode material

Based on the recorded results of the previous sections, a material with a ratio of elemental sulfur and DIB input precursors was chosen for the preparation of the electrode paste in the ratio 70:30 wt. %. This material was chosen for characterization because of all the samples it has the lowest solubility in electrolytes due to the lowest DIB content,

this is related to the largest theoretical capacity for the total weight of the electrode of all prepared samples. The conductivity of the selected material is also the highest of all examined, although this difference is not significant. Electrodes whose material was ground by various methods were examined.

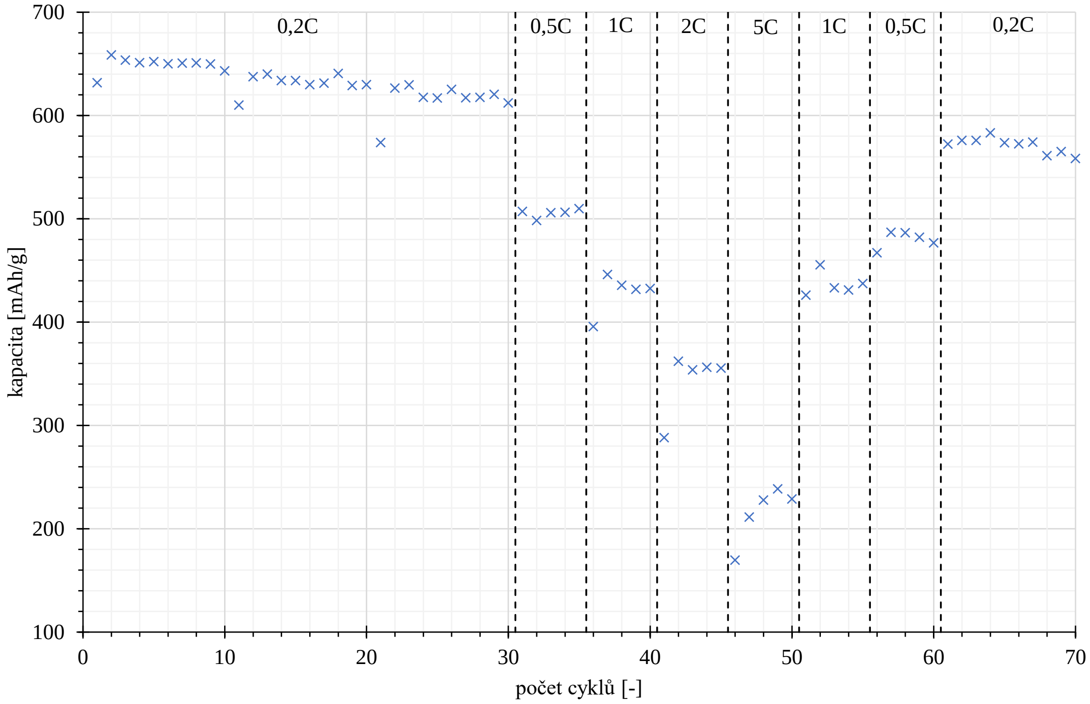

Figure 2. *Cycling of IVS with 70wt. % of sulfur.*

Conclusion

Based on the study of known methods for the preparation of polymeric sulfur, especially the method of inverse vulcanization of sulfur using 1,3-diisopropenylbenzene, sulfurized polymeric materials with different ratios of input precursors were synthesized. These materials have great potential as electroactive materials for the positive electrodes of lithium-sulfur batteries, but this technology still suffers from a number of unresolved negative aspects, and the study of new high-sulfur polymeric materials could contribute to their solution. An important factor in the inverse vulcanization of sulfur is the temperature at which the components are mixed, in this case the addition of the crosslinker 1,3-diisopropenylbenzene. The crosslinker must be added when the temperature of the sulfur melt reaches 159 ° C, otherwise there are problems with the miscibility of the two materials.

Acknowledgments

This work was supported by the specific graduate research of the Brno University of Technology No. FEKT-S-20-6206. CzechNanoLab project LM2018110 funded by MEYS CR is gratefully acknowledged for the financial support of the measurements at CEITEC Nano Research Infrastructure.

Sodium-ion batteries: research of carbon based negative electrode materials

J. Libich[a]*, M. Sedlaříková[a], J. Máca[a],P. Čudek[a], T. Kazda[a], G. Fafilek[b] and
J. J. Santana Rodríguez[c]

[a]Brno University of Technology, Faculty of Electrical Engineering and Communictaion,
Department of Electrical and Electronic Technology, Technická 12, 616 00 Brno, Czech Republic
[b]Vienna University of Technology, Getreidemarkt 9, 1060 Vienna, Austria.
[c]Department of Process Engineering, Universidad de Las Palmas de Gran Canaria, 35017, Las
Palmas de Gran Canaria, Spain

This paper focuses on the research of hard carbon as a promising negative electrode material for sodium-ion batteries. In the paper, the sodium-ion cells are discussed, their development so far, current issues and differences compared to lithium-ion cells, as they appear to be one of the promising post-lithium technologies with the potential for rapid commercialization. In the practical part, properties of some material samples are tested with a focus on their capacity and coulombic efficiency. The emphasis in this work is put on the negative electrode materials for sodium-ion batteries based on hard carbon as an active electrode material.

Introduction

Supercapacitors Sodium-ion batteries (abbreviated as Na-ion) are currently considered a highly promising technology. However, due to historical research focus on lithium cells, they have been relatively lagging behind in development compared to them. Nevertheless, they have recently become the subject of intensive investigation. The operational principle of these batteries is analogous to lithium-ion batteries. The main difference lies in replacing lithium ions with sodium ions. Similar to lithium-ion batteries, sodium-ion cells also utilize intercalation electrodes and an electrolyte to facilitate the transfer of sodium ions between them. Sodium, like lithium, is an alkali metal, with lithium having an atomic number of 3 and sodium having an atomic number of 11. Both elements have one electron in their valence shell, but the sodium atom is larger, requiring adjustments to the materials and manufacturing processes used in lithium-ion batteries.

The main anticipated use of sodium-ion batteries is as energy storage systems for stabilizing the electrical grid. Their role will be highly significant in the future as a complement to renewable energy sources. Most renewable sources, by their nature, are unable to provide a consistent energy supply (such as solar or wind power), which creates the need for energy storage. Traditional solutions to this problem have involved pumped hydroelectric power plants, but their construction is expensive, requires suitable locations, and is not feasible on a small scale. This is why battery energy storage systems based on lithium-ion batteries are already in operation in some places around the world. Sodium-ion batteries are expected to offer lower procurement costs, better availability, and higher safety compared to lithium-ion batteries. This is partly due to sodium being much more abundant in the Earth's crust than lithium (estimated to be about 1000 times more common). Another potential application could be traction batteries for electric vehicles. Here, they could once again compete with lower costs and higher safety, albeit at the expense of lower capacity and therefore reduced range. According to current estimates, sodium-ion cells are expected to have the potential to achieve a capacity approximately 18 % lower than lithium-ion batteries. This would offer them broad utilization in applications where the emphasis is not solely on achieving the highest gravimetric energy density but also factors such as material availability, safety, and cost, making them an interesting alternative to the existing lithium-ion technology.

Anode-negative electrode materials for sodium-ion batteries

Similarly to lithium, graphite appears to be a suitable material for the anode. Carbon atoms in graphite form layers with relatively weak bonds between them, allowing for good intercalation of lithium ions. With lithium, graphite forms LiC_6 at full cell charge, providing a theoretical capacity of 372 mAh/g. However, this is not the case with sodium ions. Due to their larger size compared to lithium, sodium ions hardly intercalate into graphite. The maximum achieved capacity is only 35 mAh/g when NaC_{64} is formed, and its low charging and discharging rate make it unsuitable for this application. One possible solution has been the use of an electrolyte based on diglyme. Unfortunately, so far, this has only yielded capacities of around 100 mAh/g. An alternative could be the use of disordered, amorphous carbons (commonly referred to as hard carbon), which enable the intercalation of sodium ions even with conventional electrolytes. Carbon is not arranged in regular layers but consists of single-layer graphene sheets that are disordered and bent in various directions. Even at high temperatures, these layers cannot be straightened to transform this material into graphite. This structure is sometimes described using the "card house" model due to the resemblance of the disordered graphene layers to a collapsed house of cards. The internal structure of amorphous carbon consists of small regions with regularly ordered graphene layers, with a thickness of up to 40 Å, as well as regions of amorphous carbon with defects and nanopores. The distance between graphene layers in amorphous carbon ranges between 3.6 and 4.0 Å, which is greater than the 3.35 Å in regular graphite.

Tests have revealed excellent capacity characteristics of materials based on amorphous carbon. Capacities exceeding 370 mAh/g have been measured, with high efficiency, as shown in Figure 2 above. The measured capacity of 370 mAh/g for amorphous carbon in sodium-ion batteries reaches the level of commercially used graphite-based materials in lithium-ion cells. The vast majority of commercial lithium-ion batteries utilize the intercalation capabilities of graphite and the formation of the compound LiC_6, which achieves a theoretical capacity of 372 mAh/g. If further tests confirm these parameters, amorphous carbon (hard carbon) can be considered as the sought-after, functional negative electrode material for sodium-ion batteries, analogous to graphite used in the case of lithium-ion cells. Additionally, these materials are relatively inexpensive, readily available, non-toxic, and environmentally friendly. Their usage, therefore, appears to be highly promising and could become one of the key anode materials for sodium-ion batteries.

Acknowledgments

This work was supported by the specific graduate research of the Brno University of Technology No. FEKT-S-23-8286.

Characterisation of precursor suspensions for fibrous electrodes

V. Procházka[a], M. Havlík Míka[a], J. Kočí[a] , N. Klusoňová [a]

[a]Department of Glass and Ceramics, Institute of Chemical Technology, Prague, Czech Republic

The primary aim of this research was to synthesize and analyze precursor suspensions designed for the production of silica-based nanofibers via the electrospinning technique. The main objective of this research endeavor was to fabricate nanofiber mats with properties ranging from amorphous to semicrystalline, thereby allowing for convenient customization and practical application in electrochemical settings, specifically as separators or electrodes in amorphous glass all solid-state batteries. The characterization of the electrospun mats involved an evaluation of their conductivity, while their molecular structure was analyzed using ^{29}Si nuclear NMR spectroscopy.

Nanofibrous structures

Nano/microstructured materials have exhibited remarkable performance across diverse research and industrial domains. Notably, in the energy sector, significant advancements in nanomaterial research have been achieved, particularly concerning electrode materials, electrolytes, and membranes for fuel cells. Moreover, these innovative technologies and applications have been reported in fields such as material engineering, tissue engineering, and water and gas treatment, among others.

The distinctive feature of nanomaterials lies in their exceptionally large surface-to-diameter ratio, which confers upon them enhanced mechanical strength, flexibility, surface area-to-volume ratio, porosity, gas permeability, and structural stability compared to bulk counterparts (1, 2). As a consequence of this attribute, the utilization of nano/micromaterials offers a potential solution to circumvent numerous issues commonly encountered when employing bulk materials such as silicone electrode cracking (6). Typically, nanofibrous materials have fiber diameters ranging from 100 nm to 800 nm, with reported instances of mass-produced fibers as fine as 36 nm and even as small as 2 nm in limited quantities (3, 4).

Numerous techniques have been explored for nanofiber preparation, with electrospinning being considered the most versatile among them. This method allows for the processing of a wide range of materials, precise control over fiber diameter, and the fabrication of multicomponent configurations, including nanotubes, nanorods, or nanowires. Electrospun fibers are relatively easy to align, assemble, and integrate into applications at a relatively low cost (5). In the realm of silica-based nanofiber preparation, electrospinning stands as one of the few viable methods. Another cost-effective approach is the melt-blowing technique, although it typically results in fibers with diameters exceeding 800 nm (4).

The resulting properties of the nanofibrous products are influenced by a multitude of factors, which can be broadly categorized into three groups: 1) material properties (e.g., concentration, viscosity, conductivity, surface tension), 2) processing parameters (e.g., voltage, flow rate, collector distance, spinner configuration), and 3) ambient conditions (primarily ambient temperature and humidity) (4).

The current study centers on the synthesis of amorphous silica and alumino-silica glass nanofibers impregnated with active electrode materials through the electrospinning technique. The precursor suspensions are formulated by combining tetraethyl orthosilicate (TEOS) as a high-temperature binder for the active material, polyvinylpyrrolidone (PVP) to improve spinnability, and active material sourced from discarded batteries and solar cells. The active nanoparticles are obtained via high-energy dry and wet ball milling methods. The fibrous mats produced in this study exhibit the capacity to endure temperatures of up to 1000°C while retaining their flexibility.

References

1. Yang, X.-h., P. He, and Y.-y. Xia, *Preparation of mesocellular carbon foam and its application for lithium/oxygen battery.* Electrochemistry Communications, 2009. **11**(6): p. 1127-1130.
2. Zhang, B., et al., *Recent advances in electrospun carbon nanofibers and their application in electrochemical energy storage.* Progress in Materials Science, 2016. **76**: p. 319-380.
3. Soltani, I. and C.W. Macosko, *Influence of rheology and surface properties on morphology of nanofibers derived from islands-in-the-sea meltblown nonwovens.* Polymer, 2018. **145**: p. 21-30.
4. Zdraveva, E., et al., *Electrospun nanofibers*. 2017. p. 267-300.
5. Liu, Y., et al., *Preparation and characterization of electrospun SiO2 nanofibers.* Journal of nanoscience and nanotechnology, 2008. **8 3**: p. 1528-36.
6. Favors, Z.; Bay, H. H.; Mutlu, Z.; Ahmed, K.; Ionescu, R.; Ye, R.; Ozkan, M.; Ozkan, C. S. *Towards Scalable Binderless Electrodes: Carbon Coated Silicon Nanofiber Paper via Mg Reduction of Electrospun SiO2 Nanofibers.* Scientific Reports 2015, 5 (1), 8246. DOI: 10.1038/srep08246.

Anthracite as anode material for sodium-ion batteries

A. Šimek, T. Kazda and O. Čech

Department of Electrotechnology, Brno University of technology, Brno 616 00, Czech Republic

This article addresses the issue of development of anode materials for sodium-ion batteries. As graphite cannot be used for this technology in contrast to of lithium-ion technology, the aim is to find a substitute. Anthracite appears to be a promising material as with its very low cost and availability is also more geo-politically favorable than graphite. The experimental part then deals with the characterization of calcined anthracite and the subsequent electrode fabrication, complemented by the electrochemical characterization of the prepared electrodes.

Introduction

Today, lithium-ion (Li-ion) battery technology represents the majority of the global battery market. This is mainly due to their good operating characteristics, such as high gravimetric and volumetric energy density. Other advantages include their relatively long lifetime and the fact that they are now a time-proven technology in various market sectors. However, this type of technology suffers from socio-economic material constraints. Considering the widespread presence of sodium in the Earth's crust and its very similar properties, sodium-ion (Na-ion) battery technology appears to be a suitable complementary technology to Li-ion technology. [1]

Anode materials for sodium-ion batteries

The large ionic radius of sodium results in the difficulty of finding a suitable anode host material. Other problems include higher working potential leading to lower energy density, low coulombic efficiency and volume change during cycling. The development objective is therefore to find a material that will provide a theoretical capacity of approximately 300 $mAh.g^{-1}$ to match Li-ion technology. [2]

Carbon-based materials are among the first choices in the development of anode materials for Na-ion, as graphite is one of the most commonly used in Li-ion technology today. However, graphite intercalates sodium ions poorly, hence surface deposition rather than intercalation occurs. Thus, expanded graphite, non-graphitic carbons, carbon nanomaterials or metal organic frameworks can be alternative substitutes for graphite. [2]

Anthracite is a type of coal, but it contains a very small amount of volatile matter (2-12%) compared to the fixed-carbon content (86-98%) [4]. Although anthracite ranks as the rarest form of coal, its abundance and price make it a promising candidate for future development of anode materials for Na-ion technology [2].

Experimental

Calcined anthracite from a local supplier was used in the experimental part. This material was supplied in the form of grains ranging in size from 3 to 7 mm, as can be seen in *Figure 1a). Figure 1b)* shows the XRD spectrum of calcined anthracite. For further processing, it was therefore necessary to grind the material in a ball mill. From this coarsely ground sample, a first electrode sample was prepared. To achieve finer grinding, the anthracite sample was ground in a planetary mill, thus ensuring a smaller particle size. From this finely ground sample, a second sample of electrode material was prepared.

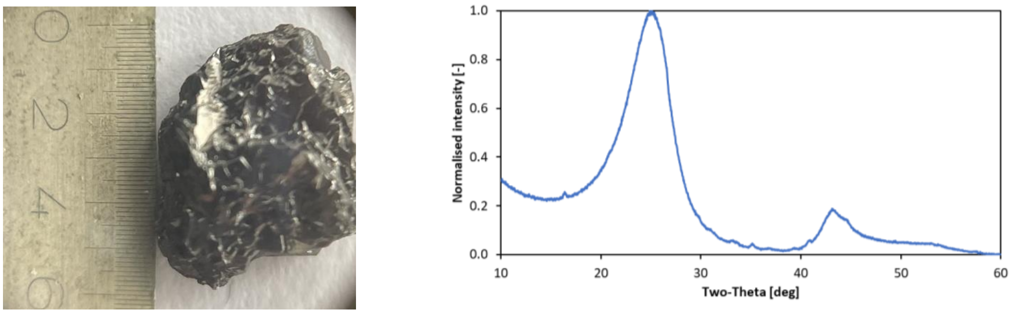

a) b)

Figure 1. *a) anthracite as received and b) XRD spectrum of calcinated anthracite*

The electrode material was prepared from ground anthracite, SuperP and polyvinylidene fluoride in a ratio of 80:10:10 respectively. N-Methyl-2-pyrrolidone was used as solvent. After sufficient mixing of all components, a 200 µm layer of electrode material was deposited on the aluminum foil. After drying, 18 mm diameter electrodes were die-cut and subsequently crimped with 3 tons of pressure.

e)

Figure 2*a)* and *b)* shows an SEM images of the electrodes for comparison of the grain size of the active material. From the prepared electrodes, the EL-CELL® measuring cells were assembled in a Jacomex glove box (under argon inert atmosphere). Lithium metal, Whatman GF/C glass separator and electrolyte labeled 1M NaPF6 in EC:PC (1:1) were used to assemble the half-cells. Electrochemical measurements were then performed on a Bio-Logic multi-channel potentiostat.

e)

Figure 2*c)* and *d)* then show the results of cyclic voltammetry (CV) and

e)

Figure 2*e)* shows a comparison of the cycling results.

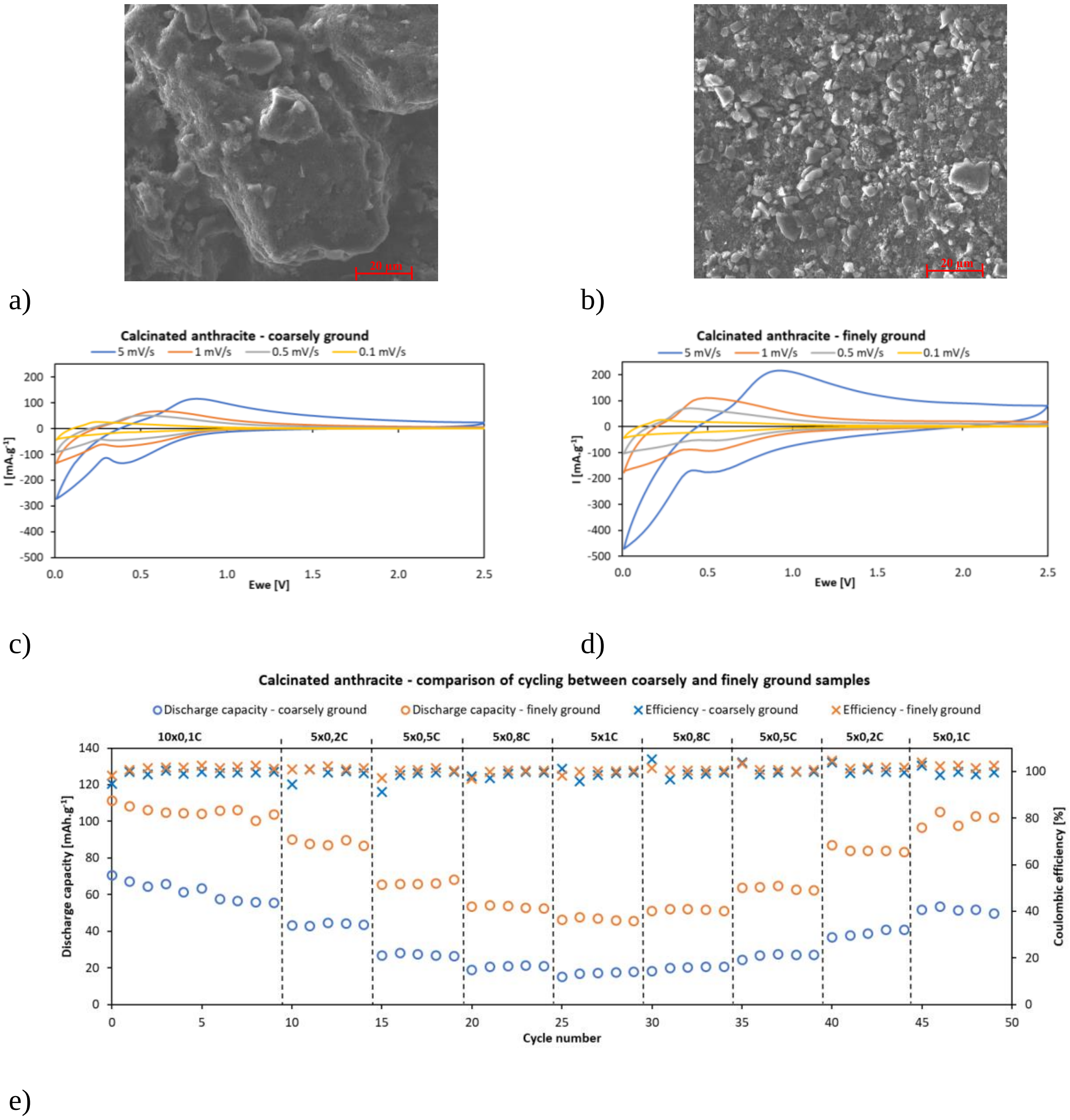

a) b) c) d) e)

Figure 2. *SEM images of electrode with a) coarsely ground and b) finely ground anthracite; results of CV measured on c) coarsely ground and d) finely ground anthracite and e) comparison of cycling results for coarse and finely ground anthracite*

Results and conclusion

From the measured results it can be observed that the particle size significantly affects the performance of the anode. As can be seen on SEM images coarsely ground anthracite had a particle size of approximately 100 um, whereas finely ground anthracite had a particle size of approximately 5 um. The particle size is then associated with the active surface, which significantly affects the overall capacity of the electrode. It is then possible to observe in the CV results a larger current response and better peak rendering for finely ground anthracite. When comparing the discharge capacity, a larger discharge capacity and smaller capacity loss can then be observed for the finely ground sample. These results could be further improved by chemical cleaning and further calcination of the anthracite sample, which remains a task for future research. Overall, anthracite can be used as a relatively cheap anode material with promising characteristics, which could help the future development of Na-ion technology.

Acknowledgments

This work was supported by the specific graduate research of the Brno University of Technology No. FEKT-S-23-8286. We acknowledge CzechNanoLab Research Infrastructure supported by MEYS CR (LM2023051).

References

1. Z. Jiang *et al.*, “Anthracite-based reduced graphene oxide/antimony composites as anode materials for high performance sodium ion batteries”, *Journal of Alloys and Compounds*, vol. 925, 2022, doi: 10.1016/j.jallcom.2022.166631.
2. T. Perveen, M. Siddiq, N. Shahzad, R. Ihsan, A. Ahmad, and M. I. Shahzad, “Prospects in anode materials for sodium ion batteries - A review”, *Renewable and Sustainable Energy Reviews*, vol. 119, 2020, doi: 10.1016/j.rser.2019.109549.
3. Y. Li *et al.*, “Advanced sodium-ion batteries using superior low cost pyrolyzed anthracite anode: towards practical applications”, *Energy Storage Materials*, vol. 5, 2016, doi: 10.1016/j.ensm.2016.07.006.

Interface Engineering in Energy Conversion and Storage Employing Oxide Semiconductors

L. Kavan[a], M. Zlamalova[a,b], V. Mansfeldova[a], H. Krysova[a], H. Tarabkova[a]

[a] J. Heyrovsky Institute of Physical Chemistry, Academy of Sciences of the Czech Republic,
Dolejskova 3, CZ-18223 Prague 8, Czech Republic

[b] Department of Inorganic Chemistry, Faculty of Science, Charles University, Hlavova 2030,
CZ-128 40 Prague, Czech Republic

E-mail: kavan@jh-inst.cas.cz

Semiconducting oxides (such as SnO_2, TiO_2 and ZnO) find salient applications in batteries, photovoltaics (both dye-senstized and perovskite), photocatalysis and solar fuel generation. Characterization of electronic structure near the conduction band minimum (CBM) provides deeper understanding of the photo/electro/chemical activity. Yet, literature about these three generic oxides is overloaded by highly inconsistent data [1]. We addressed these inconsistencies by interfacial engineering and advanced characterizations, based on a combination of electrochemical impedance spectroscopy, photoelectrochemical methods, photoelectron spectroscopy (XPS, UPS, including NAP-techniques), Kelvin probe measurements and scanning probe microscopy (AFM, KPFM) [2]. Our studies show that the CBM positions and/or work functions of these oxides can vary in a surprisingly broad range of nearly 1 eV depending on the actual sample environment and on the details of its synthetic history [2,3]. The macroscopic single crystals of various phases and orientations along with high-quality compact layers made by optimized procedures based on atomic layer deposition (ALD) or spray pyrolysis appear to be the ideal reference materials for addressing the above-mentioned contradictions. This knowledge provides rationale for optimization of oxide semiconductors in a range of technologies of energy conversion and storage.

Acknowledgment

This work was supported by the Grant Agency of the Czech Republic (contract No. 22-24138S).

References

1. PATEL, M.Y., MORTELLITI, M.J., DEMPSEY, J.L., A Compendium and Meta-analysis of Flatband Potentials for TiO2, ZnO, and SnO2 Semiconductors in Aqueous Media, Chem. Phys. Rev., 3 (2022) 011303.
2. ZLAMALOVA, M., MANSFELDOVA, V., TARABKOVA, H., KRYSOVA, H., KAVAN, L., Variable work function of semiconducting thin-film oxide electrodes: a case study of SnO2 and TiO2, J. Solid State Electrochem., 27 (2023) 1935-1943.
3. MANSFELDOVA, V., ZLAMALOVA, M., TARABKOVA, H., JANDA, P., VOROKHTA, M., PILIAI, L., KAVAN, L., Work Function of TiO2 (Anatase, Rutile, and Brookite) Single Crystals: Effects of the Environment, J. Phys. Chem. C, 125 (2021) 1902-1912.

Melanin-Organic Polymer with Semiconductor Properties as Unusual and Effective Material for the Energy Industry

[3]E. Shembel, [2]V. Kyrychenko, [1]V. Redko, [1]T. Pastushkin, [1]B. Kutnick, [3]A. Markevich

[1]Enerize Corporation, Coral Springs, FL, 33067, USA

[2] Sunoil-Agro, Pavlograd, 51400, Ukraine

[3] Scientific Research Laboratory of Chemical Power Sources of Ukrainian State University of Chemical Technology, Dnipro, 49005, Ukraine

Melanin is a biological organic polymer and has semiconductor properties. The structure of organic semiconductors – like melanin determines the mechanism of their semiconductor nature, electrical and catalytic properties. Principal common structure of melanin. C18H10N2O4. Molecular Weight 318 g/mol. Density: 1.6 to 1.8 g/cm^3.

Our goal is to use Melanin - as an unusual material for investigating and following scaling up in the innovative energy industry based on the Melanin technologies.

1. Generating energy in hybrid systems, which include: a) Melanin-organic polymer with semiconductor properties; and b) Silicon or other inorganic semiconductor.
2. Our results confirm that Melanin is an effective modifier for electrodes and for increasing the energy and power of batteries.
3. Generating the innovative solid polymer electrolytes without binder for high energy Li–ion batteries and other batteries, like Mg-ion batteries

The Ukrainian production of Sunoil-Agro, Ukraine, has developed an innovative technology for the synthesis of melanin under the leadership of the Director Mr. Kyrychenko Volodymyr N., and produces the melanin in the amount of up to 200 kg per year. Various types of Melanins are produced.

Now we present some results of research and testing of an innovative hybrid energy system based on an organic semiconductor – melanin, and an inorganic semiconductor –silicon. For comparison, we will provide a conventional energy system - a solar cell based on a silicon wafer.

Results below show the unique performance of the hybrid system based on melanin and silicon: as the illumination level decreases, the open circuit voltage of the hybrid system increases significantly. In this case, the electromagnetic properties of the system components are affected.

1. Characteristics of the energy system – solar cell based on a silicon wafer

The characteristics (open circuit voltage) of the No. 113 silicon wafer solar cell in high and low light are shown below in Figure 1. The presented results show that as the illumination value decreases, the open circuit voltage of the solar cell decreases sharply.

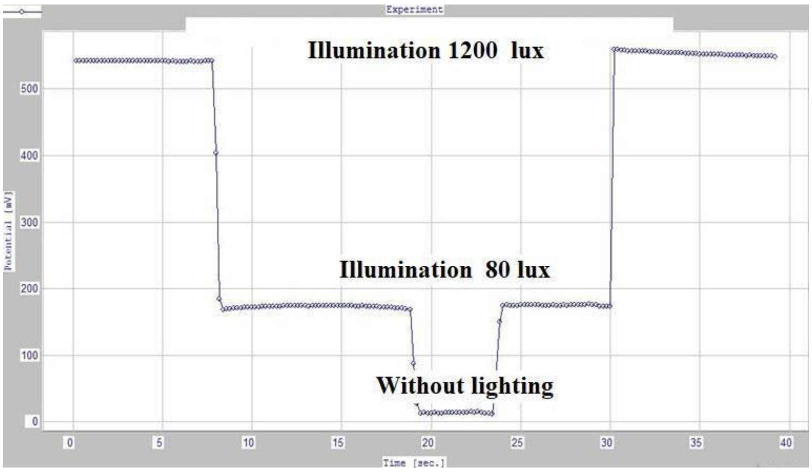

Figure 1. *Open circuit voltages of the No. 113 silicon solar cell are under strong illumination (approximately 12,000 lux), low illumination (80 lux), and at no illumination.*

2. Characteristics of the hybrid energy system – based on the melanin and silicon wafer.

Characteristics of an innovative hybrid energy system based on an organic semiconductor – melanin and an inorganic semiconductor - silicon wafer shown on Figure 2

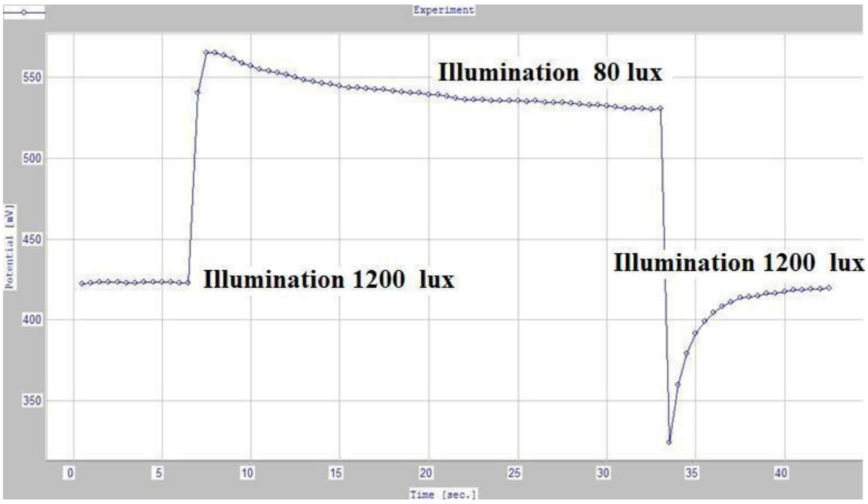

Figure 2. *Dependence of the open circuit voltage on the illumination of a hybrid system, including a melanin and silicon.*

During presentation we will also present:

1. How melanin effectively modifies the electrodes of the Li-ion and increasing the energy and power of battery
2. Properties of the polymer electrolyte synthesized based on melanin

References

1. X. Gu, S. Zhang, and Y. Hou. *Chin. J. Chem*., **34**, 13 (2016).
2. H. Zhang, X. Li, and H. Zhang. Li-S and Li-O2 Batteries with High Specific Energy. Springer Briefs in Molecular Science. Pages 1-48, Springer, Singapore (2017).
3. Z. Wei Seh, W. Li, J.J. Cha, G. Zheng, Y. Yang, M.T. McDowell, P-C. Hsu, and Y. Cui, *Nat Commun*., **4**, 1331 (2013).
4. W. Zhou, Y. Yu, H. Chen, F.J. DiSalvo, and H.D. Abruña, *J. Am. Chem. Soc.*, **135** (44), 16736 (2013).
5. E. Shembel, V. Kyrychenko, I. Maksyuta, V. Redko, N. Zaderey and M. Tkach, *ECS Trans.*, **99** (1), 47 (2020).
6. M. Naoi, W. Maruyama and P. Riederer. *Encyclopedia of Movement Disorders*, p. 169, Academic Press (2010).
7. Yu. Polishchuk, E. Shembel and Andrea Straková Fedorková. *ECS Trans.*, **99** (1), 133 (2020).

Tilt angle adjustment for solar panels mounted on solar ships to optimize the charging cycle of connected batteries

R. Bayer[a], J. Maxa[a], P. Šabacká[a], P. Dostálová[a]

[a] Department of Electrical and Electronic Technology, Brno University of Technology,
Technická 10, 616 00 Brno, Czech Republic

These days many solar ship projects exist such as TURANOR PlanetSolar, Solar Voyager, Solaris, SoelCat 12 and the Helios yacht [1-4], which use solar energy obtained from solar panels mounted on their deck or from solar sails. For this reason, each of these solar ships needs a good quality battery to power its engine and accessories when sunlight is not available. This article compares the stability of usable solar heat flux incident on horizontally and vertically mounted solar panels surface based on the season and latitude at which they are supposed to be used. This article also compares two different ways to charge the ships' batteries throughout the day, which are maximizing the power gathered from sun regardless the power peaks at specific times of the day and optimizing the power output of the panels to be as smooth as possible throughout the day. All simulations were calculated using the ANSYS simulation software.

Introduction

These days the number of applications in which solar panels can be used grows rapidly. One of these applications is using the solar panels to power ships and other vessels and accumulate the energy gathered from the sun to batteries used on those vessels.

However, using solar panels on ships have both advantages and disadvantages. Advantages include, for example, the energy self-sufficiency of the ship, lower operating costs of the vessel and a greener and quieter operation compared to ships powered by internal combustion or diesel engines.

On the other hand, disadvantages of using solar panels on ships include the dependence of such a system on sufficient sunlight and the cleanliness of the active area of the panels. The cover glass of solar panels should also have a protective layer that is resistant to aggressive environmental conditions such as salt water, higher UV exposure, etc [5-8].

This article aims at and compares the differences, advantages and disadvantages between vertical and horizontal solar panels mounting in terms of stability of the usable solar heat flux incident on their surface.

Methods and calculations

The current Experimental Chamber consists of two chambers separated by a small opening that simulates the condition created by differential pumping in an electron microscope.

For calculations and simulations of incident radiation on both horizontally and vertically mounted panels, we used ANSYS simulation software, because of its ability to calculate not only the incident radiation on the panels directly from the sun, but also the radiation reflected from the water surface [9-10].

Ship model used in the calculations was heading towards north and calculations were made for positions 0°N, 0°E; 40°N, 0°E and 80°N, 0°E. On each side of the ship model a vertically mounted panel with surface of 1 square meter was modeled at a varying inclination angle of 0°, 15° and 30° inwards from vertical walls creating a truncated pyramid with a horizontal panel on its top side. Simulations were calculated for two specific dates, 21st June (summer solstice) when the sun trajectory over the sky is longest and 21st December (winter solstice) when it is shortest. As shown on Fig. 1, the *sunshine factor* reflecting the sky clarity was set to 1, meaning clear sky.

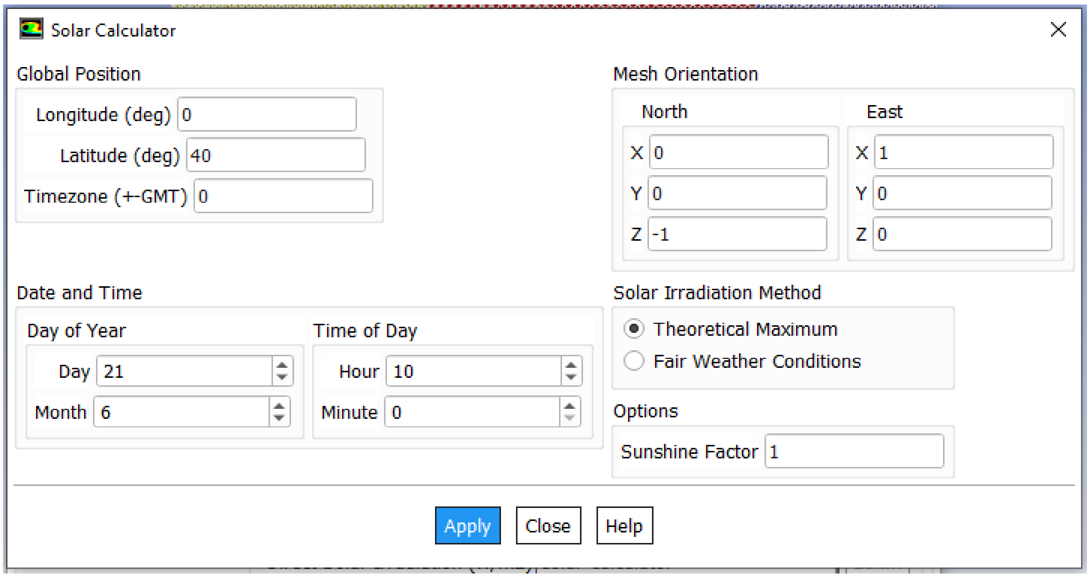
Solar Calculator

Global Position
Longitude (deg) 0
Latitude (deg) 40
Timezone (+-GMT) 0

Mesh Orientation
North: X 0, Y 0, Z -1
East: X 1, Y 0, Z 0

Date and Time
Day of Year: Day 21, Month 6
Time of Day: Hour 10, Minute 0

Solar Irradiation Method
● Theoretical Maximum
○ Fair Weather Conditions

Options
Sunshine Factor 1

Figure 1. *Example of conditions used for calculations of absorbed solar heat flux*

In all simulations a theoretical maximum solar heat flux specific to every single location was used and time interval of the day was chosen from 5am to 10pm with timestep of 1 hour.

Results and Discussions

As shown on Table 1, horizontally mounted solar panel absorbs much more incident solar radiation in midday than set of vertical panels (see *Avg. vertical* column) and the average absorbed solar radiation is also higher (see Table 2 below).

TABLE I. *Amount of absorbed solar heat flux including radiation reflected from water surface*

21st June; 0°N, 0°E; 15° wall inclination							
Hour	**Solar heat flux [W/m2]**						
	Western	**Eastern**	**Upper**	**Northern**	**Southern**	**Avg. vertical**	**Vertical / horizontal**
5	0,00	0,00	0,00	0,00	0,00	0,00	-
6	56,10	442,00	58,68	207,50	58,82	191,10	326 %
7	180,89	919,27	370,90	501,61	184,16	446,48	120 %
8	296,11	1132,10	727,56	716,94	297,47	610,66	84 %
9	389,85	1189,20	1040,50	878,85	388,50	711,60	68 %
10	458,52	1133,20	1280,70	994,45	454,27	760,11	59 %
11	499,24	985,87	1430,40	1062,50	492,08	759,92	53 %
12	757,35	771,96	1485,20	1088,40	507,50	781,30	53 %
13	974,58	508,45	1436,20	1065,00	493,57	760,40	53 %
14	1126,80	461,78	1292,40	999,78	457,47	761,46	59 %
15	1188,80	394,71	1057,10	886,93	393,34	715,95	68 %
16	1139,30	302,36	747,90	727,83	303,74	618,31	83 %
17	938,19	188,32	392,63	516,37	191,68	458,64	117 %
18	471,74	61,76	70,17	223,20	64,68	205,34	293 %
19	0,00	0,00	0,00	0,00	0,00	0,00	-
20	0,00	0,00	0,00	0,00	0,00	0,00	-
21	0,00	0,00	0,00	0,00	0,00	0,00	-
22	0,00	0,00	0,00	0,00	0,00	0,00	-

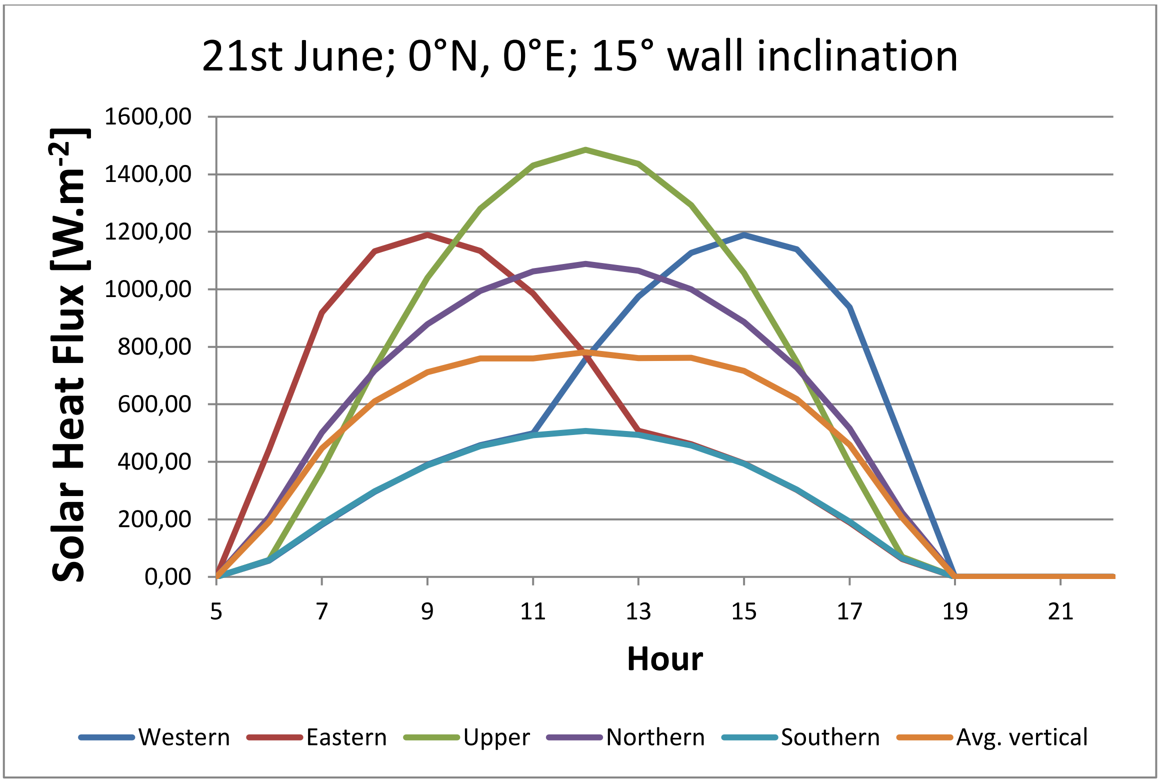

Figure 2. *Graphical representation of the amount of absorbed solar heat flux including radiation reflected from water surface*

TABLE II. *Solar heat flux absorbed by horizontally and vertically mounted solar panels*

21st June; 0°N, 0°E; 15° wall inclination				
Solar heat flux [W/m2]				
Horizontal		**Vertical**		
58,68		191,10		min
876,18		598,56		avg
1485,20		781,30		max
817,50	-93 %	-68 %	407,46	avg-min
609,02	70 %	31 %	182,74	max-avg
1426,52		590,20		0,00

Conclusions

According to simulation results, when using vertically mounted solar panels the average amount of absorbed solar energy is lower by 5 % to 45 % compared to average solar energy absorbed by horizontally mounted solar panels, whereas the stability of absorbed solar energy throughout the day is much better when using vertically mounted solar panels. That means vertically mounted solar panels can supply ship's batteries with more constant power and there is no need to use such powerful power resistors in Battery Management System to burn excess power to avoid batteries overcharging. This can also prolong both Battery Management System's and batteries' lifetime.

Acknowledgments

This research was supported by Brno University of Technology specific research program: Materials and technology for electrotechnics IV, reg. no. FEKT-S-20-6206.

References

1. Six sun-powered ships. Engadget [online]. [cit. 2023-07-23]. Available from: https://www.engadget.com/2016/09/24/six-sun-powered-ships/
2. Sun River - an electric boat on the Rideau Canal. SunRiver [online]. 2023 [cit. 2023-07-20]. Available from: https://sun-river.ca/
3. G.S. Spagnolo, D. Papalillo, A. Martocchia, G. Makary, Solar-Electric Boat, J. Transp. Technol. (2012). doi:10.4236/jtts.2012.22015.
4. S.M. Lutful Kabir, I. Alam, M. Rezwan Khan, M.S. Hossain, K.S. Rahman, N. Amin, Solar powered ferry boat for the rural area of Bangladesh, in: 2016 Int. Conf. Adv. Electr. Electron. Syst. Eng. ICAEES 2016, 2017. doi:10.1109/ICAEES.2016.7888005.
5. T. Hwang, S. Kang, J.T. Kim, Optimization of the building integrated photovoltaic system in office buildings - Focus on the orientation, inclined angle and installed area, in: Energy Build., 2012. doi:10.1016/j.enbuild.2011.10.041.
6. F. Bayrak, G. Ertürk, H.F. Oztop, Effects of partial shading on energy and exergy efficiencies for photovoltaic panels, J. Clean. Prod. (2017). doi:10.1016/j.jclepro.2017.06.108.
7. C. Norberto, C.N. Gonzalez-Brambila, Y. Matsumoto, Systematic analysis of factors affecting solar PV deployment, J. Energy Storage. (2016). doi:10.1016/j.est.2016.04.003.
8. R. Haselhuhn, P. Maule, Fotovoltaické systémy, 1. české vydání, rev. 1, Česká fotovoltaická asociace, Plzeň, 2017.

9. M.Z. Jacobson, V. Jadhav, World estimates of PV optimal tilt angles and ratios of sunlight incident upon tilted and tracked PV panels relative to horizontal panels, Sol. Energy. (2018). doi:10.1016/j.solener.2018.04.030.
10. G.E. Lau, E. Sanvicente, G.H. Yeoh, V. Timchenko, M. Fossa, C. Ménézo, S. Giroux-Julien, Modelling of natural convection in vertical and tilted photovoltaic applications, Energy Build. (2012). doi:10.1016/j.enbuild.2012.10.014.

Modular PV System Design and Evaluation

J. Fabián[a], P. Šafl[a]

[a] Brno University of Technology, Brno, Czech Republic

In applications such as mobile workstations, disaster relief or military applications, the only energy sources used nowadays are gas or diesel generators, which could be replaced by more environmentally friendly renewable energy sources. The presented paper aims to provide insight into key elements and design principles for modular PV system design. Furthermore, two such proposed designs, which focus on modularity and mobility, are evaluated as a replacement for the generator-only solution that is used nowadays. We also propose ways of further optimization of the systems.

Design principles for modular PV systems

During the process of designing modular PV systems, many factors need to be taken into account. Depending on the intended use of the system, we must consider the choice of devices (i.e., inverters or batteries) to create a modular system that could be used in mobile and stationary applications and ensure easy scalability. PV systems usually consist of PV modules, inverters and (nowadays) also batteries. In the following subchapters, we discuss the key parts of PV systems and their importance in the design process of modular systems.

Inverters

The main element of a PV system is an inverter, which converts the direct current from PV panels to alternating current as well as controls the maximum power point (MPP) of the connected PV arrays. For the design of modular PV systems, it is important to know, whether a one-phase or three-phase system is needed. The appropriate inverter is then chosen based on this, the expected load characteristics, and the requirements for an on-grid or off-grid system. [1] Furthermore, depending on the AC or DC coupling of the batteries, we may want to utilize battery inverters. Although the AC coupling connection suffers from additional losses, it enables us to easily scale the system's battery capacity.

Batteries

Batteries are used in PV systems to increase overall efficiency by storing surplus energy, but in off-grid systems, they are necessary for the proper functioning of the whole system. As mentioned before, they can be connected directly to the photovoltaic inverter or through their separate battery inverters which regulate the energy flow to the load. [2, 3] When designing a PV system, we often need to make a compromise between battery capacity and the initial cost.

Generators

In standalone off-grid PV systems, we are unable to ensure energy supply in all conditions. Due to this, we can utilize AC generators to provide power in adverse conditions as well as eliminate the need for more PV arrays and higher battery capacity. [3, 4]

Evaluation of proposed designs

Modular PV systems can be in practice used in many applications, especially with mobility in mind, such as mobile workstations, disaster relief, or military applications [4, 5, 6] In this paper, we aimed to evaluate two proposed designs of modular PV systems. Both designs were created to be modular and easily transportable. Both PV systems are off-grid systems with the utilization of backup generators which were designed and simulated in PV*Sol. The first system aims to provide energy for a military field service station [7], whereas the second design focuses on a mobile command center used in crises [4].

The first design consists of PV panels mounted on the roof of ISO1C containers (Fig. 1) with an installed power of 17.6 kWp, eight 1,7 kW microinverters, 310 kWh battery capacity and an 8 kW back-up generator. The main disadvantage of this off-grid system is the low installed power due to insufficient mounting space. However, the proposed PV system is still capable of covering the estimated yearly consumption of the field service station (45 000 kWh) using solar energy with a solar fraction of 32.6%. The rest is covered by the back-up generator. Further optimization of the system could be done by reducing the battery capacity, which was chosen to ensure two days of autonomy.

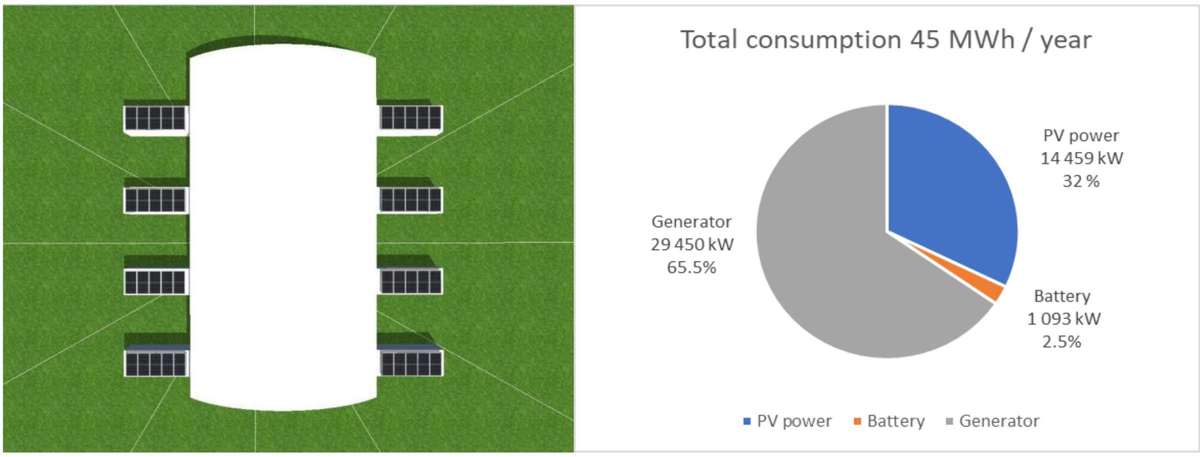

Figure 1. *First PV system design visualization and simulation results. Source: Author*

The second PV system was designed for a mobile command center that should operate for 6 months (April – September) with total consumption of 10 000 kWh. This design focuses on higher mobility with transportable PV panels construction (Fig. 2), installed power of 10.8 kWp, two one-phase inverters, 60.4 kWh battery capacity and a 4 kW back-up generator. Although the proposed design covers 40% of the consumption using solar energy (with a solar fraction of 69%) and can be scaled to eliminate the need for a back-up generator [4], in short-term deployment, the cost-efficiency of such a system would be low.

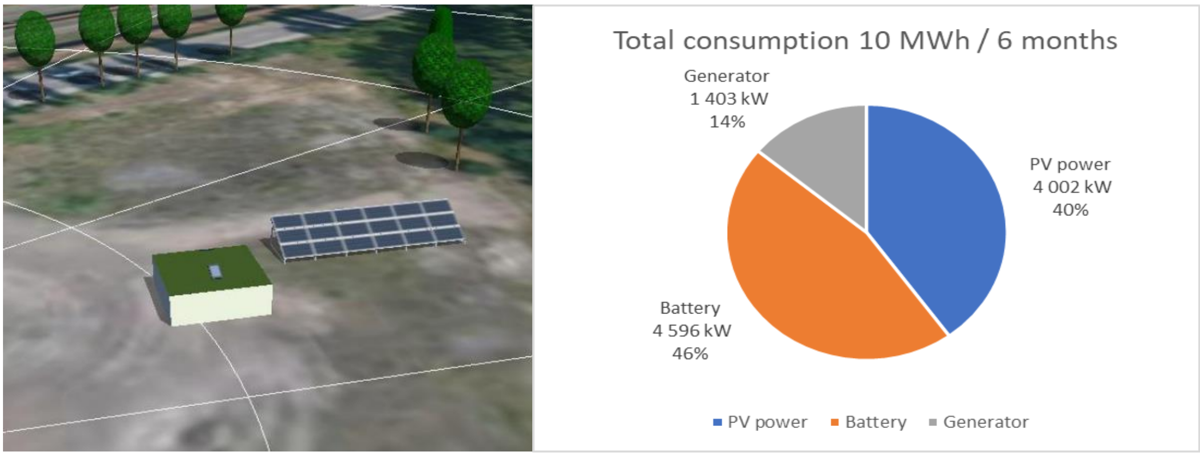

Figure 2. *Second PV system design visualization and simulation results. Source: Author*

Conclusion

The paper focuses on presenting key elements of photovoltaic systems from the point of view of designing modular systems and the evaluation of two proposed PV system designs. The proposed designs are both off-grid PV systems with the utilization of a back-up generator and were designed with modularity and mobility as their key aspects. The first design aims to provide renewable energy and energy sustainability to military field service stations, and the second design focuses on a mobile command center for disaster relief. Both systems present good examples of practical modular PV systems, although both systems could be further optimized for better cost-efficiency.

Acknowledgments

This work was supported by the specific graduate research of the Brno University of Technology No. FEKT-S-23-8286.

References

1. SALAS, V. a E. OLÍAS. Overview of the state of technique for PV inverters used in low voltage grid-connected PV systems: Inverters below 10kW. *Renewable and Sustainable Energy Reviews* [online]. 2009, **13**(6-7), 1541-1550. ISSN 13640321. Retrieved from: doi:10.1016/j.rser.2008.10.003
2. EL HAMMOUMI, A., S. CHTITA, S. MOTAHHIR and A. EL GHZIZAL. Solar PV energy: From material to use, and the most commonly used techniques to maximize the power output of PV systems. *Energy Reports* [online]. 2022, **8**, 11992-12010. ISSN 23524847. Retrieved from: doi:10.1016/j.egyr.2022.09.054
3. MANIMEKALAI, P., R. HARIKUMAR a S. RAGHAVAN. An Overview of Batteries for Photovoltaic (PV) Systems. *International Journal of Computer Applications* [online]. 2013, **82**(12), 28-32. ISSN 09758887. Retrieved from: doi:10.5120/14170-2299
4. FABIÁN, J., T. BINAR and P. ŠAFL. Photovoltaic system design for strategic infrastructure and mobile command centre. *Acta Innovations* [online]. 2023, (46), 81-92. ISSN 2300-5599. Retrieved from: doi:10.32933/ActaInnovations.46.6

5. BINAR, T., J. ZIMÁKOVÁ, J. FRIDRICH and M. SEDLARIKOVA. Use of Renewable Energy Sources for Power Supply of Variable Traffic Signs. *ECS Transactions* [online]. 2021, **105**(1), 269-280. ISSN 1938-5862. Retrieved from: doi:10.1149/10501.0269ecst
6. QAZI, S. Mobile Photovoltaic Systems for Disaster Relief and Remote Areas. *Standalone Photovoltaic (PV) Systems for Disaster Relief and Remote Areas* [online]. Elsevier, 2017, 2017, 83-112. ISBN 9780128030226. Retrieved from: doi:10.1016/B978-0-12-803022-6.00003-4
7. EISENWORTH, L. *USING INDUSTRY 4.0 PRINCIPLES FOR MOBILE WAREHOUSE DESIGN*. Brno, 2023. Master’s thesis. Brno University of Technology

Nano-Structured Innovative Transparent Polymers Replace the Glass and Increase the Energy of PV Modules

E. Shembel[b], V. Redko[a], T. Pastushkin[a], B. Kutnick[a], K. Sukhyy[b],
Y. Pustovalov[c], D. Kaszuba[c],

[a]Enerize Corporat ion, Coral Springs, FL, 33067, USA

[b]Scientific Research Laboratory of Chemical Power Sources of Ukrainian State
University of Chemical Technology, Dnipro, 49005, Ukraine

[c]INT Sp z o.o.,Ul Pilsudskiego 17/4, 34-074 Rzeszów, Polska.

Traditional photovoltaic modules with the glass are complex, non-flexible, & expensive, requiring the antireflection coating and adhesive polymer between glass and semiconductor. Encapsulation and protective coating using innovative single layer with special structure of nano polymer with high level transparency provides new design of thin film flexible photovoltaic modules and increases the energy of the PV modules**.**

Benefit using nanostructured highly transparent polymer material for compare the PV modules with glass:

1. Nanostructured highly transparent polymer material is applied directly to the PV module surface.
2. This process of polymerization can proceed at low temperatures (80^{o}C) as compared with glass lamination.
3. Enerize polymer material eliminates the need for the adhesives required with glass and some other polymers.
4. This eliminates the multi-layer structure including the reflective surfaces present with glass.
5. No glass is used with this polymer coating.
6. The polymer can be formed as a flat smooth surface or as a “crinkle coat”.
7. The “crinkle coat” version further enhances photon collection efficiency due to the light concentrating effect of the polymer material and its surface morphology.

Images of PV Modules Coated with the Polymer

The crinkle coat surface morphology covers the surface of the solar cell module with the optically transparent polymer layer. Incident light 1; absorbed light 2; reflected light 3 is incident at another point along the surface of the polymer. Solar cell module covering the entire surface with the optically transparent polymer layer.

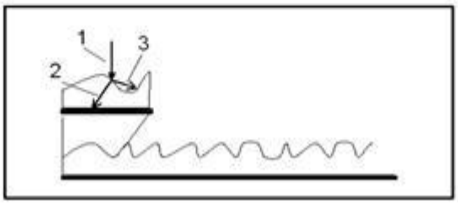

Nanostructure of Transparent Polymer for Encapsulation Silicon or Other Semiconductor for Solar Cells

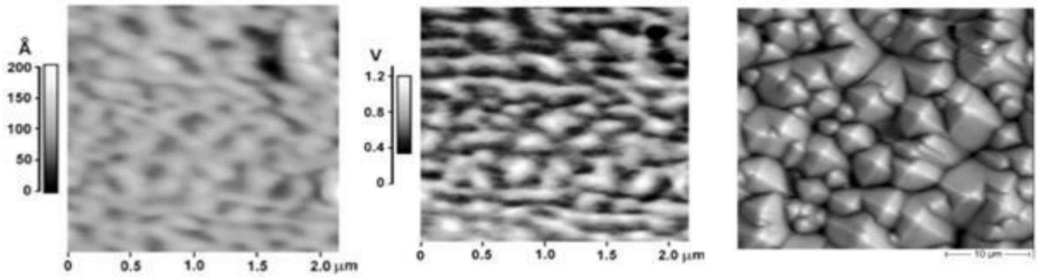

This effect could be titled “Reduction of Lens Reflexion by the "Moth Eye" Principle

Independent center for testing PV modules at Florida International University tested Enerize PV modules based on mono c-Si encapsulated with NSTP. During tests artificial hurricane conditions were modeled using a special test bench. Pictures on the right show the PV modules which have been tested.

Major advantages of PV modules encapsulated with nanostructured transparent polymer

- Increase efficiency by 20% - 30% thus allowing higher electrical output under the same illumination.
- Reduce production costs by 30%
- Reduce weight by 30% compared with traditional methods
- Longer durability of thin film PV modules with Enerize coating

- Works with different types of solar cells: monocrystalline, multicrystalline, amorphous silicon photovoltaics and solar cells based on non-silicon systems such as CIGS.
- Effective utilization of shorter wavelength ranges of the spectrum, including UV, due to the high transparency of the polymeric coating.
- More resistant to degradation by UV and ionizing radiation (so-called photon degradation).
- Stability when exposed to high and low temperatures and thermal-cycling, mechanical impact, and high relative humidity.
- Nanostructured graphite, which developed and produced by company INT Sp z o.o can successfully modify nanostructured transparent polymer and additionally increase the energy of the PV modules

The quote from the NATO Chief Jens Stoltenberg, who suggested battle tanks with solar panels as militaries go green: https://www.thenationalnews.com/world/europe/nato-chief-suggests-battle-tanks-with-solar-panels-as-militaries-go-green-1.1160313 “NATO should do its part to look into how we can reduce emissions from military operations,” he told the Chatham House event. “We know that heavy battle tanks or fighter jets and naval ships consume a lot of fossil fuel and emit greenhouse gasses and therefore we have to look into how we can reduce those emissions by alternative fuels, solar panels or other ways of running our missions

References

1. E. Shembel, T, Pastushkin, V. Redko, etc. *Photovoltaic Module*. US Patent application No. 12/082,859
2. E. Shembel, V. Redko, T. Pastushkin, etc. Nanostructured Transparent Polymer Provides Innovation Design for Solar Cells *The ECS Transactions* 87 (1) pp 231-236
3. Y. Pustovalov, E. Shembel, L. Vishnyakov, etc. Carbon material for electrodes of lithium-ion power sources and method of production thereof. US Patent application No. 10/898631
4. V. Redko, E. Shembel, T. Pastushkin, etc. Method and Device for Rapid Non - Destructive Quality Control of Powdered Materials. US Patent No. 8,102,181

Comparative Photoelectrochemical Characteristics Of Heterostructure And Composite Based On $BiVO_4$ And WO_3

V. O. Smilyk[1*], S. S. Fomanyuk[1], I. A. Rusetskyi[1], M. O. Danilov[1], G. Ya. Kolbasov[1]

[1]V. I. Vernadskii Institute of General and Inorganic Chemistry of the Ukrainian NAS, prospekt Palladina 32/34 Kyiv 03142, Ukraine

*Corresponding Author E-mail Address: VitaliySmilyk@i.ua

Bismuth vanadate has recently attracted more and more attention as a photosensitive material in the visible area of the solar spectrum [1]. The theoretical efficiency of solar energy conversion into chemical hydrogen energy for bismuth vanadate approaches 9% with a maximum current density of approximately 7 mA*cm^{-2} [2]. However, the generation of $BiVO_4$ photocurrent by photoanodes is usually limited by high electron-hole recombination and low charge transfer efficiency at the interfacial boundary, so the experimental value of the photocurrent density is much lower than the theoretically calculated value [2]. The creation of composites or heterostructures based on $BiVO_4$ can improve the efficiency of photoconversion by reducing recombination in photosensitive materials [3]. For this purpose, we conducted comparative studies of the photoelectrochemical efficiency of the composite and heterostructure based on $BiVO_4$ and WO_3.

$BiVO_4$ films were obtained at an anodic current of 0.5 mA/cm^2 from an acidic (HNO_3) electrolyte pH = 4.7 based on 0.01 mol/l $Bi(NO_3)_3$ and 0.035 mol/l $VOSO_4$. The thickness of the coatings was determined by the method of two-beam interferometry [4]. The obtained $BiVO_4$ films with a thickness of 150 nm were annealed in air for three hours at 500 °C. The $BiVO_4/WO_3$ heterostructure was obtained by deposition of WO_3 on top of a $BiVO_4$ film from a peroxide solution: 0.1 mol/l Na_2WO_4, 0.2 mol/l H_2O_2 and H_2SO_4 (pH= 1.1) with a cathode current of 1.5 mA/cm^2. Composites ($BiVO_4$-WO_3) were obtained as follows: colloidal solutions of tungsten trioxide were obtained in a solution of glycerol (25 ml) and $NaWO_4$ (2 g), with the addition of sulfuric acid HNO_3 (5 ml). Then, to obtain the composite, the WO_3 colloidal solution was added to the $BiVO_4$ deposition solution. Thin coatings of the composite were deposited at an anodic current of 2 mA/cm^2. To obtain a homogeneous composite, WO_3 colloidal particles were mixed in the $BiVO_4$ deposition solution. The obtained films based on the composite and heterostructure were annealed in air for three hours at 500 °C. The thickness of the films was 150÷300 nm.

The ratio of WO_3 in the 50/50 mol% WO_3 and $BiVO_4$ composite was selected using the gravimetric method - the WO_3-$BiVO_4$ film (obtained by electrodeposition with WO_3 particles) was weighed on analytical balances, after which WO_3 was etched from the composite by the action of ammonia at pH = 9, in which stable $BiVO_4$ itself. Then the undissolved $BiVO_4$ precipitate was weighed. At the same time, approximately equal thicknesses (d) of the composite 50-50 mol% WO_3-$BiVO_4$ - 300 nm and heterostructures with thicknesses of $BiVO_4$ -150 nm and WO_3 - 150 nm were selected.

Studies of the quantum yield of the photocurrent showed that in the obtained films of the WO_3-$BiVO_4$ composite (Fig. 1 curve 3), in contrast to the heterostructure (Fig. 1 curve 2), a higher value of the quantum yield of the photocurrent is observed in the area of light absorption of pure $BiVO_4$.

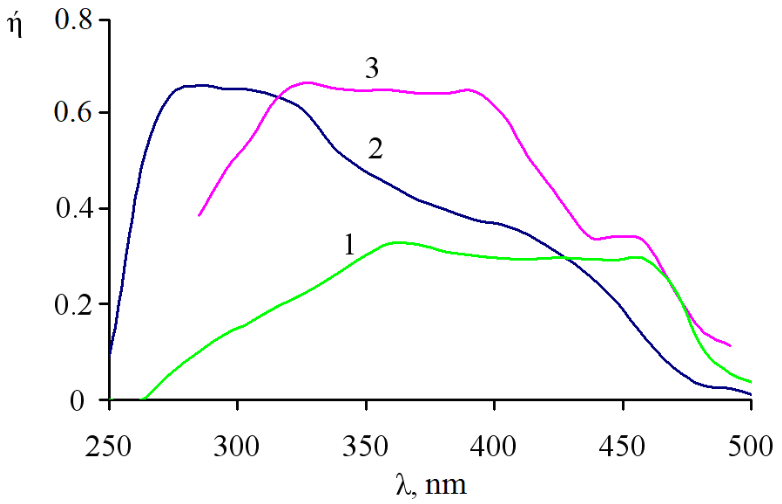

Figure 1. Spectral dependences of the photocurrent quantum yield for 1 - a thin film of $BiVO_4$, 2 - a heterostructure, and 3 - a composite of $BiVO_4$ with WO_3 in a 0.1 M Na_2SO_4 solution at a potential of +0.8 V relative h.s.e.

The reason for such a positive effect may be the reduction of energy losses associated with the recombination of electrons and holes in $BiVO_4$, which, as it was established from photoluminescence studies (Fig. 2), is spent on radiative processes in the longer wavelength region of the spectrum, depending on the excitation wavelength. Fig. 2 shows that the most intense photoluminescence is observed for wavelengths of excitation with UV radiation (i.e. higher energy hν), which indicates a significant contribution to photoluminescence of surface radiative recombination. Therefore, to increase the efficiency of photoconversion, it is important to increase the contact area of $BiVO_4$ with WO_3, in which efficient electron transfer takes place [3] and, obviously, reduces radiative recombination losses.

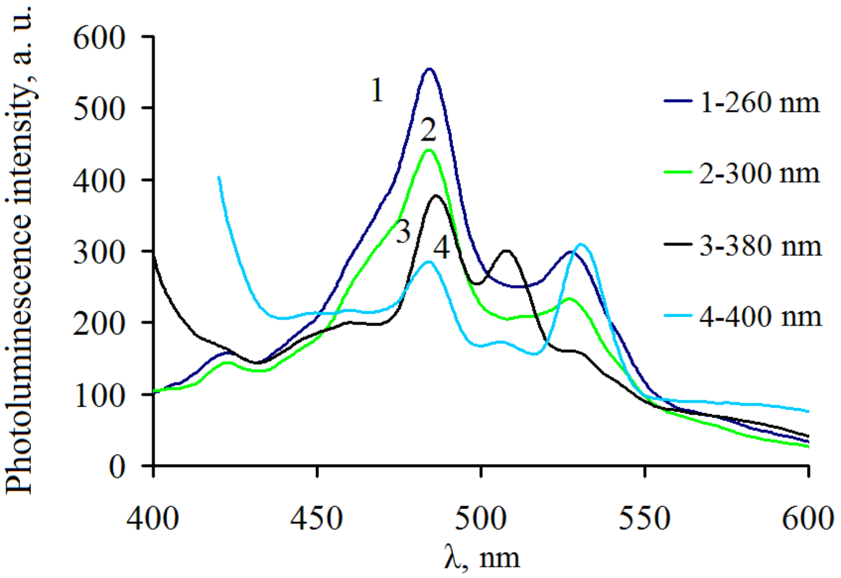

Figure 2. Photoluminescence spectra of thin $BiVO_4$ coatings with a thickness of 140 nm depending on the excitation wavelength.

Thus, it is shown that in the films of WO_3-$BiVO_4$ composites, in contrast to the $BiVO_4$/WO_3 heterostructure, there is an increase in the photocurrent quantum yield in the visible light range of

350-500 nm. This is due to the fact that the contact area of WO_3-$BiVO_4$ in the composite is larger than in the corresponding heterostructure, which leads to a decrease in recombination in the composite and an increase in photoelectrochemical efficiency.

References

1. Brack P, Sagu J-S, Peiris T, McInnes A, Senili M, Wijayantha K, Marken F, Selli E 2015 *Chem. Vapor Depos.* **21** 41
2. Huang Z, Pan L, Zou J, Zhang X, Wang L 2014 *Nanoscale* **6** 14044
3. Hong S, Lee S, Janga J, Lee J **2011** *Energ. Env. Scien.* **4** 1781
4. Smilyk V, Fomanyuk S, Kolbasov G, Rusetskyi I, Vorobets V, **2019** *Res. on chem. intermed.* **45** 4149

Innovate, Collaborate, Regulate: Navigating Through Lithium-ion Battery Transport Regulations

Andreas Gigl, BSc

Research institutes, when collaborating with external project partners, can face the necessity to send Lithium-ion or Lithium-metal cells and batteries that were produced in their own lab to places outside their own facility. As soon as such a cell or battery is being transported, the rules of the ADR (Agreement concerning the International Carriage of Dangerous Goods by Road) apply and must be followed to avoid penalties and safety risks.

In addition, the quality management programme mentioned in the ADR is a valuable source for implementing a system to enhance the quality and reproducibility of manufactured cells and batteries. Furthermore, it supports ensuring the safety of these products whether they will be kept in the producing facility or be shipped externally. The nine points of this programme can also be used for knowledge and innovation management, which can create additional value for the research group or institute.

This lecture will commence with the acquisition of the current version of the ADR. It is necessary to only use the original and most updated version of this UN treaty. the starting point for the topic of Lithium-ion/-metal cells and batteries will be shown and how to follow the different forks for different applications and products. Based on a case study, the applicable rules and regulations will be explained This will lead to the above-mentioned quality management programme, where all points will be discussed regarding the ideas and goals behind them and how these requirements can be met. These requirements will also be presented with their use for knowledge and innovation management to show how following these rules can have an additional value. At the end, there will be a discussion about the guideline to read through the ADR and the requirements it contains.

Impact of rolling temperature over mechanical and corrosion behavior of austenitic steel

Rahul Singh, B. Kranthi Kumar and Abhishek Kumar*

Department of Applied Mechanics, Motilal Nehru National Institute of Technology Allahabad,
Prayagraj -211004, India

*Corresponding author: abhishek@mnnit.ac.in

Abstract

Stainless steel, a cost-effective material, is considered a promising electrode for green electrochemical energy storage and conversion systems. In the present work, 316-austenitic stainless steel was severely deformed to 90% thickness reduction employing cryorolling and room temperature rolling to study its effect on its mechanical properties and corrosion behavior. Cryorolling resulted in improved tensile strength and microhardness of 2056 MPa and 500 VHN as compared to 1751 MPa and 460 VHN for room temperature rolling. The enhancement in properties of cryorolled steel is evident of accumulation of higher dislocation density as compared to room temperature rolled steel. The corrosion behavior were estimated via linear polarization corrosion tests and electrochemical impedance spectroscopy. Resistance to corrosion decreased with increasing strain during both used process of rolling for steel sheets.

Keywords: Cryorolling (CR), Room temperature rolling (RTR), Austenitic stainless steel (Type-316), Mechanical properties and corrosion behavior.

Results and Discussion

Mechanical properties

Figure 1 (a) & (b) shows reflexes of effect of rolling over the mechanical properties. Rolling at room temperature as well rolling at cryo temperature condition remarkably enhanced ultimate tensile strength (UTS). Yi Xiong et al [1], Xiong et al. [2] and Zheng et al. [3] to confirmed the same trends for different steels, this is all because of suppression of dynamic recovery i.e., resulting in accumulation of large number of dislocations, however dynamic recovery in room temperature rolled specimens resulted in the values to lower end. The other factor responsible for enhancement in UTS and hardness values is evolution of strain induced martensite phase and material strain hardening during cryo-deformation.

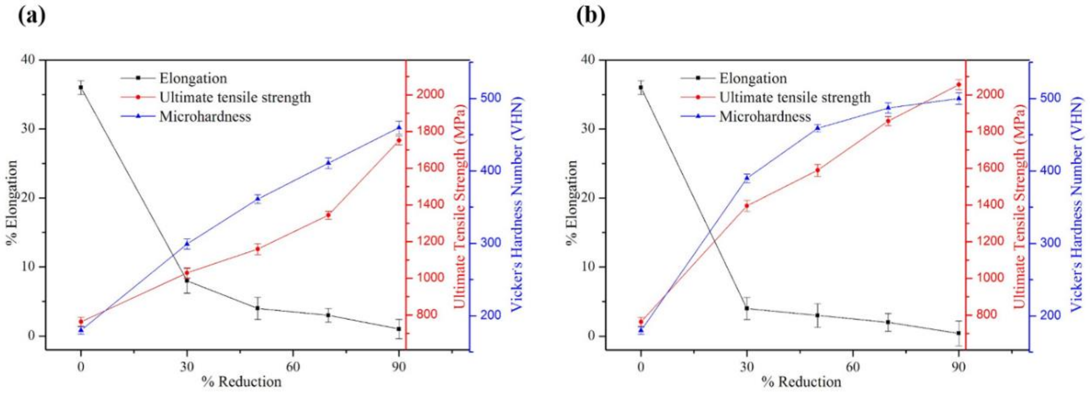

Figure 1. Elongation, ultimate tensile strength (UTS) and micro hardness of RTR (a) and CR (b) 316 austenitic steel at different percentage of thickness reductions.

Corrosion analysis

Fig. 2 shows the linear polarization plots for room tempere rolled and cryorolled samples in the 3.5% NaCl solution. Decrease in corrosion resistance occurs for both room temperature and cryorolled conditioned samples, which may be attributed to increased level of lattice defects (mainly high dislocation density and high low angle grain boundaries). The atoms seated at these sites goes in to the solution because of their less stable crystalline domain. As rate of corrosion reaction is directly proportional to the concentration of reactive sites, as the concentration of lattice defects increases, corrosion rate is increased. In addition, corrosion rate is also in direct relation to the total amount of α′-martensite. Several studies pertaining to cold roliing of different austenitic steels have reported decreased corrosion resistance [4-6]. Lower values of corrosion potential and higher values of corrosion current density for both rolling routes proves processed steel corrodes rapidly.

Fig. 3 depicts (a) Nyquist diagram and (b) Bode phase formalism for undeformed (0% RTR) and room temperature rolled sample, where (c) and (d) represents niquest and bode phase formulation for cryorolled conditioned samples. It is apparent that the Nyquist plots are unfinished semicircle, similar nyquist plots are also outlined as unfinished capacitance arc [4]. This suggest more the diameter of semicircle, better the resistance of the film. It also suggest with increasing deformation, the resistance of film deplete. From bode plots, the adverse effect of rolling is mirrored at low frequency side.

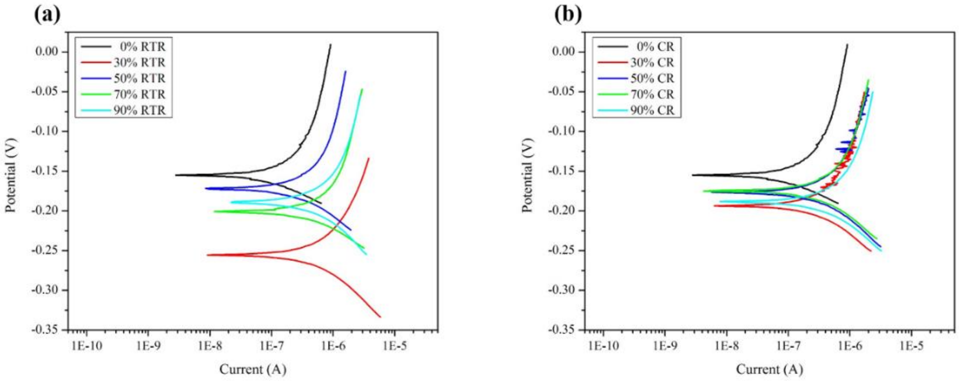

Figure 2. Linear polarization curves of 316 steel rolled at different temperature condition: (a) room temperature and (b) cryo temperature.

Table 1. *Electrochemical corrosion parameters obtained from the linear polarization curves as a function of various room temperature percentage thickness reduction (% RTR).*

Specimen condition	**OCP**	**E_{corr} (mV)**	**β_a (mV/dec)**	**β_c (mV/dec)**	**I_{corr} (μA)**	**Corrosion rate (mm/Yr)**	**Polarization resistance (kΩ)**
0% RTR	-0.153	-199.16	77.175	202.6	490.4nA	0.0056984	49.493
30% RTR	-0.235	-255.35	104.25	184.86	1.0018	0.011641	28.899
50% RTR	-0.125	-172.16	95.675	311.34	660.36nA	0.00776733	48.131
70% RTR	-0.148	-200.53	74.257	173.11	818.04nA	0.0095056	30.44
90% RTR	-0.156	-189.13	155.69	576.46	1.7486	0.020319	27.58

Table 2. *Electrochemical corrosion parameters obtained from the linear polarization curves as a function of cryo deformation (% CR).*

Specimen condition	**OCP**	**E_{corr} (mV)**	**β_a (mV/dec)**	**β_c (mV/dec)**	**I_{corr} (μA)**	**Corrosion rate (mm/Yr)**	**Polarization resistance (kΩ)**
0% CR	-0.153	-199.16	77.175	202.6	490.4nA	0.0056984	49.493
30% CR	-0.151	-193.55	111.41	338.86	769.27nA	0.008939	47.335
50% CR	-0.146	-176.8	98.414	225.7	670.24nA	0.007788	44.407
70% CR	-0.136	-174.81	102.16	265.85	762.25nA	0.008857	42.048
90% CR	-0.151	-188.61	100.83	241.03	850.95nA	0.009888	36.283

Table 3. *Equivalent circuit parameters for 316 austenitic steel as a function of cryorolling.*

Specimen condition	**R_S (Ω)**	**R_P (kΩ)**	**CPE**	
			Y_0 (μmho)	n
0% CR	23.6	125	39	0.879
30% CR	35.8	78	79.6	0.861
50% CR	24.9	54.2	85	0.907
70% CR	25.5	57.3	85.1	0.872
90% CR	48.4	40	70.6	0.88

Table 4. *Equivalent circuit parameters for 316 austenitic steel as a function of room temperature rolling.*

Specimen condition	**R_S (Ω)**	**R_P (kΩ)**	**CPE**	
			Y_0 (μmho)	n
0% RTR	23.6	125	39	0.879
30% RTR	23.6	25.9	64.5	0.886
50% RTR	26	50.7	33.9	0.833
70% RTR	26.2	30.5	35.2	0.822
90% RTR	25.4	32.6	91.9	0.877

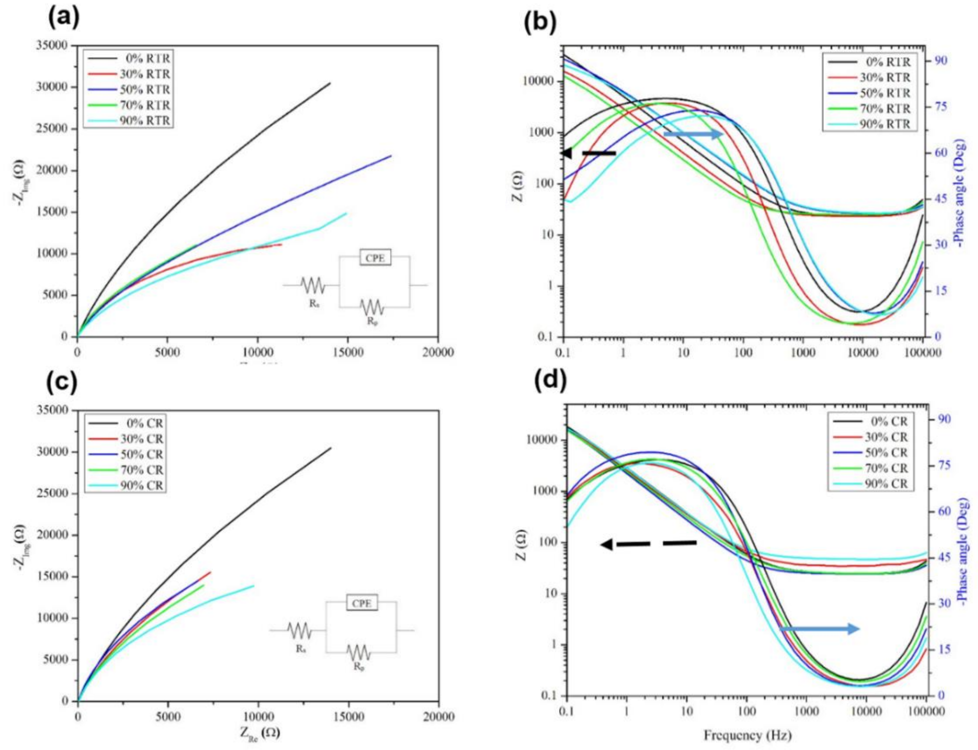

Figure 3. *Niquest plot for (a) room temperature rolled condition (c) cryorolled condition, (b) and (d) representing corresponding bode plots.*

Conclusions

- The UTS of undeformed steel (i.e. 0% RTR) is improved to approximately 129 % after 90% RTR, i.e, 763 MPa to 1751 MPa, while for cryorolling UTS is improved to approximately 169 % after 90% CR from 763 MPa to 2056 MPa.
- The hardness values have increased from 180VHN to 460 VHN (gross increase 156%) after completion of 90% room temperature rolling. Simillarly the gross increase of 178% in hardness is noted for cryorolled 316 austenitic steel. The hardness values have increased from 180VHN to 500 VHN.
- According to the linear polarization and electrochemical impedance tests, the uniform corrosion rate increases and the corrosion resistance decreases with increasing percentage reduction (RTR & CR). Lower values of corrosion potential and higher values of corrosion current density for both rolling routes proves processed steel corrodes rapidly and EIS results shows that the passivating film becoming less resistant with redution in thickness.

References

1. Xiong Y, Yue Y, Lu Y,et al. Cryorolling impacts on microstructure and mechanical properties of AISI 316 LN austenitic stainless steel. Materials Science & Engineering A. 709: 2018; 270-276.
2. Xiong Y, He T, Wang J, et.al. Volinsky, Cryorolling effect on microstructure and mechanical properties of Fe–25Cr–20Ni austenitic stainless steel, Materials & Design. 88: 2015; 398-405.

3. Zheng J, Li C, He S, et.al. Deformation twin and martensite in the Fe–36%Ni alloy during cryorolling, Materials Science and Technology. 33: 2017; 1681-1687.
4. Shukla S, Patil A P, Tandon V, et.al. The effect of cold work by rolling on electrochemical behaviour of Cr-Mn austenitic stainless steel in chloride environment, Materials Research Express. 5: 2018; 066535.
5. Tandon V, Patil A P, Rathod R C, et.al. Correlation of martensite content and dislocation density of cold worked 316L on defect densities of passivating film in acidic environment, Materials Research Express. 5: 2018; 086515.
6. Tandon V, Patil A P, Rathod C R, et.al. Influence of cold work on electrochemical behavior of 316L ASS in PEMFC environment, Materials Research Express. 5: 2018; 026528.

Numerical Simulation of Battery Storage Systems on Low Earth Orbits

M. Mačák[a,b], J. Zíka[b], T. Kazda[a]

[a] Department of Electrical and Electronic Technology, Brno University of Technology, Brno 616 00, Czech Republic

[b] TRL Space Systems s.r.o., Brno 602 00, Czech Republic

Reliable prediction of the battery system behavior is one of the most important aspects for a mission success. During the operation, the batteries experience transient current loads, varying temperatures, mechanical stresses or radiation effects. Numerical models must be able to capture these effects on battery behavior in order to provide accurate predictions as the battery degradation might require adjustments of the satellite operation. This study focuses on the development of a temperature-dependent equivalent circuit model.

Introduction

The constant improvement of space technologies, especially small satellites (CubeSats) lead to high-performance and low-cost missions comparable to larger satellites. The application of energy-demanding subsystems and payloads, while maintaining long life cycles of the CubeSats led to higher demands on the energy storage systems [1]. In order to ensure good reliability of battery systems, it is necessary to carry out extensive experimental testing, which includes monitoring battery capacity, internal resistance, maximum discharge rate and the influence of temperature [2]. Currently, there is still large difference between reported operable temperatures for Li-ion batteries used in space. In the most extreme cases, it may be between -20 °C and 60 °C. However, these temperature variations significantly influence the battery behavior and its degradation. Ideally, batteries should stay between 20 °C and 30 °C, which makes them the most sensitive and as a result the most critical subsystem for the mission's success [3].

Most of the currently launched small satellites in Low Earth Orbits (LEO) are in altitudes between 500 km and 600 km. The average orbital period in this area is around 95 min, with the average time in sunlight being 60 min and 35 min in the Earth‘s shadow [4]. On average, batteries have to undergo 16 cycles in a day, which makes their operation very demanding, as their State of Charge (SoC) should not decrease under 80 %. Experimental measurements, while necessary, are usually time consuming and are often unable to cover all foreseen operation regimes. To efficiently observe Li-ion battery characteristics in LEO environment, it is necessary to develop simplified experimentally based models, which would be able to apply initial experimental measurements to predict the battery behavior in future. Equivalent Circuit Models are the most common empirical model for the description of battery performance, in which the behavior is described by an electrical circuit. Their advantage lies in their accuracy, adaptability and simplicity [5]. This study focuses on the development of a temperature sensitive equivalent electric model of a Li-ion battery operating in a LEO environment, which would be able to predict the battery degradation based on its operation regime.

Experimental

A set of 3350 mAh Samsung 18650-35E batteries has been chosen for the experimental testing. In order to build an ECM of the battery. A 2 R-C model (shown in Fig. 1) has been selected to properly describe the battery transient behavior. Each R-C pair represents a time constant of the system. The battery behavior dependence on the applied was investigated between 0.1 C and 1 C. The ECM parameters were obtained from the electrochemical impedance spectroscopy every 25% of SoC. Impedance spectra were then fitted using a Matlab script.

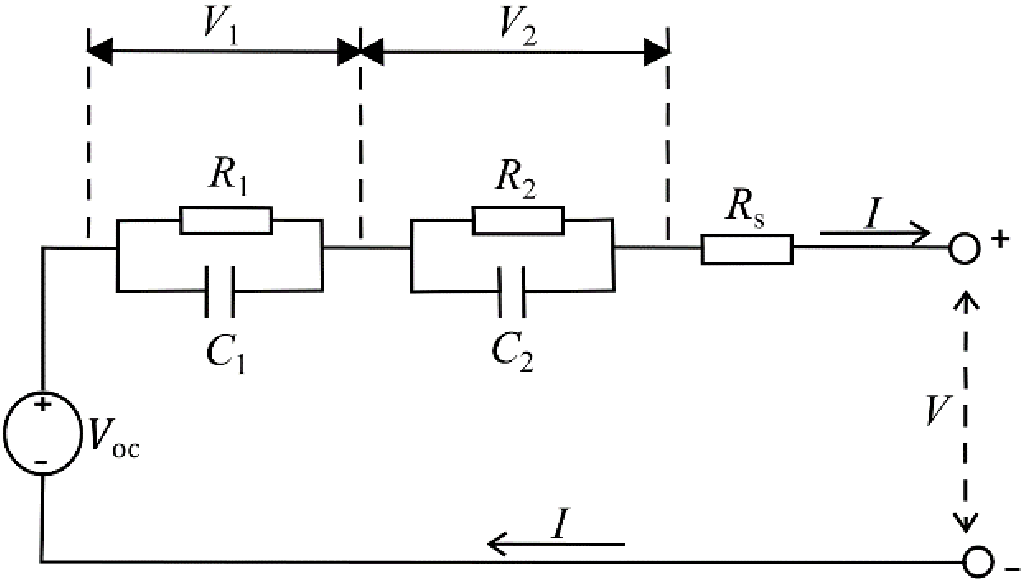

Figure 1. *Li-ion battery equivalent circuit model [7].*

In this case, the battery was cycled with a defined current profile based on the foreseen CubeSat mission. Figure 2 shows the current profile, which consists of a periodic change between sunlight and eclipse periods. Visible peaks represent operations of the subsystems such as transmission or payloads (usually scientific or for Earth observation). Batteries are discharged by approximately 0.1 C and charged by approximately 0.2 C during the nominal operation.

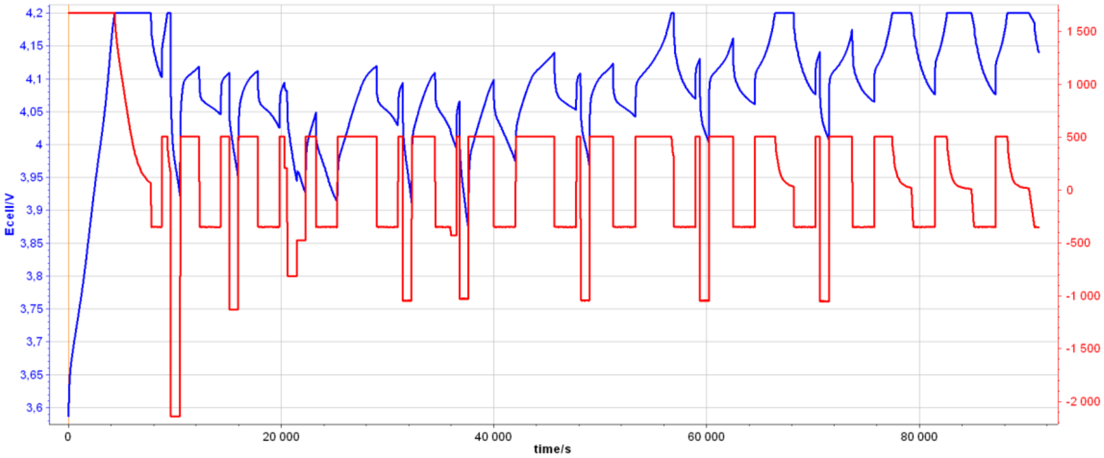

Figure 2. *Current and voltage profile of a Low Earth Orbit CubeSat mission.*

Conclusions

Current approach in the characterization of Li-ion batteries for space applications lies in the extensive experimental testing procedures at defined environmental conditions. However, battery temperature, which can significantly change during the orbit, is one of the most important factors which influence battery behavior and degradation. In order to develop precise models, it is necessary to study and replicate conditions, which will the battery systems experience during the operation in space. Equivalent circuit modelling is a suitable approach for the battery modelling in space as this method is simple, accurate and is able to capture battery transient behavior and temperature dependence.

Acknowledgments

This work was supported by the specific graduate research of the Brno University of Technology No. FEKT-S-23-8286.

References

1. S. Baccari, F. Vasca, E. Mostacciuolo, L. Iannelli, S. Sagnelli, R. Luisi, and V. Stanzione, *2019 European Space Power Conference (ESPC)*, 1-6 (2019).
2. F. C. Krause, J. P. Ruiz, S. C. Jones, E. J. Brandon, E. C. Darcy, C. J. Iannello, and R. V. Bugga, *J. Electrochem. Soc.*, **168**(4) (2021).
3. V. Alcayde, A. Vercher-Martínez, and F. J. Fuenmayor, *Adv. Space Res.*, **68**(4),1975-1988 (2021).
4. E. Morsch Filho, L. O. Seman, and V. de Paulo Nicolau, *Appl. Therm. Eng.*, **193** (2021).
5. M. -K. Tran, M. Mathew, S. Janhunen, S. Panchal, K. Raahemifar, R. Fraser, and M. Fowler, *J.Energy Storage*, **43** (2021).
6. P. Vyroubal and T. Kazda. *J.Energy Storage*, **15**, 23-31 (2018).

In situ Monitoring of Battery Electrode Materials Changes using Raman Spectroelectrochemistry

Z. Vlčková Živcová[1*], M. Jindra[1], F. J. Sonia[1], M. Müller[3], J. Červenka [3], A. Fejfar[3] and O. Frank[1]

[1] J. Heyrovský Institute of Physical Chemistry, Czech Academy of Sciences, 182 23 Prague, Czech Republic

[2] Department of Physical Chemistry, University of Chemistry and Technology, 16628 Prague, Czech Republic

[3] Institute of Physics of the Czech Academy of Sciences, 182 21 Prague, Czech Republic

zuzana.vlckova@jh-inst.cas.cz

One of the important features for controlling and improving the stability of battery systems is the ability to monitor chemical and structural changes in the electrode material during battery operation. In situ Raman spectroelectrochemistry (SEC) is a very useful non-destructive and real-time technique combining Raman spectroscopy and electrochemistry to study the key processes at different potentials applied. The selection of an appropriate measurement setup (such as a traditional glass spectroelectrochemical cell, micro-droplet setup, or a coin cell with an optical window) is essential based on the nature of the investigated system to facilitate accurate analysis. This study will focus on electrode characterization utilizing the SEC technique for two different rechargeable battery systems, namely Li-ion batteries (LIBs) and aqueous batteries (ABs).

The promising anode material for next-generation LIBs is silicon, which, thanks to its high theoretical specific capacity of 3579 mAh/g (for $Li_{15}Si_4$ the highest lithiated phase achievable for the ambient temperature lithiation), can replace the most commonly used graphite with ca. ten times lower specific capacity (372 mAh/g for LiC_6) [1]. However, since silicon is a non-conductive material, it is still necessary to use carbon as a conductive matrix in the form of silicon/carbon composite anodes. The key degradation processes in the composite anode prepared using Si nanoparticles (10 nm) with a conductive carbon-based matrix (carbon black) were studied [2]. These processes, such as the crystal lattice changes (expansion/contraction) and possible degradation/amorphization of Si nanocrystals, the solid electrolyte interphase (SEI) layer formation on the electrode surface during the charge/discharge reactions, and the stability of the carbon-based matrix, significantly affect the performance of Si-based LIBs in many ways. Especially, the large silicon volume expansion (more than 300%) and associated stress cause mechanical instability resulting in rapid capacity fading. Using in situ Raman SEC in coin-cells (CR2032) as a half-cell configuration with optical window, the initial degradation mechanisms of the SEI layer formation, as well as possible structural changes caused by the volume expansion of silicon nanoparticles were determined. The shift of the first-order Raman peak of Si at 521 cm^{-1} which is assigned to crystalline silicon is related to the stress evolution in nanoparticles caused by the (de)lithiation-induced stress (tensile-to-compressive transition) in Si nanoparticles and the native oxide on their surface. Additionally, the detailed in situ Raman measurement of the first and second lithiation cycle allowed us to detect the decomposition of the electrolyte ($LiPF_6$ in EC/DMC) which is associated with SEI layer formation. A decrease in the intensity of the Raman vibrational modes (700–1050 cm^{-1}) of EC/DMC corresponding to the decomposition of the electrolyte was observed at reduction potentials 0.8 V and 0.3V vs. Li/Li^+ corresponding to the same potentials determined by cyclic voltammetry.

Aqueous batteries (ABs) are based on a saline aqueous electrolyte and a carbon-based electrode material. The low electrochemical stability window of common aqueous electrolytes (1.23V) can be significantly enlarged by using highly concentrated “water-in-salt” (WIS) electrolytes [3] in combination with the appropriate electrode material. For the application in ABs with highly corrosive environments we investigated the p-type semiconducting (band gap 5.5 eV) boron-doped diamond (BDD) due to its excellent chemical stability and wide potential window compared to other carbon-based materials. The polycrystalline BDD films were grown by microwave plasma-enhanced chemical vapor deposition (MPECVD) with different quality (sp^2 carbon content) and boron doping levels (boron/carbon ratio in the gas phase). In situ Raman SEC measurements were performed in aqueous electrolytes in a standard glass cell [4] as well as in a micro-droplet setup [5]. It was observed that in the case of BDD films containing a high amount of sp^2 (low quality), the modes belonging to sp^2 carbonaceous phases changed their intensities. The intensity of the D, G, and D′ Raman peaks increased in the cathodic direction, while in the anodic direction bleaching of these peaks was observed. The diamond films prepared with almost no sp^2 carbon content (high quality) exhibited no spectroelectrochemical changes of sp^3 diamond lattice in the potential region tested. In both cases of BDD (LQ and HQ) the modes belonging to boron incorporated into the diamond lattice exhibited no changes with the applied potential suggesting the good stability of this material.

References:

1. M. Winter and J. O. Besenhard, *Electrochimica Acta*, **45**, 31 (1999).
2. Z. Vlčková Živcová, M. Jindra, S. F. J., M. Muller, J. Červenka, A. Fejfar and O. Frank, *in preparation* (2023).
3. Z. A. Zafar, G. Abbas, M. Silhavik, K. Knizek, O. Kaman, F. J. Sonia, P. Kumar, P. Jiricek, J. Houdková, O. Frank and J. Cervenka, *Electrochimica Acta*, **404**, 139754 (2022).
4. Z. Vlčková Živcová, O. Frank, V. Petrák, H. Tarábková, J. Vacík, M. Nesládek and L. Kavan, *Electrochimica Acta*, **87**, 518 (2013).
5. Z. Vlčková Živcová, M. Bouša, M. Velický, O. Frank and L. Kavan, *Nanomaterials*, **11**, 1256 (2021).

Acknowledgment:

This work was supported by the Czech Science Foundation, projects Nos. GA18-08959S and GA23-05895S.

Corrosion Processes of Sintered Materials Based on Fe

M. Sedlaříková[a], M. Zatloukal[a], J. Kuchařík[a], P.Čudek[a], G.Fafilek[b]

[a)] Department of Electrical and Electronic Technology, FEEC, Brno University of Technology,
Technická 10, 616 00 Brno, Czech Republic

[b)] Institute of Chemical Technologies and Analytic, TU Wien, Getreidemarkt 9, 1060 Wien

Powder metallurgy is a long-known method of manufacturing metal and ceramic products. There are several ways to sinter metal powder. One way is to use modern laser sintering technology. Another method is to compress the powder under high pressure in the matrix and then fire it. Fillers can also be used to bind the powder together and the resulting mixture is cast into a matrix with subsequent firing in a protective atmosphere.

The polymer filler can be, for example, polyurethane, which embeds metal powder in its porous structure, which will continue to carry this structure after firing. A significant disadvantage is that polyurethane contains oxygen [1], which moves into the metal material during firing and creates new oxide bonds.

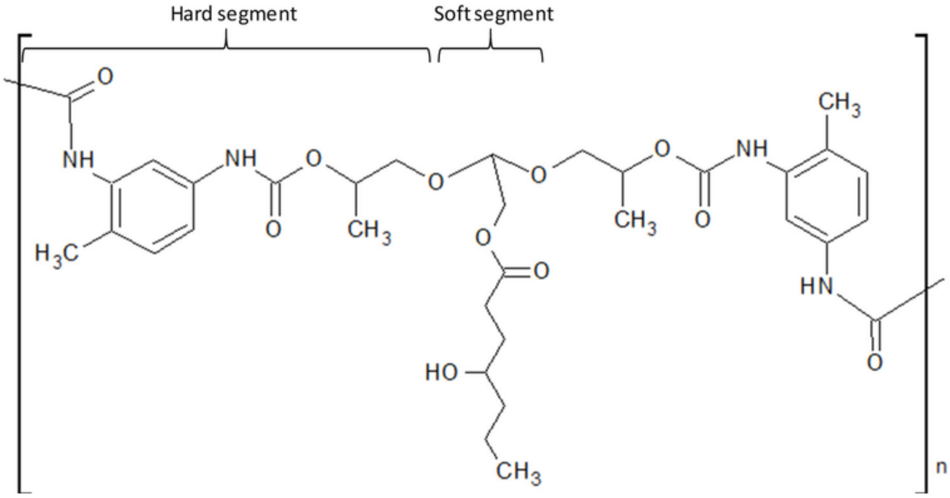

Figure 1. *Chemical structure of polyurethane [1]*

The problem with contained oxygen in the base material of the polymer is solved by polystyrene, which does not contain any oxygen in the bond [2]. In addition, carbon and hydrogen bonds are broken during firing, and these free atoms can bind to each other the oxygen contained in the metal powder.

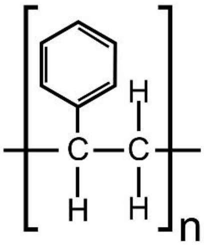

Figure 2. *Chemical structure of polystyrene [2]*

The samples were made by the last of the named methods, when three different amounts of binder were used (0.5, 1.0, 1.5g). Polystyrene dissolved in acetone was chosen as the binder. 10 g of iron powder was mixed with this dissolved polymer and cast into a mold. This was followed by drying at 37°C for 24 hours. The subsequent firing in a protective argon atmosphere was at a temperature gradient of 5° C/min to 450° C, where the temperature remained for 2 hours and then the temperature increased to 1000° C with the same gradient. Firing at 1000° C lasted hour. This was followed by gradual cooling of the furnace.

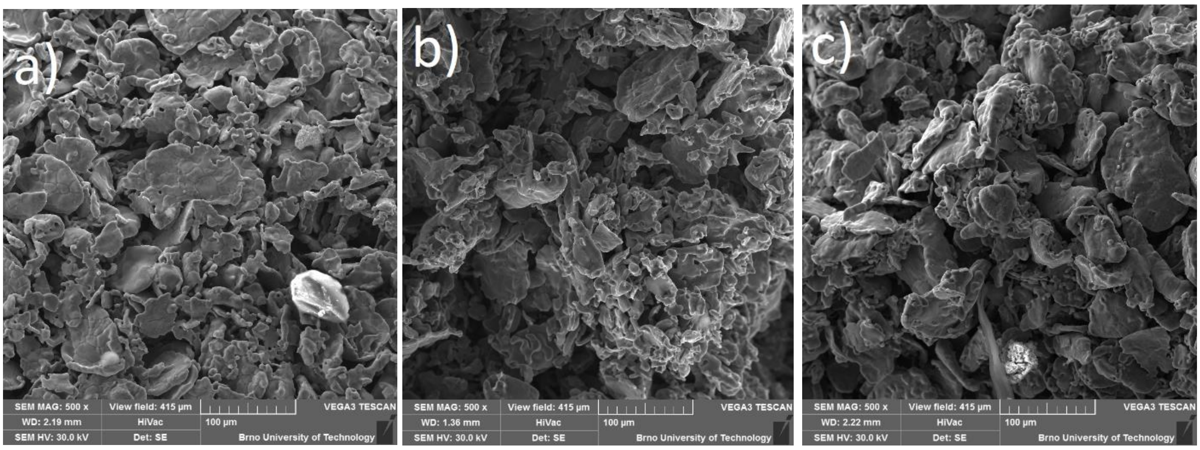

Figure 3. *Environmental scanning electron microscope image of internal structure of sample: a) with 0.5g PS, b) with 1.0g PS, c) with 1.5g PS*

The prepared samples were first observed with an electron microscope, then the initial corrosion current was measured. Afterwards, the samples were placed in a solution of 0.9% sodium chloride and the corrosion current of these samples was measured at regular intervals.

Acknowledgements

This work was supported by the specific graduate research of the Brno University of Technology No. FEKT-S-23-8286.

References

1. Ahmad, Zulfiqar & Md Jamil, Siti Nurul Ain & Choong, Thomas & Luqman Chuah, Abdullah & Mastuli, Mohd Sufri & Othman, Nurhanisah & Jiman, NurNazurah. (2019). Green Flexible Polyurethane Foam as a Potent Support for Fe-Si Adsorbent. Polymers. 11. 2011. 10.3390/polym11122011.
2. Findlay, Catherine. (2018). Development of FTIR tomography for thermal-source imaging of 3D biochemical distributions in micro-samples of cells and fibers. 10.5203/THESIS_FINDLAY_1.

Battery Thermal Management System for Greater Lifetime and Safety: a mini-review

Seyed Saeed Madani and Carlos Ziebert

Institute of Applied Materials-Applied Materials Physics, Karlsruhe Institute of Technology, 76344 Eggenstein-Leopoldshafen, Germany; seyed.madani@kit.edu, carlos.ziebert@kit.edu

*Correspondence: seyed.madani@kit.edu; Tel.: (+49-72160828540)

Abstract. An efficient thermal management system for lithium-ion batteries is crucial to assure that the lithium-ion battery pack works in the specified temperature scope, especially for high charge and discharge conditions. One of the lithium-ion battery's thermal design and thermal management objectives is to climb down the heat generation boundary perpendicularly and decrease the lithium-ion battery cell's maximum temperature, especially at high working conditions. The aforementioned could be useful to lessen the sophistication of the lithium-ion batteries' thermal management systems. This study reviews different investigations which were employed to accomplish and display thermal behaviour and cooling arrangement in the lithium-ion battery pack and different techniques for simulating and modelling the thermal management of lithium-ion batteries. It was concluded that multiple inlets and outlet flow are more advantageous than a single one because they can avoid the hottest region concentration in the cooling system.

Keywords: Lithium-ion Batteries, Thermal Management, Lifetime, and Safety.

Introduction

One of the world's most significant critical concerns is tackling the growing energy demand without polluting the environment. Carbon dioxide emissions have increased rapidly, and their concentration in the atmosphere is quickly growing. Lithium-ion batteries could be the principal technology to solve these problems.

Lithium-ion batteries are appropriate for completely electric and hybrid electric vehicles attributable to their big energy density and specific energy compared to other rechargeable cell chemistries. Nevertheless, these lithium-ion batteries have not been extensively employed commercially in completely electric and hybrid electric vehicles yet attributable to low-temperature performance, cost, and safety which are all concerns connected with lithium-ion battery thermal management systems.

Heat loss measurement of lithium-ion batteries was done. The most significant temperature and heat losses were found adjacent to the upper part of the lithium-ion battery pack. The most negligible temperature and heat losses were located on the bottom of the lithium-ion battery pack. It was concluded that the non-uniform temperature and heat loss distribution on the lithium-ion battery pack might be diminished by altering and modifying the lithium-ion battery pack's geometry.

Thermal management of lithium-ion batteries was accomplished using different techniques. Figure 3 illustrates the lithium-ion battery thermal management system. This methodology could be applied to commercial lithium-ion battery cells, while information concerning lithium-ion battery cell assembly and chemistry is restricted. It was concluded that the lithium-ion battery's maximum temperature at the end of discharge was decreased with the enhancing heat transfer coefficient or flow velocity. Air-cooling's temperature profile was approximately identical to direct liquid cooling; nevertheless, it has a more significant temperature impact on the lithium-ion battery cell. Experimental heat generation data of the lithium-ion battery was used as a source term. The velocity of air cooling was assumed to be 20 m/s. Different configurations were applied to the thermal management of the lithium titanate oxide battery pack. The distance between lithium titanate oxide-based batteries was assumed to be 50 mm. The discharge current rate was assumed to be 65 A. The amount of heat generation was proportionate to the cooling flow velocity. The temperature of the lithium-ion battery could be manageable with an immense velocity of coolant fluid. Notwithstanding, with an increase of cooling flow velocity to greater than 20 m/s, V=0.01 m/s, and V=0.05 m/s for air cooling, direct liquid cooling, and direct liquid cooling, correspondingly, a considerable cooling of the lithium-ion battery could not be obtained. The investigated cooling approaches dissipated approximately the identical heat from the lithium-ion battery cell at a flow velocity of 20 m/s for air cooling and 0.01 m/s for direct liquid cooling, and 0.05 m/s for indirect liquid cooling. Compared to air cooling, direct liquid cooling, and indirect liquid cooling, fin cooling has the lowest maximum temperature decrease due to the comparatively big heat capacity. One of the modifications to improve the thermal management of lithium-ion batteries could be relocating the current tabs to opposite endings of the lithium-ion battery. The electrochemical reaction rate is escalated as a consequence of a more significant temperature gradient. More considerable current rates might distinguish this occurrence in various portions of the lithium-ion battery as a consequence of a significant temperature gradient. The advancement of concentration gradients and current in the battery is created by the great discharge rates, which are needed for lithium-ion batteries attributable to the electric vehicle's abrupt acceleration. The electrical conductivity of the negative electrode is considerably more excellent than that of the positive electrode. This occurrence brings on smaller temperatures in the neighbourhood of the current collecting tab of the positive electrode than the negative one. The aforementioned challenges additional research for superior comprehension of the heat generation mechanisms and thermal management of lithium-ion batteries because of the lack of comprehensive analysis of lithium-ion batteries.

systems is shown in Figure 2. An exclusively established thermal control system is the exclusive method to decrease the heterogeneous temperature distribution in lithium-ion batteries.

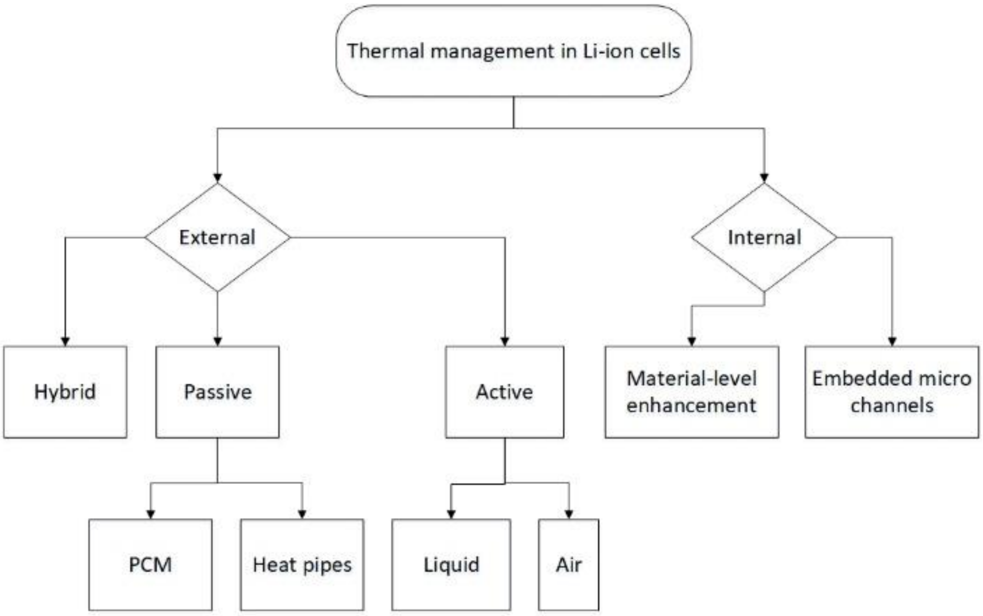

(a)

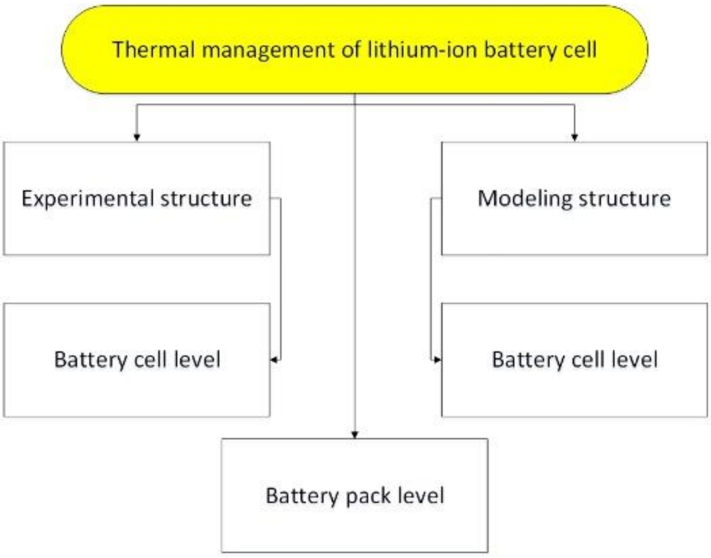

(b)

Figure 2. *(a): Classification of different thermal management approaches, (b): Organization of thermal management systems.*

Conclusion

The thermal management of lithium-ion batteries, including different cooling strategies and cooling configurations, was reviewed. Different configurations were used by different researchers for the thermal management of lithium-ion battery packs. For this purpose, different assemblies for lithium-ion battery thermal management were selected. Different liquids, including water/glycol, were used as the coolant fluid in the arrangement of fin cooling. It should be noted that indirect liquid cooling appends more additional heaviness than direct liquid cooling because of the density. Usually, a non-homogeneity of temperature is seen on the surface of lithium-ion batteries. Correspondingly, modifications are required to stop this unappealing thermal behaviour. It is recommended that physical properties, as well as material properties, could be modified. Besides, improvements in the thermal management system could be included. It was concluded that the arrangement of the lithium-ion battery pack, including different inlet and outlet positions, can shift the location of the hottest region in the pack. The hottest region is distributed in the system by increasing the number of air-cooling outlets and inlets. Notwithstanding the reduction of fluid flow around the hottest lithium-ion batteries will face an increase in temperature in these areas. Lack of uniform distribution of fluid within the channels might increase the hot spot regions in the arrangement. It was concluded that the coolant fluid's entrance temperature plays a critical role in the lithium-ion batteries' thermal management system. Notwithstanding, there should be a restriction on the increase in the entrance temperature of coolant fluid. There should be a trade-off between some of the cooling method's advantages and disadvantages for different applications and cooling performance. For instance, in cases where the system's safety is more critical than other factors, more attention should be given to cooling performance than the system's cost.

Thermal Modeling of Lithium-ion Batteries: a mini-review

Seyed Saeed Madani and Carlos Ziebert

Institute of Applied Materials-Applied Materials Physics, Karlsruhe Institute of Technology,
76344 Eggenstein-Leopoldshafen, Germany;

*Correspondence: seyed.madani@kit.edu

Abstract- The non-uniform distribution of temperature in lithium-ion batteries may stem from internal heat generation. Understanding the thermal behavior of lithium-ion batteries and implementing temperature control strategies for battery packs is crucial. Models developed to study the thermal behavior of lithium-ion batteries contribute to a better understanding of their thermal management under different operating conditions. This study examines various investigations that have employed simulations and models to analyze the thermal characteristics, behavior, and runaway phenomena of lithium-ion batteries. The review aims to highlight the potential of the characterization techniques used and the impact of critical parameters such as current rate and temperature on thermal behavior. Typically, it is easier to enhance the thermal design systems rather than the design of lithium-ion batteries themselves. Therefore, this thermal review work primarily focuses on the thermal system. The provided summary offers a broad overview of the research findings, and for a more comprehensive understanding, reference to the specific published accounts and associated modeling work is necessary.

1. Introduction

Figure 1 depicts the categorization of lithium battery systems. Among them, lithium-ion batteries show the most promise as a storage technology to decrease greenhouse gas emissions in the transportation sector. With their high power and energy densities, lithium-ion batteries are well-suited for a wide range of renewable energy storage applications. The versatility of lithium-ion battery technology makes it suitable for various uses, each with its own specific requirements. Additionally, lithium-ion batteries find applications in military, aerospace, and residential sectors due to their safety, reliability, substantial power capacity, and long lifespan.

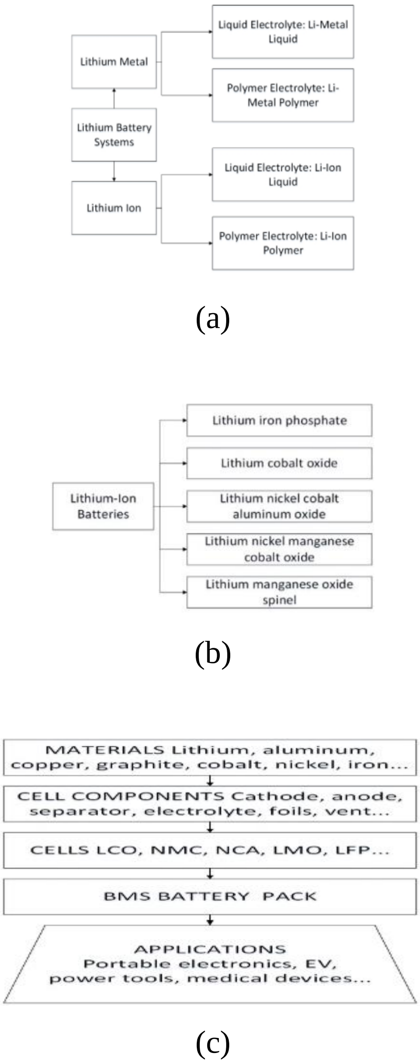

Figure 1. *Categorization of lithium battery systems according to (a): The nature of their electrolyte, (b): Their cathode chemistry, and (c): The construction configuration of lithium-ion battery manufacturing .*

Dafen Chen et al. [1] conducted a comparative analysis of various cooling methods for lithium-ion batteries, including direct liquid cooling, indirect liquid cooling, and air-cooling (active cooling method). The study combined numerical simulations with experimental laboratory data. The findings indicated that air-cooling exhibited the smallest reduction in maximum temperature due to the relatively low thermal conductivity and heat capacity of air. While air requires less power to circulate, it is not as effective in rapidly dissipating heat during rapid discharging. Indirect liquid cooling introduced additional weight compared to direct liquid cooling, as the density of aluminum is roughly three times higher than that of mineral oil. In the case of fin cooling, water/glycol served as the coolant fluid. The study also determined temperature distributions across the surface of the lithium-ion battery under different velocities and flow directions for air-cooling and direct liquid cooling.

The utilization of experimental data from battery calorimeters for thermal analysis of lithium-ion batteries is crucial because these batteries experience significant temperature rise and heat dissipation gradients during charging and discharging in practical applications, primarily due to irreversible and reversible heat. Developing a dynamic and time-dependent heat generation model for lithium-ion batteries using battery calorimeters can help address this issue. To mitigate the non-uniform temperature distribution and heat generation on the surface of lithium-ion battery cells, modifications to the battery cell's geometry can be considered. For example, placing the negative and positive tabs on opposite sides of the battery cell or increasing the tab size to enhance contact between the electrodes' current collectors and external tabs are potential suggestions. Different configurations of current collectors in the lithium-ion battery cell can be explored, and the most optimal design should be chosen if modifying the design by lithium-ion battery manufacturers is not feasible.

In their study, M. Shadman Rad et al. [2] focused on the thermal modeling of lithium-ion batteries. They developed thermal models based on heat generation data obtained from various experiments. The experimental setup was constructed in accordance with modern simulation laboratories. The thermal model was employed to analyze the heat generation and temperature changes of a lithium-ion battery cell. Furthermore, the model-calculated heat generation and temperature were compared with the experimental data to validate the accuracy of the model.

In their research, Cong Zhu et al. [3] developed a thermal model specifically tailored to the configuration and geometry of lithium-ion batteries. The simulation results obtained from the model were compared to measurements conducted in the laboratory. Additionally, the proposed thermal model for lithium-ion batteries was evaluated and found to be capable of predicting the thermal behavior of the batteries. Panchal et al. [4] conducted a thermal analysis of lithium-ion batteries and observed temperature variations on the surface of the battery cells, particularly at high current rates. This phenomenon can be attributed to significant heat dissipation resulting from larger temperature gradients. Previous studies have compared different methods for managing and analyzing the thermal behavior of lithium-ion batteries during various cycling and operational conditions. Different configurations and assemblies have been examined in the literature to understand the thermal characteristics of lithium-ion batteries. Efficient thermal management of lithium-ion batteries is essential to limit temperature increases and prevent further exothermic reactions, thus controlling heat generation and avoiding thermal runaway. Various simulations have been conducted to estimate the thermal characteristics of lithium-ion batteries, and suggestions have been made to improve their thermal behavior. However, comprehensive comparisons and investigations of different arrangements for the thermal characteristics of lithium-ion batteries are still limited. Researchers and lithium-ion battery manufacturers can utilize this study to gain insights into the thermal behavior of lithium-ion batteries under diverse conditions. The study highlights the need for further comprehensive research on thermal characteristics, considering the significant progress made in understanding the workings and mechanisms of lithium-ion batteries. Consequently, it is crucial to assess the current state and the latest advancements in thermal modeling research for lithium-ion batteries.

Conclusion

This article presents a thorough evaluation of existing approaches used for analyzing the thermal properties of lithium-ion (Li-ion) battery systems. By providing an overview of different models, algorithms, and methods, this review establishes a basis for the development of more effective techniques to model and diagnose the thermal characteristics of Li-ion batteries, thereby enhancing battery safety. Accurate measurement of heat generation rates within Li-ion cells is vital to ensure safety and optimize performance. The temperature distribution within a cell affects its performance, cycle life, and overall system safety, which are influenced by the rate at which heat is generated inside the cell and dissipated from its surface. While theoretical models exist for predicting heat generation rates, there is limited literature available on experimental measurements, particularly at high discharge rates. The establishment of a dedicated thermal model system is necessary to reduce the uneven temperature distribution in lithium-ion pouch cells. To achieve this, a suitable thermal model for Li-ion batteries is required. These models can be applied to Li-ion battery cells, even when information about cell assembly and chemistry is limited, enabling the design of diverse thermal management and characterization systems. More precise data on heat generation and thermal characteristics contribute to better investigations of thermal management systems for Li-ion batteries and facilitate the incorporation, establishment, and development of thermal models specific to battery applications. Researchers have employed various techniques to analyze the thermal characteristics of Li-ion batteries with the aim of designing efficient, simplified, and cost-effective thermal management systems. This information can be utilized by battery manufacturers to analyze and improve Li-ion batteries, as well as by researchers in the field. The non-uniform temperature distribution within Li-ion battery packs highlights the uneven dissipation of heat across the pack, with areas of higher temperature indicating greater heat loss. These findings can guide the design and optimization of advanced thermal management systems for Li-ion batteries. The outcomes of these studies hold value for both the industry and research community, contributing to the advancement of Li-ion battery thermal management systems that allow for precise determination of temperature changes over time and prediction of electrical, thermal, and chemical processes. Based on the researchers' findings, specific methodologies are recommended for evaluating crucial thermal parameters of Li-ion pouch cells. These include using calorimeters to determine heat capacity and thermal conductivity, employing the heat loss method to assess the entropic factor, and utilizing the pulse method to determine internal resistance. Further research is necessary to address specific aspects of thermal issues associated with Li-ion batteries. Specifically, there is a need for a comprehensive thermal management technique that incorporates features such as cold storage to mitigate capacity degradation, rapid heating to enhance performance, uniform cooling to simplify electrical balancing schemes and improve energy extraction, and rapid cooling during critical heating events while minimizing auxiliary power consumption.

Reference

1. Chen, Dafen, Jiuchun Jiang, Gi-Heon Kim, Chuanbo Yang, and Ahmad Pesaran. "Comparison of different cooling methods for lithium-ion battery cells." Applied Thermal Engineering 94 (2016): 846-854.
2. Rad, M. Shadman, D. L. Danilov, M. Baghalha, M. Kazemeini, and P. H. L. Notten. "Adaptive thermal modeling of Li-ion batteries." Electrochimica acta 102 (2013): 183-195.
3. Zhu, Cong, Xinghu Li, Lingjun Song, and Liming Xiang. "Development of a theoretically based thermal model for lithium ion battery pack." Journal of Power Sources 223 (2013): 155-164.
4. Panchal, S., I. Dincer, M. Agelin-Chaab, R. Fraser, and M. Fowler. "Experimental and theoretical investigation of temperature distributions in a prismatic lithium-ion battery." International Journal of Thermal Sciences 99 (2016): 204-212.

Thermal modeling of lithium-ion battery packs

M. Sedlařík[a], P. Vyroubal[a]

[a] Brno University of Technology, Technická 10, 616 00 Brno, Czech Republic

This work deals with the thermal management of lithium-ion pouch batteries. Behavior of lithium-ion batteries are strongly dependent on their operating temperature. In the case of deflection, the degradation mechanisms of the batteries are affected, therefore it is necessary to keep the batteries at optimum operating temperature. In this work, the effectiveness of different types of battery pack cooling is monitored and compared. The experiment includes a model of battery pack contains 6 cells that are thermally analyzed with discharge currents of 1C, 3C and 5C using passive air cooling and active non-contact liquid cooling.

Introduction

The thermal management of lithium-ion batteries is significantly important in terms of their performance, lifespan and reliability. Increasing the temperature of a battery can accelerate its degradation mechanisms, accelerating battery ageing, leading to a reduction in reliability. Conversely, critically low temperatures lead to a significant reduction in overall capacity. If the power is not limited, lithium-ion precipitation can occur, causing irreversible degradation and potential safety hazards. Generally, the optimum operating temperature for lithium-ion batteries is between 10 and 30 °C. In high-power applications such as electromobility, batteries reach higher temperatures. In these cases, it is necessary to investigate the heat dissipation of the battery, as the batteries could be exposed to continuous thermal stress, which would accelerate their degradation and could lead to a fire if the batteries reach a critical temperature. [1]

Various cooling methods are used to regulate the temperature of lithium-ion batteries and prevent them from overheating. The common way of cooling method for lithium-ion batteries is air cooling. Air cooling involves the use of natural convection or forced airflow through the battery pack to dissipate heat generated during operation. This method requires no additional components other than adequate ventilation and can be implemented with simple design considerations. Liquid cooling is a more advanced cooling method used to regulate the temperature of lithium-ion batteries efficiently and precisely. This technique involves circulating a cooling fluid, typically water or a specialized coolant, through channels or pipes within the battery pack. The cooling fluid absorbs heat from the battery cells and carries it away to an external heat exchanger, where the heat is dissipated into the surrounding environment. Batteries can also be immersed directly in a non-conductive coolant such as silicone-based or mineral oils.

Experiment

The model includes a battery pack, which consists of 6 battery cells that are connected as 2 modules in series, where the module consists of 3 cells in parallel. One Li-ion battery cell is in a pouch package based on NMC technology, which is represented by a cube with dimensions 97x512x8 mm and has a capacity of 78 Ah.

The battery cell model is created using experimentally measured discharge curves at discharge currents of 0.1C; 0.2C and 0.5C. These curves are used to derive the model parameters U and Y, which represent the depth of discharge (DoD) function used to form the semi-empirical ntgk model.

The battery pack will be subjected to thermal analysis at discharge currents of 1C, 3C and 5C. In the process, the temperature at the edge and center cell is monitored under two different cooling systems. The first type is air cooling, where the heat transfer coefficient is set at 5 W/m^{2}K and the ambient temperature is set at 300 K. The second type is an aluminum shell through which water flows.

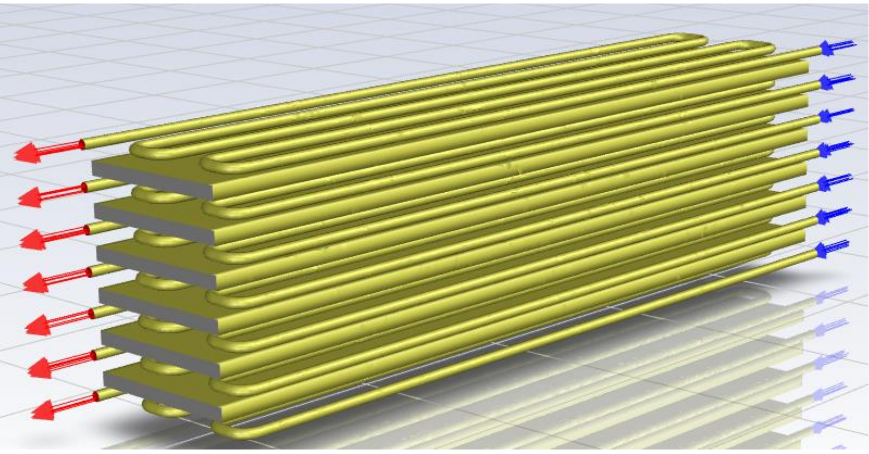

Figure 1. *Active liquid cooling non-contact method*

Results

In the case of passive air cooling (Figure 2), the temperature rises sharply as the battery discharge current increases, especially at 5C. Air cooling is unable to dissipate heat at higher discharge currents and other types of cooling must be used.

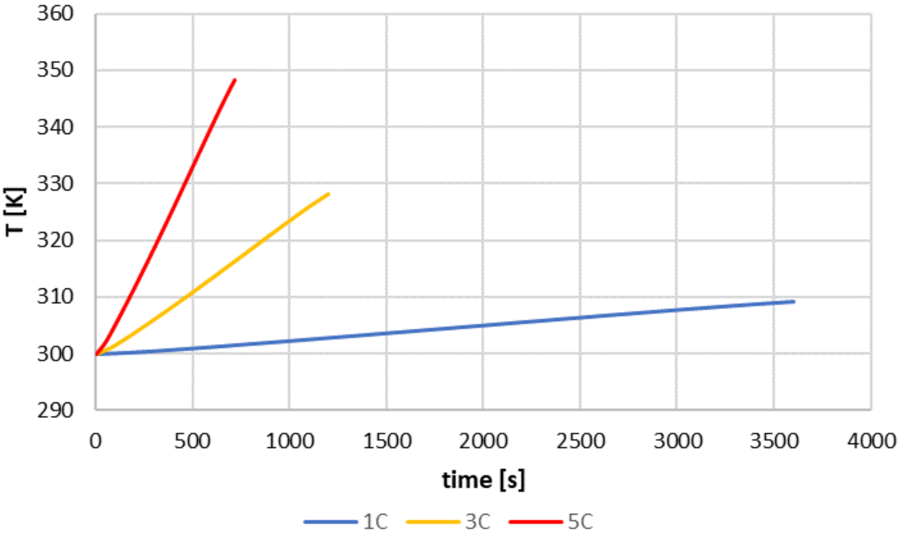

Figure 2. *Thermal analysis of passive air cooling*

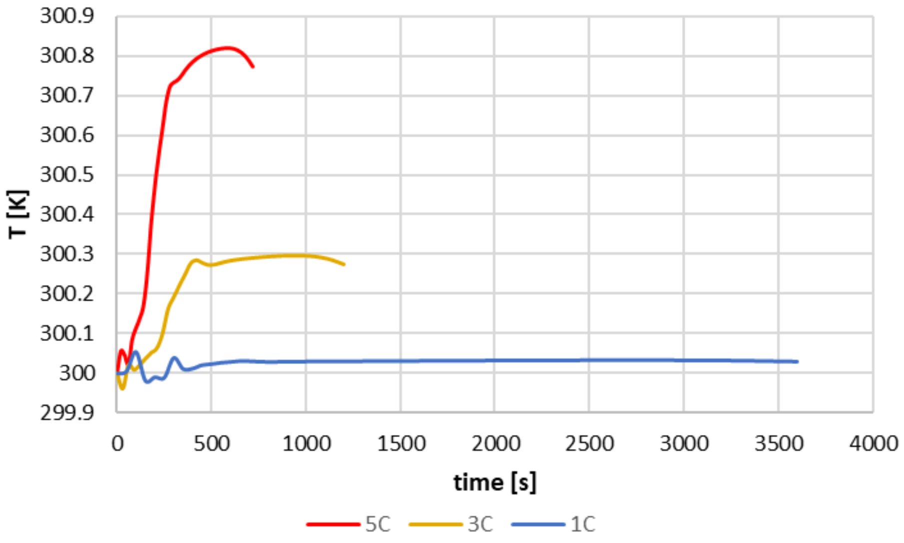

Figure 3. *Thermal analysis of active liquid cooling*

Conclusion

The experiment shows the effectiveness of active liquid cooling at higher discharge currents where air cooling is no longer sufficient. At 1C discharge current is not such a significant difference in cooling and the batteries could be cooled by airflow only. The highest battery pack temperature simulated on the internal batteries reaches 348 K at a discharge current 5C in 720 s. For active liquid cooling, a maximum increase of 0.82 K was observed and in this case is necessary to use active cooling of battery pack.

Acknowledgements

The publication was created within the project of specific research at BUT (No. FEKT-S-23-8286).

References

1. JUNQIU, Li. Modeling and Simulation of Lithium-ion Power Battery Thermal Management. Springer Nature Singapore, 2022. ISBN 2662-2920.

Non-Destructive Non-Contact Testing for Investigation of Initial Materials and During Production of Li Batteries, Solar Cells, and in Other Industries.

Ensuring High Quality and Reliability.

V. Redko[b], T. Pastushkin[a], E. Shembel[c], B. Kutnick[a], Y. Pustovalov[d], D. Kaszuba[d]
V. Khandetskyy[a], N. Zaderey[c], A. Redko[c]

[a]Enerize Corporation, Coral Springs, FL, 33067, USA

[b]Inter-Intel, Dnipro, 49005, Ukraine

[c]Scientific Research Laboratory of Chemical Power Sources of Ukrainian State
University of Chemical Technology, Dnipro, 49005, Ukraine

[d]INT Sp z o.o.,Ul Pilsudskiego 17/4, 34-074 Rzeszów, Polska

Continuous application of appropriate non-destructive testing procedures to materials and components before, during and after the manufacturing process is the most cost effective method to achieve the highest possible product quality and reliability.

The safety and reliability of Li battery are determined mainly by its basic design and chemistry. However, without adequate quality control during manufacture, defects in even the best designs can lead to inconsistent performance and early failure. Deployment of automated quality assurance technology at every stage of the manufacturing and assembly process will increase the reliability and safety of batteries while lowering overall manufacturing costs by reducing wastage and preventing defective components from being incorporated into the finished product. Non-destructive methods and equipment are innovative tools for successful coordination of R&D, manufacturing, and applications of Li batteries

Methods, which authors of this abstract are developed, are based on the interaction of different vector and scalar fields.

1. Wave acoustic fields of different polarization.
2. Potential electrical and magnetic fields.
3. Vector eddy magnetic fields.
4. Gradient heat fields (infra-red spectrum).
5. Electron emission fields.
6. Glow fields of high voltage pulse discharges.
7. Mathematical constructs are used for process description and modeling. They provide indications of main analytical dependences between the parameters of the excitation / probe fields and geometric and electro-physical characteristics of the test article.

8. Describing the wave process of elastic waves in isotropic and anisotropic media.
9. Maxwell and Lap lace equations.
10. Mathematics of spectral transformations in different orthogonal bases.
11. Theory of wave diffraction processes.
12. Methods of defection of identification and treatment of images using fuzzy logic and artificial neural networks.
13. Noise resistant method of the wavelet analysis image processing, etc.

Below presented Non-destructive Non-contact methods and equipment for using during Li batteries production.

1. Combined Electromagnetic Eddy-Current & Capacitance methods for testing & evaluation of the powder materials, liquids & slurry compositions
2. Electromagnetic eddy-current method for evaluation the interface resistance between current collector and active electrode mass
3. Electromagnetic Eddy-Current & Capacitance Methods for thickness measurement & quality assurance during electrode coating
4. Holographic Interferometry for evaluation the hidden defect in electrodes, solid electrolytes and other components.
5. Gas Discharge Visualization – High Voltage Electric Field method for quality assurance of hermetically sealed devices, for example - batteries
6. Electromagnetic non-destructive test weld quality in ultracapacitors and batteries
7. Electromagnetic non-contact eddy-current testing conductivity of thin film of solid & polymer electrolytes
8. Electromagnetic inspection of the hidden defects in multiple layer structure (for examples, Jelly Roll) in battery and ultracapacitor.

Our Intellectual Property in the area of NDT Testing

1. Method of Non-Contact Measuring Electrical Conductivity of Electrolytes with Using Primary Measuring Transformer. US Patent No. 7,071,684. .
2. Method and Apparatus for Measuring Conductivity of Powder Materials Using Eddy Currents. US Patent No. 7,288,941.
3. Method and Apparatus For Eddy Current-Based Quality Inspection Of Dry Electrode Structure. US Patent No. 7,355,395.
4. Method and Apparatus for Electromagnetic-Based Quality Inspection of Battery Dry Electrode Structure. UK Patent GB No. 2435575.
5. Method of Nondestructive Tightness Testing Based on Gas Discharge Visualization. US Patent No. 7,498,817.
6. Integrated Non-destructive Method and Device for Electrochemical Energy System Diagnostics. US Patent No. 7,783,438.

7. Apparatus and Method for Determining Service Life of Chemical Energy Sources Using Combined Ultrasonic and Electromagnetic Testing. US Patent No. 7,845,232.
8. Holographic Interferometry for Non-destructive Testing of Power Sources. US Patent No. 7,911,618.
9. Method and Eddy Current System for Non-Contact Determination of Interface Resistance. US Patent No. 7,982,457.
10. Method and Device for Rapid Non-Destructive Quality Control of Powdered Materials. US Patent No. 8,102,181.
11. Method and Apparatus for Detecting and Inspection Through-Penetrating Defects in Foils and Films. US Patent No. 8,284,247.
12. Methods and Systems for Non-Destructive Determination of Fluorination of Carbon Powders. US Patent No. 8.309,024. Issue Date November 13, 2012

During the 24th ABAF International Conference we will present information about Non-Destructive Non-Contact methods and equipment that we have developed for use in the production of Li batteries, Solar cells and other industries.

Degradation processes of polymeric materials

P. Šafl[1], J. Fabián [1], K. Smutková[2]

[1]Brno University of Technology, Technická 10, 616 00 Brno, Czech Republic

[2]Brno University of Technology, Technická 2, 616 00 Brno, Czech Republic

The aim of the work was to evaluate the climatic effects on the material for 3D printing - composite nylon carbon. This composite material was chosen because nylon-carbon is a suitable material for the production of spare parts for e-motorsport. A degradation chamber was used for degradation, which is able to degrade the material in an accelerated mode. Without this chamber, the degradation would take on average four times longer. The climate chamber works with a combination of light, heat and increased humidity. The degradation processes are then examined by mechanical tests.

Intruduction

As development is progressing, there are various changes in mindsets and views on e-motorsport components. The market has been damaged in previous years, where pandemics and war have caused and continue to cause supply shortages or complete production shutdowns. These realities force motorsport development and production to adapt and not be dependent on imports. One solution is the use of additive technologies such as 3D printing. This technology is particularly suitable for the production of structural parts, which have become more widely used than mass-produced parts. As a result, design teams are now able to replace shortage parts quickly and with high quality.

The implementation of the production described above often takes insufficient account of the properties of the materials themselves. Often overlooked is the fact that materials processed by 3D printing have different characteristics than those formed by conventional injection molding. Therefore, it is essential to run studies that focus on assessing the behaviour of materials affected by 3D printing and, if necessary, modifying its properties to ensure that the material is functional and failure-free throughout its life cycle. As these materials affected by 3D printing are used more and more frequently, it is also necessary to take into account their aging, degradation and the effect of the environment on the material in order to avoid destruction or weakening of the resulting parts.

Experiment

For the purpose of the impact tests, it was necessary to select a suitable test body that would comply with the applicable standard describing the tests. Due to the lack of a specific standard focused on testing materials for 3D printing, a standard that regulates the tensile properties of metallic materials was chosen. Specifically, the standard used was ČSN EN ISO 148, which specifies the exact procedure for conducting tests under different temperature conditions. A cuboid-shaped test body was chosen to perform these tests.

The bodies themselves were created using 3D printing, using a full perimeter technique where the print head created a layer of material by tracing the outline of the body from the outer wall towards the centre. This procedure achieved a high similarity of mechanical properties between the printed bodies, which was essential to achieve valid experimental results. Subsequently, notches were created in the bodies. In order to achieve high accuracy, the notches were created after the printing was completed. The dimensions of the samples were determined according to the specifications of the standard and the printing machine used.

The specimens used for the Charpy hammer test were 80 mm long, 10 mm wide and 4 mm high. The groove on the sample was in the shape of an isosceles triangle, with 45° outliers. These test samples were printed in block form and the notch was subsequently made using a Ceast Notchvis notching machine.

Testing was carried out with two sets of test bodies, each set containing three pieces. This multiplication made it possible to achieve a statistical average of the measured values and to allow a comprehensive evaluation of the results. One of the sets was placed in a climatic chamber, while the other remained in normal conditions. After cycling in the climate chamber, both sets of bodies were subjected to mechanical tests to assess their overall mechanical characteristics.

Used technique

The Ultimaker 2+ printer was used to produce the test bodies, which has a hardened nozzle for printing abrasive materials.

For material degradation purposes, a xenon chamber from Q-LAB (see Figure 1), specifically the Q-SUN-Xe3 model, was used. This type of chamber was chosen as it fully meets the relevant standards for testing plastics intended for outdoor applications according to ASTM D2565 and plastics intended for indoor applications according to ASTM D4459. Day-light-Q filters were used in the chamber to simulate midday summer light.

To test the mechanical properties, a notch toughness test was performed using the Charpy method. Zwick 5113.100 was used as the test device, which was sufficient to break up the body.

CEAST NOTCHVIS 6951 was used for notching, which is capable of producing a notch of triangular equilateral shape with an angle of 45°. Notches are not generally made in polymer samples, but since this is more of a composite material, notches were necessary.

Measurement procedures

Phase I procedure:

1. The first step was to determine the glass transition temperature of the material to ensure that the material would not be deformed due to high temperature. This step was carried out experimentally using a Voltcraft DL-111K temperature datalogger. The datalogger has a K-type temperature sensor that is capable of measuring a temperature range from -200 to 1370 °C. This cell has a diameter of 2.5 mm and therefore holes of 2.5 mm diameter were drilled in the object to be measured and the cell was inserted into these holes.
2. After the insertion of the datalogger, different heating temperatures were set in the furnace and the glass transition temperature was determined to be 135 °C.

3. After the glass transition temperature was determined, the limiting temperature in the chamber was set to 120 °C.
4. Next, the chamber cycles were set to match the desired simulation environment.
5. After the cycling, the samples had to be labeled and prepared for mechanical testing.

The climate chamber was set to cycle in 24-hour intervals, with the illumination time of the samples was 8 hours. The selected illumination intensity was increased from 80 W/m^2 to 150 W/m^2 and then decreased again. The average illumination value was 115 W/m^2. The humidity in the climate chamber with the illumination on was selected to be 35 %. The cycle also included spraying the samples with distilled water for half an hour.

In 1 month a total of 80952 kJ/m^2 was radiated in the climate chamber and 150470 kJ/m^2 in 2 months. The second value of the radiated energy is less than twice as much as the chamber was stopped for the last 4 days to change the xenon lamp. For comparison with the data measured in the real environment, these data should be converted to Wh/m2 according to the ratio 1 Wh/m2 = 3.6 kJ/m^2. The value for 1 month of illumination is therefore 22487 Wh/m^2 and for 2 months 41797 Wh/m^2. In Prague, the highest value of radiated power is around 5647 Wh/m^2 per day.

In polymers, including nylon, UV radiation commonly causes a colour change in the irradiated object due to crystallisation of the material on the surface, as described in a study [74] carried out at the University of Alabama at Brimingham. However, due to the black colour of the tested material, no colour changes are visible. It can be argued that the radiated energy values do not reach sufficient values to test more robustly the effect of solar radiation on the material characteristics. For further detailed study, it would be advisable to expose the samples to radiation for a longer period of time, to use a more powerful radiation source, or to test the samples outdoors exposed to direct sunlight.

Phase II procedure

1. The first step was to create notches in the test bodies to ensure that all bodies broke equally during the test.
2. In the second step, the hammer was placed at the selected height and the test body was positioned in the holder.
3. Measurements could then be started by releasing the hammer, which then broke the test sample.
4. After breaking the sample, the measured value was read.
5. The test bodies that were required to be heated had to be stabilised in the chamber at 80 °C. These test pieces had to be tested within 10 seconds of leaving the chamber.
6. The methodology of the previous point was repeated for samples frozen in liquid nitrogen.

The standard deviation σ and the variance of the D (X) values were calculated for the measurement results. The hammer loss energy was subtracted from all the measured data and the average values for the different temperatures and degradation stages of the measured materials were plotted in a table for better clarity. The measured notch toughness for the Nylon CF15 Carbon material without degradation is shown in Table 1 with one month degradation in Table 2 and with two months degradation in Table 3.

Exposure of the samples to the conditions of the climate chamber for 1 month shifted the glass transition temperature above approximately 110 °C, and it was therefore not possible to determine its exact value. The same occurred for samples that were exposed to the climate chamber for 2 months. The results show that the material exposed in the chamber for one month exhibits more consistent toughness properties over a greater temperature range than material that has not been so degraded. Thus, the test samples start to get softer at higher temperatures and retain the toughness characteristics of the material for longer time. This material characteristic is due to the additional annealing in the UV chamber. The increase in values between the first and second table is due to the additional reduction of internal tension. Furthermore, we can observe a difference between the second and the third table, where after two months of degradation of the materials, photo-oxidation occurs, where the UV rays break the bond between two atoms in the chain of the macromolecule and it then breaks into smaller units. It is then easier to react with oxygen in the air. Oxidation reactions always start at the surface and gradually reach deeper layers, which then cause chemical changes in the structure of the polymers, where the macromolecules are cross-linked, leading to embrittlement and loss of elasticity of the material. This phenomenon can be seen in Figure 1, where the delamination properties of the test sample can be observed.

Figure 1. *Example of delamination after two months of degradation in a UV chamber*

Table 1. *Measured and calculated values for composite material*

Nylon CF Carbon							
T [°C]	**Samples**	**1**	**2**	**3**	**Diameter**	**D (X)**	**σ**
70	13,14,15	1,194	1,009	0,852	1,018	0,0293	1,1712
-60	2,23,24	0,221	0,221	0,221	0,221	0	0

Table 2. *Measured and calculated values for the composite material after one month of degradation*

Nylon CF Carbon 1 měsíc degradece							
T [°C]	**Samples**	**1**	**2**	**3**	**Diameter**	**D (X)**	**σ**
70	43,44,45	1,220	1,048	1,167	1,145	0,0078	0,0881
-60	19,20,21	0,271	0,221	0,283	0,258	0,001	0,0329

Table 3. *Measured and calculated values for the composite material after 2 months of degradation*

Nylon CF Carbon 2 měsíce degradace							
T [°C]	**Samples**	**1**	**2**	**3**	**Diameter**	**D (X)**	**σ**
70	73,74,75	0,234	0,419	0,419	0,357	0,0114	0,1068
-60	106,107,108	0,161	0,173	0,173	0,169	0,000	0,0069

Acknowledgements

This work was supported by the specific graduate research of the Brno University of Technology No. FEKT-S-23-8286.

References

1. ČSN ISO 2768-1. *Nepředepsané mezní úchylky délkových a úhlových rozměrů*. Federální úřad pro normalizaci a měření. Praha: Vydavatelství norem, 1992.
2. Yousif E, Haddad R.: Photodegradation and photostabilization of polymers, especially *polystyrene: review*, 23.8.2013 DOI: 10.1186/2193-1801-2-398 [online] dostupné z: https://www.ncbi.nlm.nih.gov/pmc/articles/PMC4320144/
3. ŠAFL, Pavel. *Použití technologie 3D tisku pro návrh výroby náhradních dílů* [online]. Brno, 2021 [cit. 2021-07-13]. Dostupné z: https://www.vutbr.cz/studenti/zav-prace/detail/134502. Diplomová práce. Vysoké učení technické v Brně, Fakulta elektrotechniky a komunikačních technologií, Ústav elektrotechnologie. Vedoucí práce Tomáš Binar.
4. SEPE, Mike. MICHAEL P. SEPE, LLC. *Annealing Tips for Thermoplastic Polyurethanes* [online]. 2020. 6/7. Plastics Technology, 2020, 9.9.2020 [cit. 2021-7-13]. Dostupné z: https://www.ptonline.com/blog/post/materials-part-6-of-7-annealing-tips-for-thermoplastic-polyurethanes
5. FIBERLOGY: *TECHNICAL DATA SHEET PA12+CF15*,[online]. 5. 10. 2018 Dostupné z:https://www.materialpro3d.cz/user/related_files/tds_pa12cf15.pdf

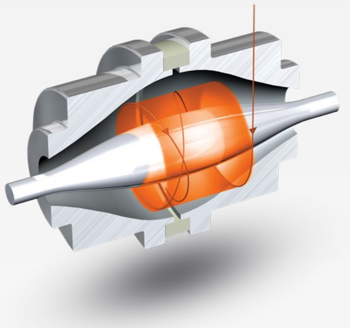

In-situ and operando Raman spectroscopy for batteries

Trusted for reliable results

Renishaw's inVia™ confocal Raman microscope and Virsa™ Raman analyser are trusted by leading researchers working on battery technology. The inVia microscope offers research-grade performance and ultimate flexibility. The Virsa analyser with its fibre probe functionality is easy-to-use and is readily transported between laboratory and manufacturing environments.

Operando (triggered) measurement

You can synchronise Raman and electrochemical measurements using either hardware or software triggering. Hardware triggering can start a series of Raman measurements with an electronic signal e.g. from a potentiostat. Software triggering enables either LabVIEW™ or Python scripts to control Renishaw's WiRE™ software via a TCP/IP connection.

Controlled laboratory environments

Renishaw's Raman spectrometers have been fitted in inert gas gloveboxes for Raman analysis of air-sensitive battery materials like $LiCoO_2$. The inVia microscope and Virsa analyser are also used in clean rooms and humidity-controlled environments suitable for manufacturing batteries.

LiveTrack™ focus-tracking technology

LiveTrack technology automatically keeps your Raman measurements in focus. Get topographical Raman images when analysing rough samples like activated carbon anodes, and uneven samples like electrode foils. If your sample swells during charge or discharge, LiveTrack technology keeps the Raman measurement in focus at the surface.

Automation and remote access

Renishaw's WiRE software can automate your Raman measurements. You can queue many samples for Raman analysis and control your experiments remotely.

www.renishaw.com/batteries

#renishaw

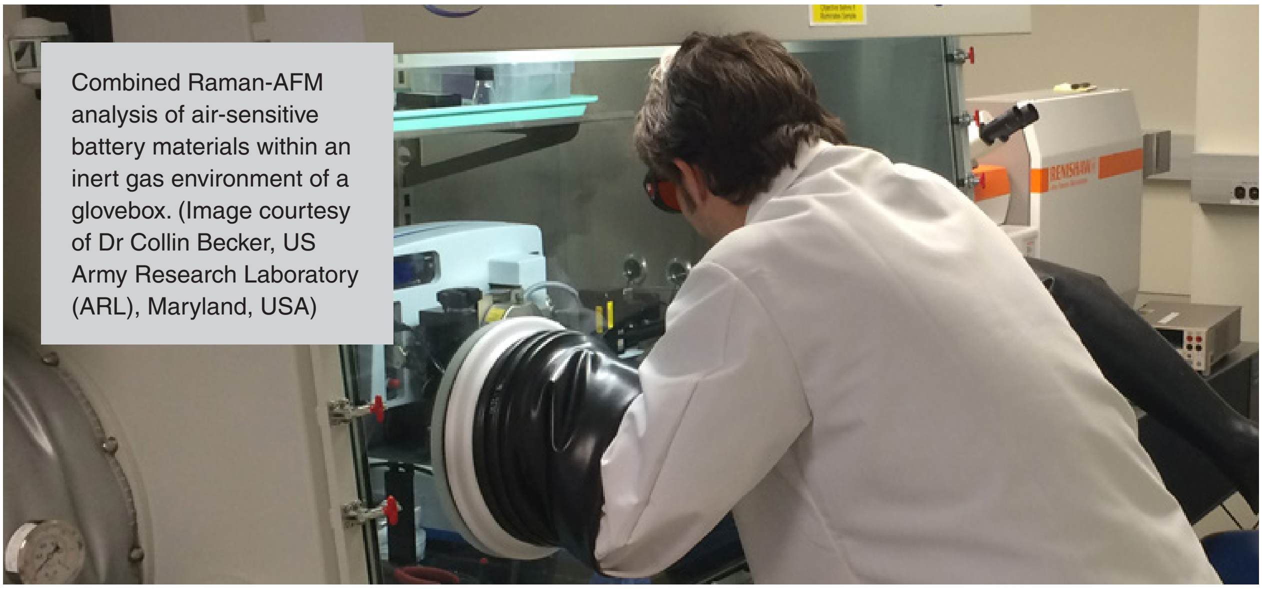

Combined Raman-AFM analysis of air-sensitive battery materials within an inert gas environment of a glovebox. (Image courtesy of Dr Collin Becker, US Army Research Laboratory (ARL), Maryland, USA)

Electrolyte characterisation

Operando Raman spectroscopy was performed using an inVia microscope to determine key electrolyte properties. Flexible sampling options are available for the required electrochemical cell orientation. (Characterising lithium-ion electrolytes via operando Raman microspectroscopy | Nature Communications, J. Fawdon, J. Ihli, F. La Mantia and M. Pasta, Nature Communications 12, 4053 (2021))

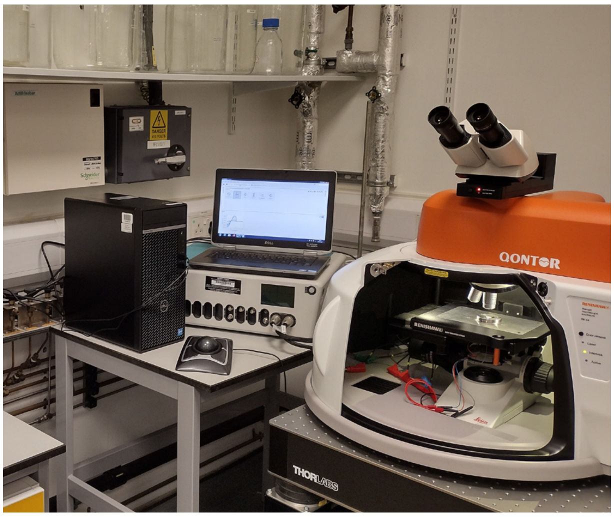

Electrochemical cell and potentiostat

Operando Raman spectroscopy performed using an inVia microscope and an EL-Cell Opto Std electrochemical cell. Hardware triggering was used to synchronise Raman acquisitions using electronic signals from a Metrohm Autolab potentiostat. (Image courtesy of Dr Rudra Samajdar and Dr Andy Wain, Electrochemistry Group, National Physical Laboratory, UK)

For more information on Raman spectroscopy for batteries, please visit **www.renishaw.com/batteries**

www.renishaw.com/raman

#renishaw

☎ **+44 (0) 1453 524524** ✉ **raman@renishaw.com**

Title: Advanced Batteries Accumulators and Fuel Cells – 24th ABAF

Edited: Marie Sedlaříková
Vítězslav Novák
Tomáš Kazda
Petr Bača

Publishing Office: Marie Sedlaříková
Vítězslav Novák
Tomáš Kazda
Petr Bača

Deadline: July 23rd 2023

Publisher: Brno University of Technology
Faculty of Electrical Engineering and Communication
Department of Electrical and Electronic Technology

Year: 2023

ISBN 978-80-214-6176-5